MSc Thesis

Identifying High Yielding Stormwater Harvesting Sites in Africa

J.R Fortuin

TU Delft

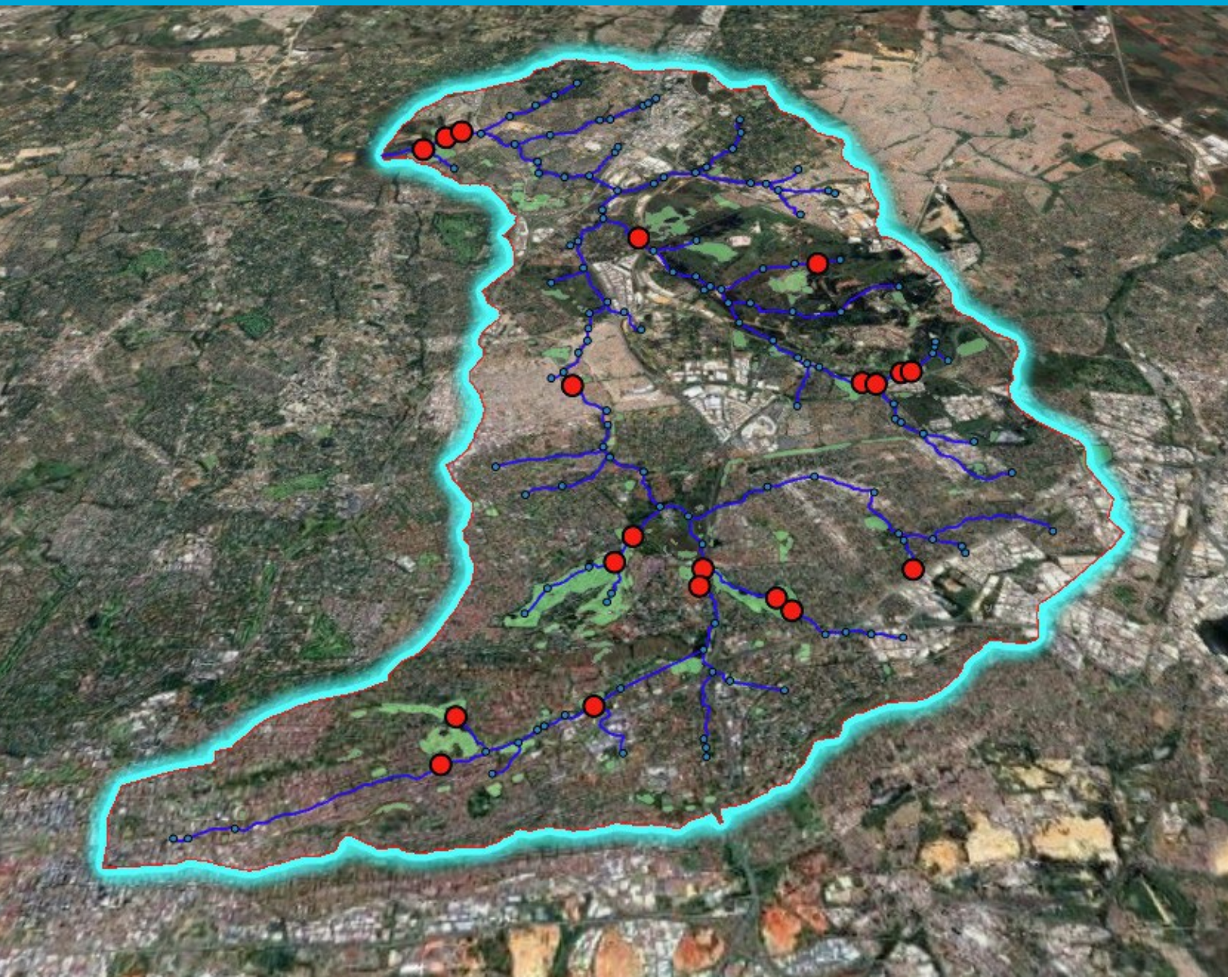

TU Delft
Delft University of Technology

Identifying High Yielding Stormwater Harvesting Sites in Africa

by

J.R. Fortuin

to obtain the degree of Master of Science

at the Delft University of Technology

to be defended on September 18th 2025.

Student Number:	4606942	
Project Duration:	November 2021 - September 2025	
Thesis Committee:	Dr. Ir. Luuk Rietveld	TU Delft, Chair
	Ir. Juan Aguilar Lopez	TU Delft
	Ir. Job van der Werf	TU Delft

Delft University of Technology

PREFACE

This thesis is submitted in fulfilment of the requirements for the MSc in Water Resources Engineering at Delft University of Technology (TU Delft). It marks the conclusion of a journey that has been both demanding and rewarding.

I am deeply grateful to my family and friends for their consistent encouragement throughout the process. Above all, my heartfelt thanks go to my wife, Trude, for her unwavering love, patience, and understanding – especially through the late nights and weekend commitments that this degree required. It truly does take a village, and mine has been extraordinary.

This thesis would not have taken shape without the early support and guidance of Martine Rutten, whose insights helped set a clear foundation. I am indebted to Luuk Rietveld, Juan Aguilar Lopez and Job van der Werf for helping me regain momentum when it mattered most and for their steady guidance in getting this thesis across the finish line. Your time, encouragement and expertise are sincerely appreciated.

My years at TU Delft have been immensely fulfilling. I have learned from and been inspired by exceptional scholars and practitioners at CiTG. Their passion and dedication have shaped many of the pages that follow, and also how I think about hydrology and hydraulics. It has been a particular honour to have studied at TU Delft in the footsteps of my great-grandfather; that connection has been a quiet source of motivation and pride throughout this journey.

I am extremely grateful for this journey at TU Delft and look forward to the new season and new adventures.

ABSTRACT

Africa is the world's second driest continent, supporting 15% of the global population with only 9% of the global renewable water resource. The 2015 to 2018 drought in the Western Cape of South Africa, where a Day-Zero scenario was narrowly avoided, highlighted the need to start looking at alternative water resources in conjunction with preserving the current water resources.

Globally, the water sector is moving towards a circular water economy - where all water sources, including wastewater, stormwater and rainwater are treated as a resource that can be used, recycled, and replenished into the system. Stormwater harvesting (SWH) has successfully been implemented in countries such as Australia, Israel, Singapore & South Africa.

The success of any SWH scheme depends on effective site selection. Yet, there is little guidance available, and site choices have traditionally relied on the subjective judgment of urban water managers. This demonstrates the need for an objective, data-driven approach that integrates multiple spatial datasets to identify optimal SWH locations.

This research develops such a method: an integrated hydrological and GIS-based screening tool that identifies high yield (hotspot) SWH sites using publicly available datasets in Africa. The collection models showed that high yielding stormwater harvesting sites can be identified with publicly available data, with all 4 weightings consistently pointing out the top 8 stormwater harvesting sites.

The storage and distribution models showed that with a storage facility that has a capacity of 10x the maximum daily demand, high reliability figures can be achieved in excess of 80% in terms of volume and time-based reliability. The storage and distribution models also showed that if the storage capacity can be increased, the reliability and resilience of the facility can also be increased.

The study also has some limitations and intrinsic uncertainties, and the framework should be used as a screening tool.

This study places focus on stormwater harvesting as an integral part of sustainable management of urban water and presents a robust, adaptable and scalable tool that can support urban areas across Africa to address the growing water demand challenges.

Contents

List of Figures

List of Tables

Acronyms

ASTER	Advanced Spaceborne Thermal Emission and Reflection Radiometer
CHIRPS	Climate Hazards Group InfraRed Precipitation with Stations
CN	Curve Number
DEM	Digital Elevation Model
EPA	Environmental Protection Agency
ESA	European Space Agency
FAO	Food and Agriculture Organisation
GIS	Geographic Information System
MAE	Mean Annual Evaporation
MAP	Mean Annual Precipitation
MAR	Managed Aquifer Recharge
ODbL	Open Database License
OSM	Open Street Maps
RWH	Rainwater Harvesting
SANRAL	SA National Roads Agency
SCS	Soil Conservation Services
SOTER	World Soils and Terrain Database
SRTM	Shuttle Radar Topography Mission
SUDS	Sustainable Urban Drainage systems
SWH	Stormwater Harvesting
SWMM	Surface Water Management Model
USDA	US Department of Agriculture
VGI	Volunteered Geographic Information

1. INTRODUCTION

1.1 Growing Water Demand

Urbanisation growth rates in Sub-Saharan Africa are among the highest globally (Ali, 2021) and it is estimated that the urban population in Sub-Saharan Africa could double by 2040 (Foster et al., 2020). The increasing population has exerted considerable pressure on the finite water resources and the rate at which the urban population is growing has surpassed the capacity of water service providers to meet the water demand (Chitonge, 2020). Africa is the world's second driest continent and has to support a global population of 15% with a global renewable water resource of 9% (Wang et al., 2014).

South Africa's urban population has increased considerably since the removal of apartheid, with the metropolitan cities accounting for 60% of the population increase. The fastest increase has been in the two Gauteng metros of Johannesburg and Tshwane, followed by Cape Town and the third Gauteng metro of Ekurhuleni (Turok & Borel-Saladin, 2014). Water demand in South Africa is predicted to be approximately 17.7 billion m^3/annum in 2030, whilst the water supply is predicted to be approximately 15 billion m^3/annum, leaving a water deficit of 2.7 billion m^3 (Mkhize et al., n.d.). The metropolitan areas of South Africa, shown **below** in **Figure 1-1**, are not well located with respect to the water resources. Gauteng province is reliant on its water supply from the Vaal River System, which in turn receives its water from the Lesotho Highlands project. The Lesotho Highlands dams are more than 300 kilometres South of Johannesburg, and the Vaal Dam is located approximately 70 kilometres from Johannesburg. It is projected that for Gauteng to avoid a water crisis, it needs to reduce its water use by 3 percent per person per year (Heggie, 2020).

It is estimated that the global population has increased by 4.4 times over the last century, compared to water withdrawal, that has increased by 7.3 times over the same time (Chitonge, 2020). The sustainable management of water resources and the protection of water environments in these ever-expanding cities is therefore of critical importance in order to address water stress and scarcity (Mohanrao, 2014). Cities will need to reduce their reliance on conventional water supply from dams and pursue alternative sources of water supply to secure their water future (Carden & Fisher-Jeffes, 2017).

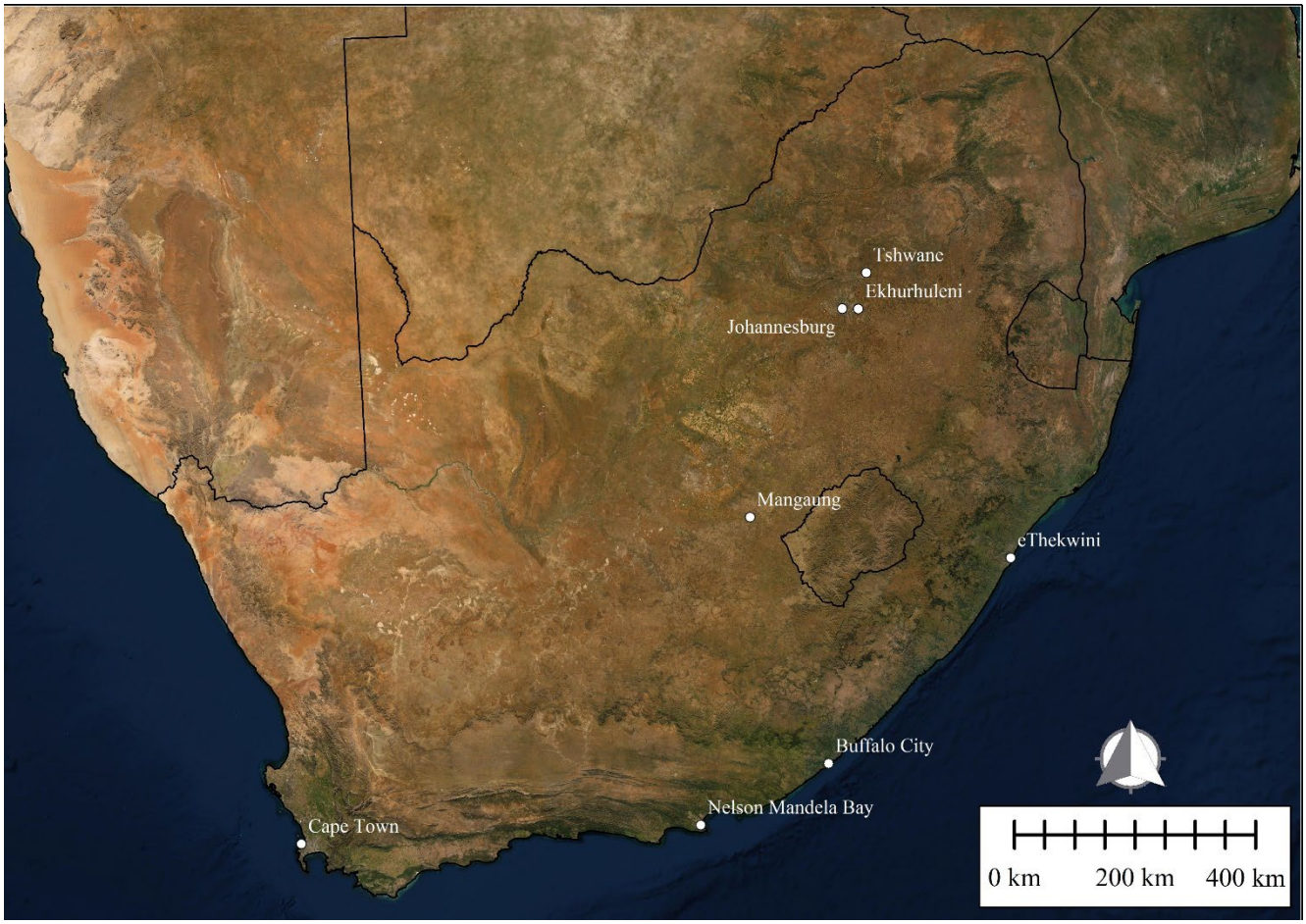

Figure 1-1: Metropolitan Municipalities of South Africa

1.2 Water Resources History

The water resources of Johannesburg have been under pressure ever since mining started along the Witwatersrand Ridge. The early water demand was driven by the need for water in the mining processes and to sustain the ever-growing population migrating towards the promise of gold riches. The demand for water was around 5.86 Mℓ/day by 1893 (Turton et al., 2007).

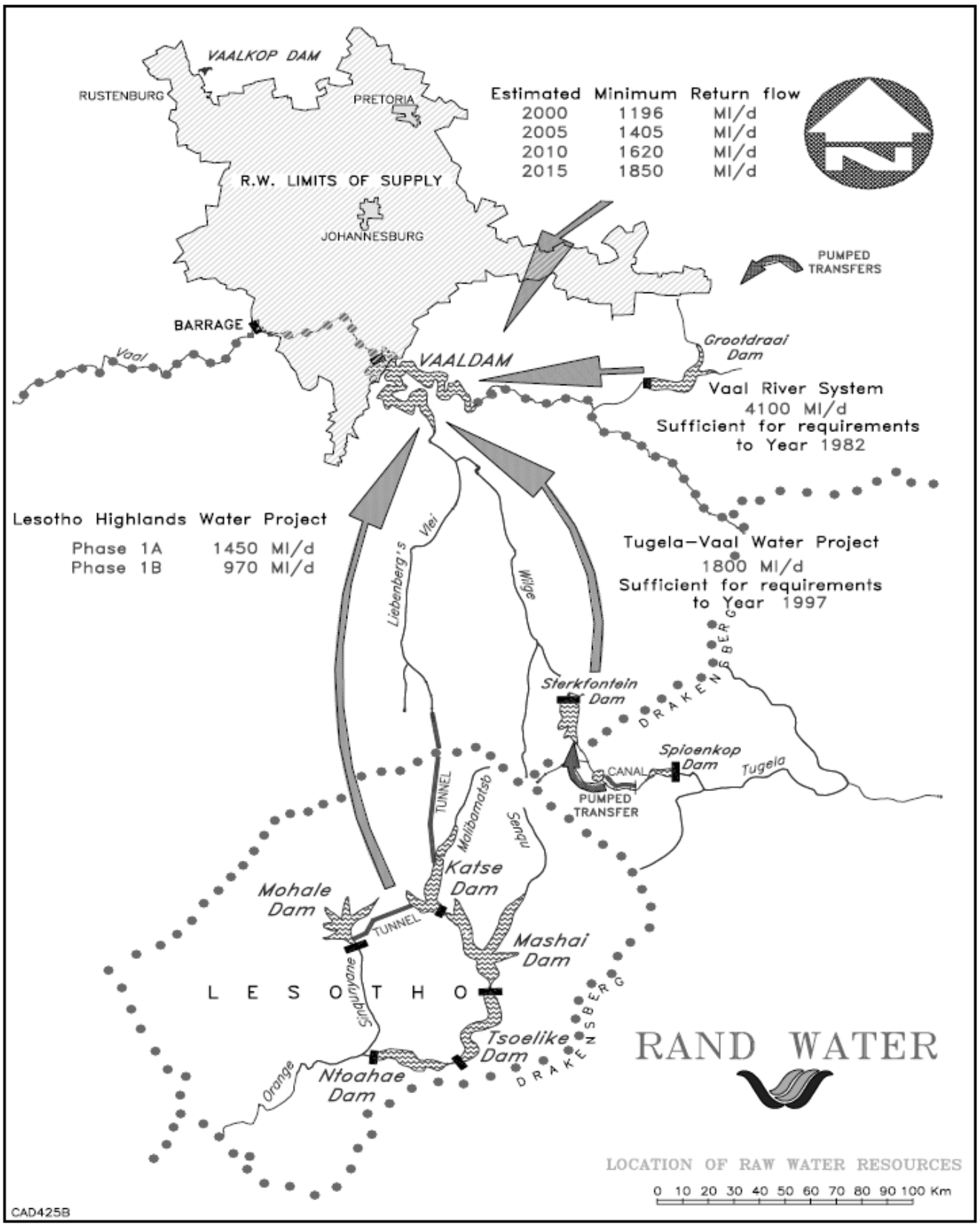

Figure 1-2: Lesotho Highlands Scheme for the supply of water to Gauteng Province (Turton et al., 2007)

By 1902, it was clear that the assurance of water supply could become a limitation to the economic growth of the city, and the Rand Water Board was established to develop a secure water supply system. The demand projections by the Transvaal Chamber of Mines estimated that the city needed 90 Mℓ/day by 1920, which consisted of 70 Mℓ/day for the mines and 20 Mℓ/day for domestic consumption. The 1913 drought in Johannesburg forced Rand Water to consider obtaining water from the Vaal River and in 1914 the Vaal River Development Scheme was adopted with plans for a barrage, a water treatment plant and a main pipeline to the Witwatersrand (Turton et al., 2007). The Vaal Barrage was constructed in the early 1920s but did not prove to be enough to meet the growing water needs of the city, and subsequently plans were made to construct the Vaal dam at the confluence of the Wilge- and Vaal River. The Vaal Dam was completed in 1938 and had a full capacity of 994 million m^3 at the time. The Vaal dam has since been lifted a few times (in 1956 and 1985) and has a capacity of 3 364 million m^3 (van Vuuren, 2008).

Further augmentation of the water supply to the Vaal Dam was done in 1974 with the Thukela-Vaal Augmentation Scheme which was the first inter basin transfer from a river basin outside of the Vaal catchment. The water is pumped from the Woodstock Dam, Driel Barrage, Kielburn Dam and Driekloof Dam situated in the Tugela catchment, into the Sterkfontein Dam that is situated in the Wilge river from where it flows to the Vaal Dam ("Thukela_Vaal Transfer Scheme," 2013).

The latest augmentation scheme is the Lesotho Highlands Water Scheme, which will double the water resources to the Gauteng region. Studies were conducted since the early 1950's to divert water from the water abundant country of Lesotho to the upper reaches of the Vaal River (Du & de Villiers, 1996). A phased approach for the development of the Lesotho Highlands Water Scheme was followed, where phase 1 was completed in 2003 and phase 2 is currently underway (*LHDA*, 2022). Phase 1 consisted of the construction of the Katse Dam, the Muela Dam and the Mohale Dam and a series of tunnels that delivers water to the Vaal catchment (European Investment Bank, 2002).

The Rand Water Supply Area and some of the major inter-basin transfers are shown in **Figure 1-2**.

1.3 Problem Statement

South-Africa has experienced several prolonged droughts in the last decade and is approaching a physical water scarcity (Makelane & Roodbol, 2020). The 2015 to 2018 drought in the Western Cape of South Africa, where a Day-Zero scenario was narrowly avoided, showed that the country and the African continent will need to start looking at alternative water resources in conjunction with preserving the current water resources. The Gauteng province of South Africa also faces the possibility of a day-zero drought in the next 10 to 20 years and has already had a near miss when the 2015-2016 El Nino drought caused the water level in the Vaal dam to dip below 25% in September 2016 (Bega, 2021).

A shift towards a circular water economy is being promoted in the water sector worldwide. A circular water economy is one where all water sources, including wastewater, stormwater and rainwater are treated as a resource that can be used, recycled, and replenished into the system (Ndeketeya & Dundu, 2022). Many cities worldwide are considering alternative water sources such as treated wastewater and stormwater harvesting to supplement existing water supplies (Dandy et al., 2019).

Traditionally, stormwater has been perceived as an inconvenience, but the increase in water demand has enhanced the recognition of stormwater as a resource and asset (Mcardle et al., 2010). Stormwater harvesting (SWH) has successfully been implemented in countries such as Australia (T. Wong, 2012), Israel (Tal, 2006), Singapore (Lim et al., 2011) & South Africa (DWAF, 2010). In South Africa the Atlantis Water Resource Management Scheme (AWRMS) is an example of a successful SWH scheme that has been in operation since 1979. To date SWH schemes have not been widely used around South Africa, with the AWRMS scheme being the exception (L. N. Fisher-Jeffes et al., 2017).

The selection of a SWH site is of critical importance for the success of SWH schemes. There is very limited guidance and methodologies available for the selection of SWH sites and has historically been done with the subjective knowledge of urban water managers (Mohanrao, 2014). Subsequently there is a need to develop an objective site selection method/model that can integrate multiple spatial datasets to determine the optimal SWH locations.

1.4 Research Objective

The research objective is to develop an objective and integrated hydrological and GIS model screening tool that determines high yielding (hotspot) stormwater harvesting sites from publicly available datasets in Africa. The model will integrate GIS functionality, scripting, remote sensing data and a hydrological model to determine and rank suitable/hotspot stormwater harvesting sites.

Research question 1 is:

> *Can high yielding (hotspot) stormwater harvesting sites be identified with publicly available data?*

Research question 2 is:

> *How reliable are these stormwater harvesting sites at supplying demand?*

2. BACKGROUND INFORMATION

2.1 Stormwater Management

The practice of stormwater management dates back thousands of years and focused primarily on flood prevention and flood control. One of the earliest stormwater regulations found is from King Hammurabi of Mesopotamia who wrote the Code of Hammurabi in 1760 BC to protect downstream landowners from negligent stormwater management practices (Echols & Pennypacker, 2015).

Traditional stormwater management was typically done with 'hard' infrastructure such as pipes and lined canals where the focus was to convey the water away as quickly as possible to prevent local flooding (Armitage et al., 2013). The article "Stormwater Management for the 1990's" summarises the historical thinking around stormwater management: "Historically, stormwater management has been limited to planning, designing and implementing storm drainage improvements. For the most part, planning and design have focused on protecting only the site being drained, with little consideration of the downstream effects of resulting increases in volume and peak flows" (Roesner & Matthews, 1990).

A paradigm shift towards water sensitive cities and sustainable stormwater management was made in the late 1990's and early 2000's (Mohanrao, 2014). Wong & Brown (2009) proposed transforming cities to Water Sensitive Cities through 6 transitions in urban water management as is shown below in **Figure 2-1** from left to right. The water sensitive city is defined by the principles of integrated urban water management (Mohanrao, 2014) and the following three pillars of practice (Wong & Brown, 2009):

1. Cities as water supply catchments.
2. Cities providing ecosystem services.
3. Cities comprising water sensitive communities.

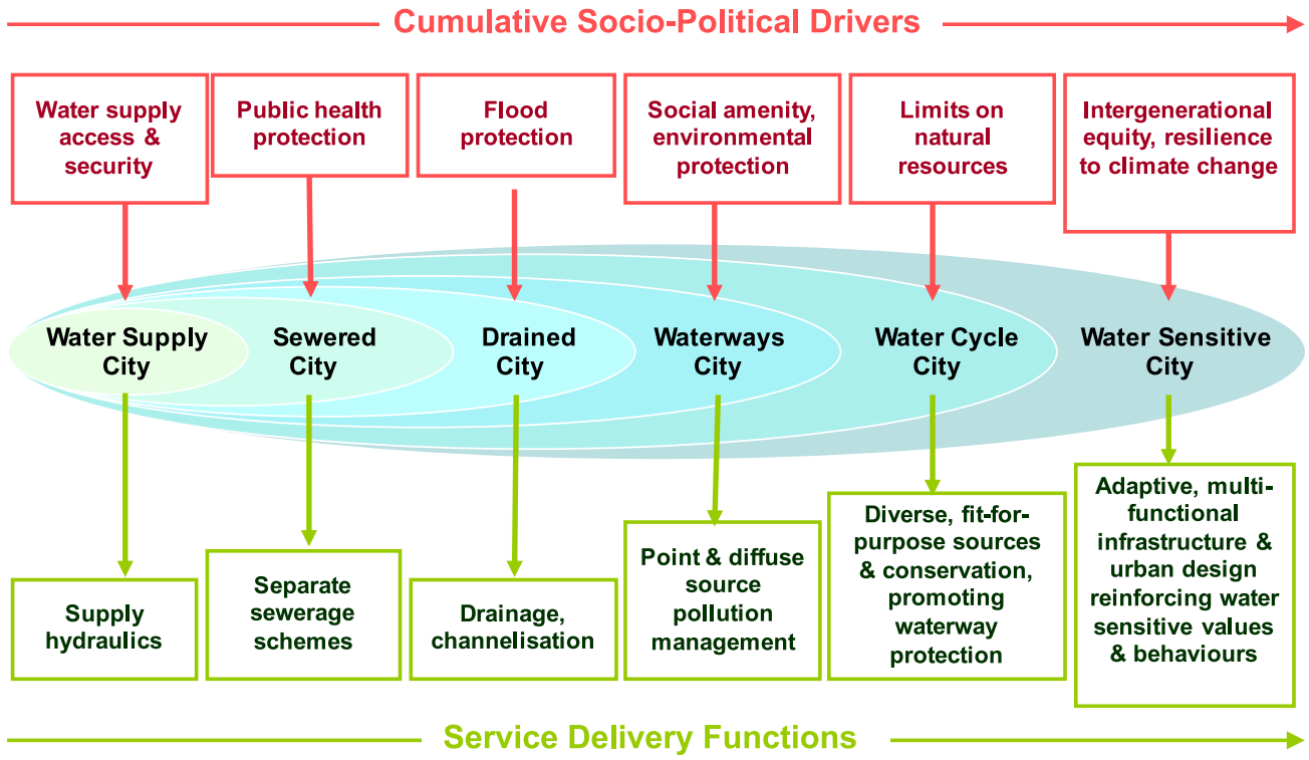

Figure 2-1: Water Sensitive Cities (Wong & Brown, 2009)

Cities as water supply catchments focuses on a supplying demand from several water sources and diverse infrastructure for harvesting, treatment, storage and distribution of water. The alterative water sources include stormwater harvesting, rainwater harvesting, recycled wastewater, managed aquifer recharge and where applicable desalination (Wong & Brown, 2009).

Cities providing ecosystem services focuses on public open spaces being public amenities that are ecologically functioning in the urban space with sustainable water management, micro-climate influences, facilitation of carbon sinks and for food production (Wong & Brown, 2009).

Cities comprising water sensitive communities focuses on the fact that technology and scientific drive will not ensure the success of water sensitive urban design (WSUD) and that institutional reform and public buy-in is needed for the adoption and long-term success of WSUD (Wong & Brown, 2009)..

2.2 Stormwater Harvesting

SWH and rainwater harvesting (RWH) are often used in literature interchangeably as the collection, storage and use of run-off. SWH and RWH are however two separate schemes, and this research will only focus on SWH. SWH & RWH in a South African context and for the purposes of this research is defined as follows (L. Fisher-Jeffes, 2015):

- **Stormwater Harvesting (SWH):** collection, storage, and use of runoff from an urban area by one or more users.
- **Rainwater Harvesting (RWH):** collection, storage, and use of runoff from roof/s on an individual property

SWH as defined above appears to have started in the 1970's and 1980's. Singapore was among the first cities in the world to do SWH to diversify their water supply sources in the 1970's (Lim et al., 2011). The literature reveals that SWH projects have been implemented in countries like the United States of America, Canada, Australia, Israel, Gaza, Malta, Namibia, Singapore & South Africa. Australia is one of the countries in which SWH has become commonplace especially in New South Wales, South Australia & Victoria with Philp et al. (2008), stating that large scale SWH outside of Australia has been very limited. Philp et al. (2008) also points out that while the majority of the projects are on a small scale, that there are several projects operating on a city-wide scale in Australia. The typical components of a Melbourne city stormwater harvesting facility are shown in **Figure 2-2** and include harvesting/collection, treatment, storage and distribution.

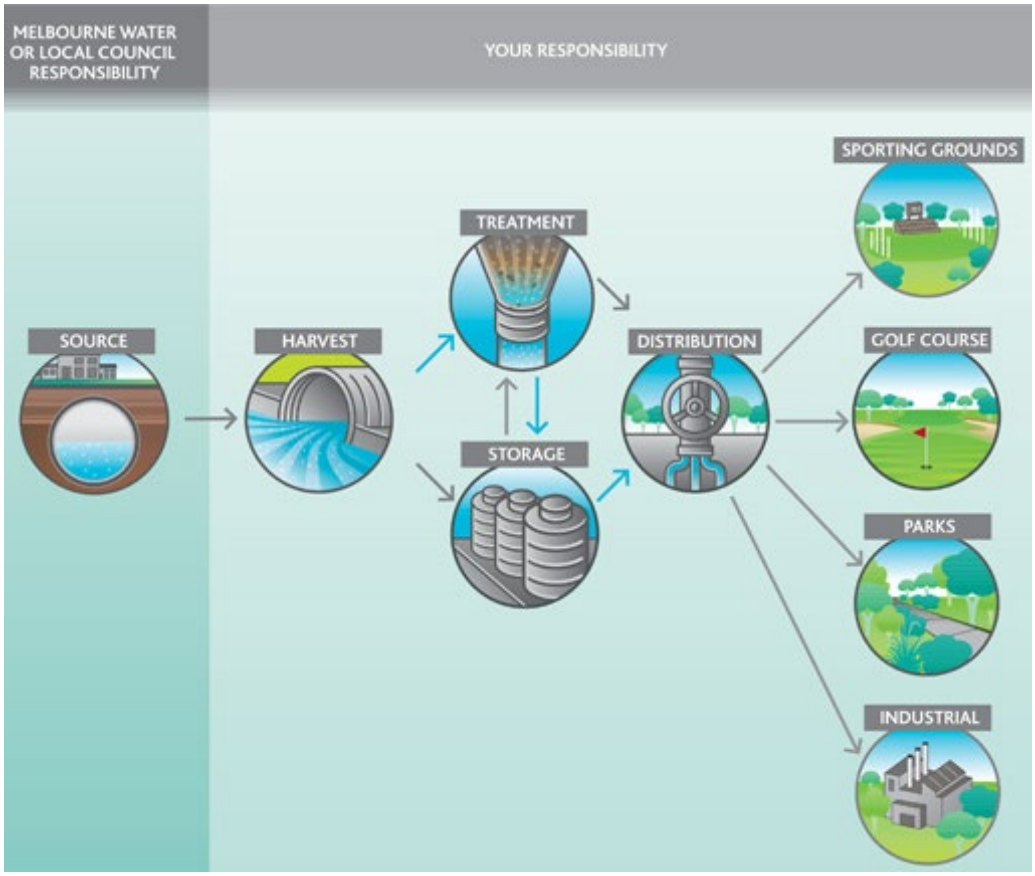

Figure 2-2: Melbourne City SWH system components (City of Melbourne, n.d.)

2.2.1 Collection

Conventional stormwater collection systems in South Africa consist primarily of pipes and canals that are focused on minimising the local flooding by conveying the stormwater as rapidly as possible. Conventional stormwater collection infrastructure offers very little water quality improvement opportunity and has very limited water losses due to the impermeable nature of the system (Rohrer, 2017). Subsequently the conventional stormwater infrastructure in South Africa tends to be concrete pipes and concrete lined canals that have minimal friction and attenuation, that facilitates the speedy routing of stormwater to downstream receiving infrastructure or water bodies. Often the natural streams or rivers in urban areas are also "upgraded" to concrete lined infrastructure to facilitate the quicker drainage of stormwater as can be seen in **Figure 2-3** of the Liesbeek River in Cape Town (*Liesbeek River Life Plan | Urban Water Management*, 2014).

Figure 2-3: Concrete Lined Liesbeek River (Liesbeek River Life Plan, 2014)

Alternative stormwater collection infrastructure or Sustainable Urban Drainage Systems (SuDS) consist of infiltration trenches & swales. These systems make use of permeable and vegetated systems that facilitate infiltration, evapotranspiration and attenuation of the flood peak that can improve the water quality and decrease the discharge volume (Armitage et al., 2013). An example of a swale canal is shown in **Figure 2-4** where the permeable aggregate material in the base of the canal allows for the infiltration and storage of water and the grass lining allows for evapotranspiration and erosion protection (Innovyze, n.d.).

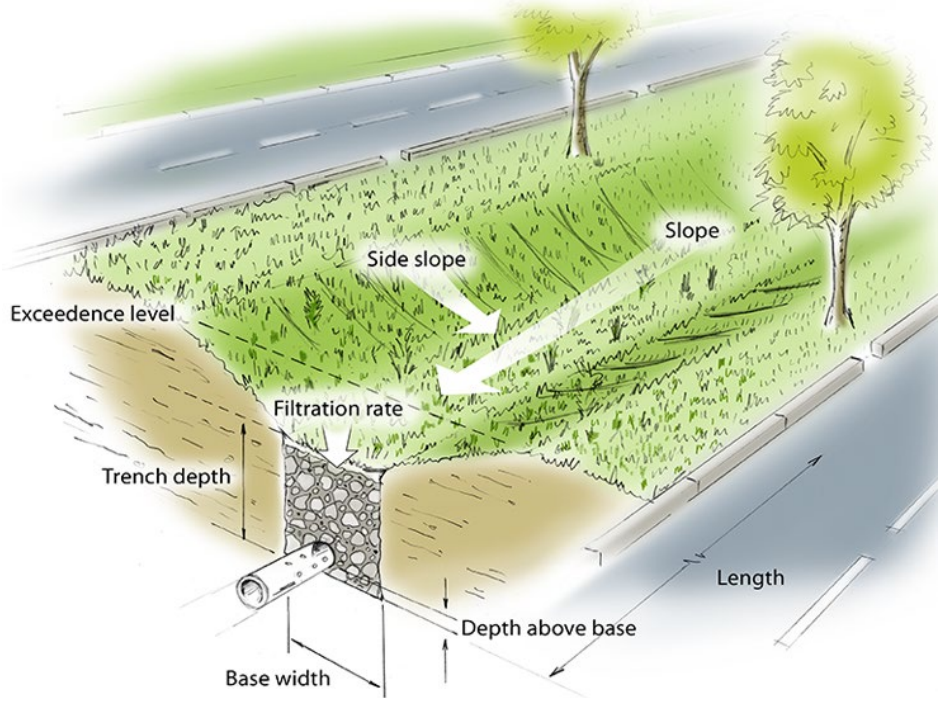

Figure 2-4: Swale Canal (Innovyze, n.d.)

The appropriate choice of either conventional or SUDS drainage collection system to match the catchment land-use is critical for the effectiveness of a SWH system and in order to have a balance of the benefits of water quality & water quantity (Mcmahon et al., 2008). A greenfield project would allow for the choice and design of appropriate collection system upfront whereas a brownfield project could allow for the retrofitting of SUDS that can improve the water quality and decrease the amount of treatment needed at the SWH facility.

2.2.2 Treatment

The treatment of the harvested stormwater in a SWH system is dependent on the water quality required by the end-user, with the literature and case studies showing that SWH has predominantly been used for non-potable water, typically used for irrigation of parks and sports fields (Mcmahon et al., 2008). Singapore has however been using SWH to supplement their potable water use since the 1970's (Lim et al., 2011). Australia also has two SWH systems that aim to supplement the potable water supply. The regional city of Orange in New South Wales is harvesting stormwater to supplement and supply up to 25% of the city's potable drinking water (Pordage, 2018), and the Kalkallo SWH & Reuse scheme aims to treat and directly inject 365Mℓ/annum treated stormwater into the drinking water system (CRC - Kalkallo, 2018).

Treatment in a SWH system can be defined in two categories:

- **Sustainable Urban Drainage Systems (SuDS) –** as stated above the aim of SuDS is to improve the water quality of stormwater. SuDS are usually implemented in a treatment train and can be installed to provide water quality improvement at a pollution source or alternatively at a local or regional scale (Armitage et al., 2013). Typically, the SuDS treatment train would form part of the collection system, however the storage facility itself can form part of the SuDS treatment train where detention ponds, or wetlands are utilized.
- **Advanced Treatment & Disinfection –** advanced treatment processes are necessary when reliable and uniform water quality is needed as is the case with potable water and certain non-potable water uses (Hatt et al., 2006; Mcmahon et al., 2008). The advanced treatment used in SWH systems is similar to those used in potable water and wastewater treatment plants (Mcmahon et al., 2008; G. Mitchell et al., 2006) and includes the following:
  - Coarse & Fine Screening
  - Dissolved air flotation (DAF)
  - Microfiltration
  - Reverse Osmosis
  - Aeration
  - Biological Treatment
  - Electrolyte flocculation

  Disinfection is required if the water end-use involves potential human contact and can be done with common disinfection techniques such as chlorination, ultraviolet radiation, oxidation and membrane filtration (Mcmahon et al., 2008).

2.2.3 Storage

The reliability of a SWH system in delivering the end-user demands is directly proportional to the storage capacity of the system, where the difference and variability between supply and demand is the optimal storage capacity needed (G. Mitchell et al., 2006). SWH systems are often constrained by the space available for storage in the urban environment which subsequently limits the total demand that the SWH system can supply (Rohrer, 2017). The final choice and design of the SWH system storage is therefore a trade-off between volumetric reliability and minimising the storage capacity and cost (L. Fisher-Jeffes, 2015).

The storage of SWH system can be broken down into three categories namely:

- **Open Storage** – all water bodies that are affected by evaporation & precipitation including retention ponds, constructed dams, lakes, wetlands (Rohrer, 2017). An example open storage SWH system is shown in **Figure 2-5** (O'Halloran, n.d.).
- **Closed Storage** – all water storage where evaporation & precipitation do not have an effect such as tanks, pipe manifolds & closed reservoirs (L. Fisher-Jeffes, 2015). An example of a closed storage SWH system is shown in **Figure 2-6** (City of Melbourne, n.d.).
- **Managed Aquifer Recharge (MAR)** – intentionally recharging and using the aquifer as storage unit to limit evaporation through infiltration ponds, percolation tanks & injection of water into the aquifer (Dillon, 2005). An example MAR SWH system is shown in **Figure 2-7** (CRC, 2018)**.**

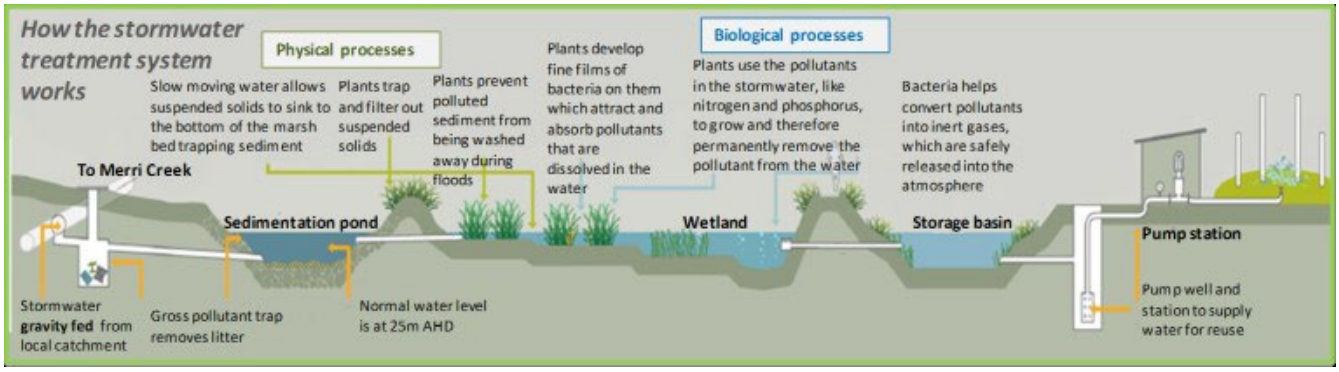

Figure 2-5: Typical Open Storage SWH System (O' Halloran, n.d.)

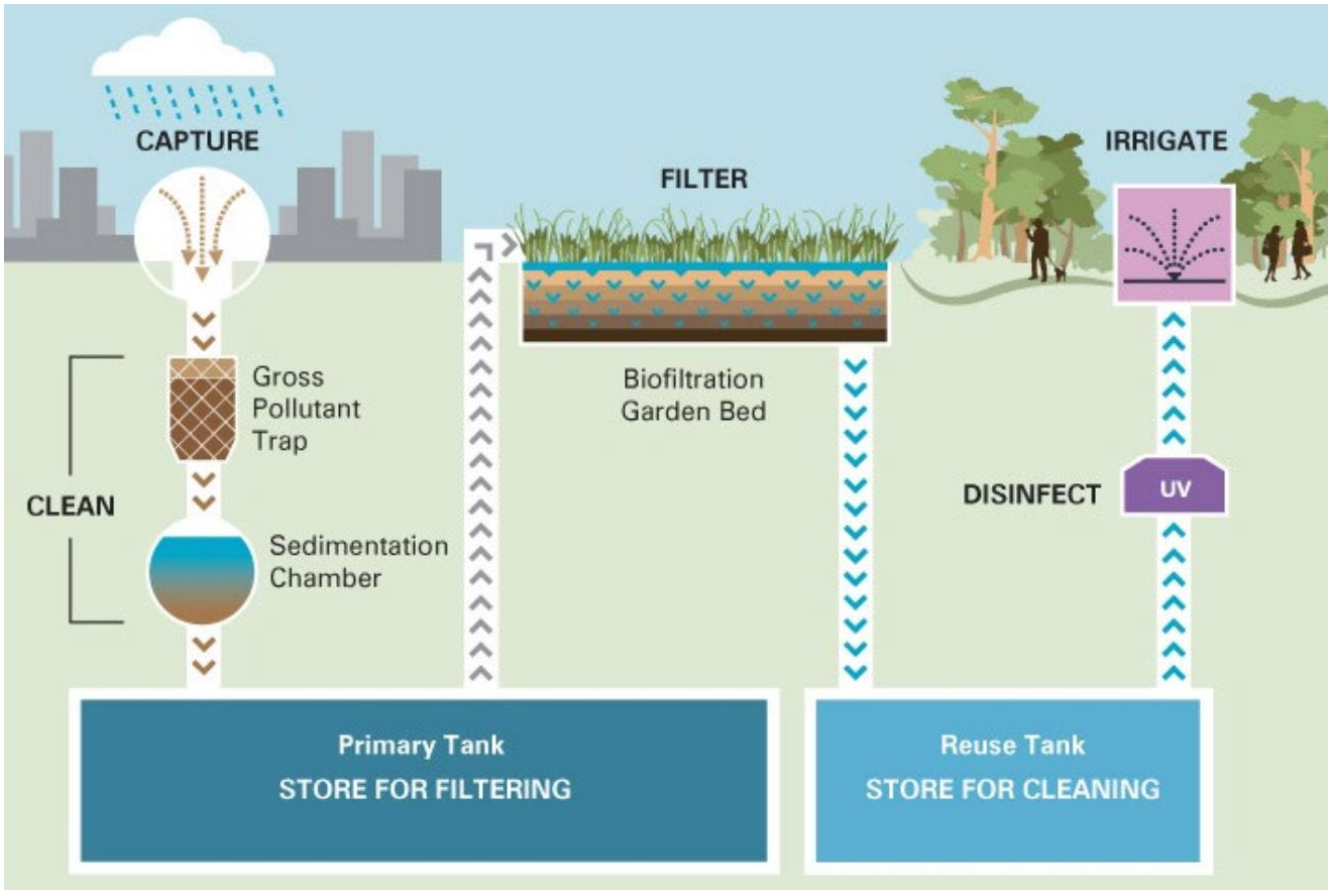

Figure 2-6: Typical Closed Storage SWH System (City of Melbourne, n.d.)

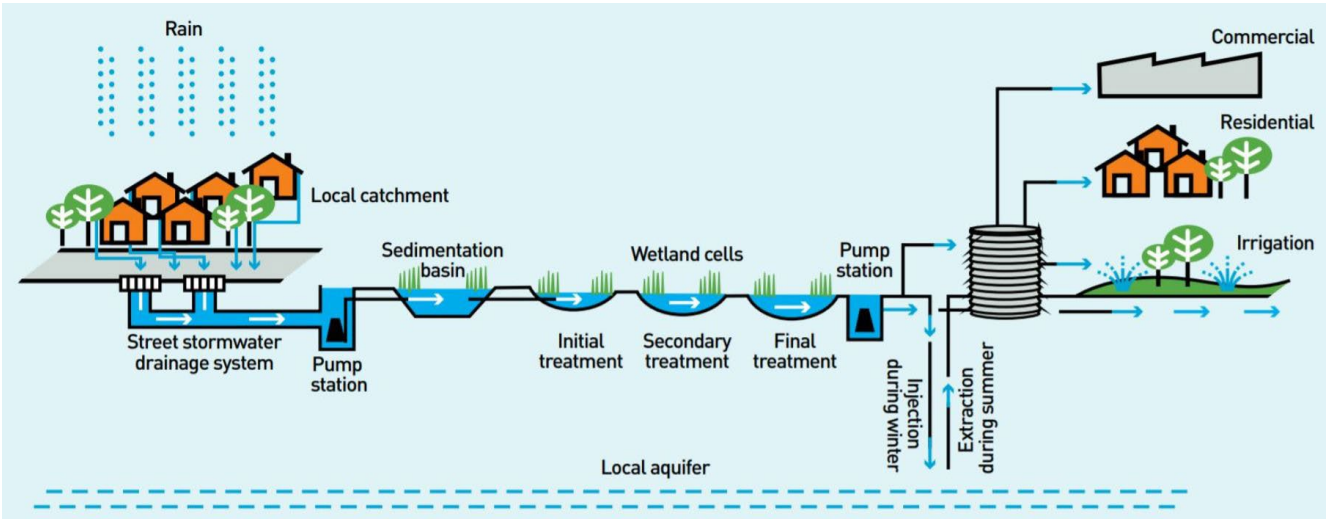

Figure 2-7: Typical MAR Storage SWH System (CRC, 2018)

2.2.4 Distribution

The distribution of a SWH system is dependent on the end-use and end-user of the treated stormwater. There are two non-potable distribution categories, namely open space irrigation (sprinkler irrigation for parks, open spaces, golf courses etc.) and dual reticulation systems (non-potable distribution systems) (L. Fisher-Jeffes, 2015). The dual reticulation systems introduce a 'third pipe' that can supply non-potable water to households and industries (Rohrer, 2017).

Potable water SWH systems can utilise the existing water distribution systems in urban areas to distribute the water to households and industries. The water quality of the cleaned stormwater from the SWH system becomes critical in order not to contaminate the potable water already in the system and in order not to contaminate the distribution network pipe infrastructure.

2.2.5 SWH Components Considered

The SWH components considered in this research are the collection, storage and distribution components as the research is primarily concerned with the water quantity component of SWH. The treatment component was not considered due to time constraints and the focus on water quantity. The collection component was addressed with the coarse models where the ideal locations for harvesting where identified. The storage and distribution components where addresses with the detailed models where the reliability of the system is dependent on the storage and the demand to which the system distributes.

3. STUDY AREA

3.1 Location & Population

The project area is the Upper Jukskei River Catchment in Johannesburg, South Africa. The location of the project area in South Africa is shown in **Figure 3-1**. Johannesburg is situated in Gauteng province and is South Africa's largest city. It is situated North-Eastern part of South Africa and is also the financial capital of the country, housing the finance, industrial and mining sectors (Mahlasela et al., 2020).

Johannesburg was formed due to the discovery of gold in the Witwatersrand and is known alternatively as eGoli, meaning 'the Place of Gold' in isiZulu. Johannesburg is one of the largest cities that is not located adjacent to the sea, a river or a lake and is also situated on a major watershed caused by the Witwatersrand, where it divides the water that flows to the Indian Ocean in the East and the Atlantic Ocean in the West (Turton et al., 2007).

Johannesburg has a population of about 5.5 million, and houses approximately 10% of South Africa's population. The population growth rate has declined from 3.5% to 2.4% since 2011 (COGTA - JHB Profile, 2020).

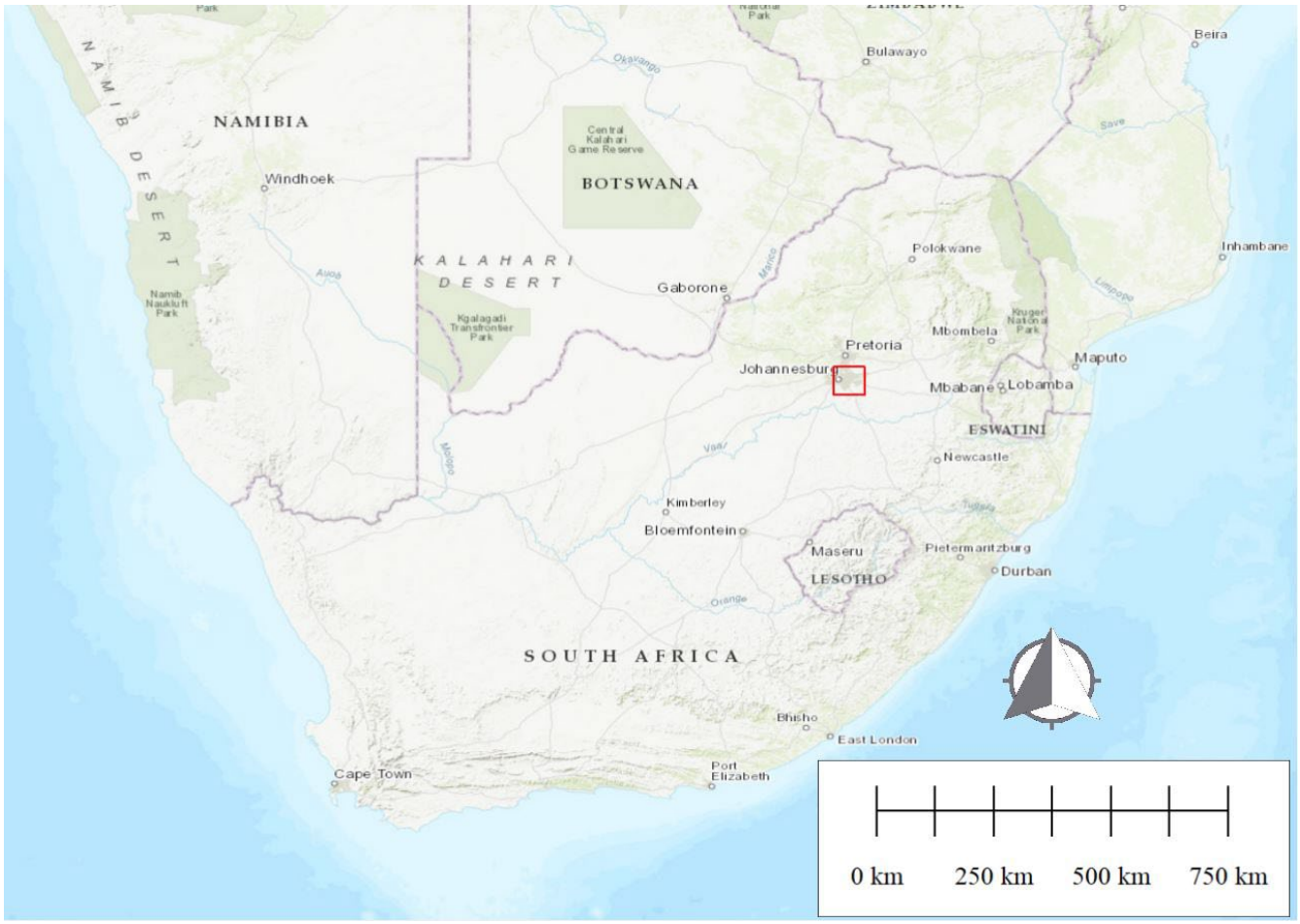

Figure 3-1: Project Area in South Africa

Johannesburg has the largest human made forest in the world (Turton et al., 2007), with an estimated 6 million trees, of which 1.2 million trees are in parks and on pavements and 4.8 million trees in private gardens.

The Upper Jukskei River catchment project area of 241km² is shown in **Figure 3-2.** The case study catchment comprises of the upper third of the Jukskei quaternary catchment A21C that supplies water to the Hartebeesboort Dam. The research catchment forms part of the Limpopo Water Management Area (WMA).

The Jukskei River has its origins in the city centre of Johannesburg near Ellis Park Stadium (shown by the blue star) and flows parallel to the R24 road in a North-Easterly direction through the suburbs of Bruma and Morninghill until it reaches Gilooly's interchange. The Jukskei river then flows in a Northerly direction past the Linksfield interchange and continues in a Northerly direction through the suburb of Lombardy and then flows through Alexandra Township and Beccleuch. The Jukskei then has a confluence with the Modderfontein river before passing through Waterfall Estate and forming a confluence with the Braamfontein spruit at the outlet of the case study area.

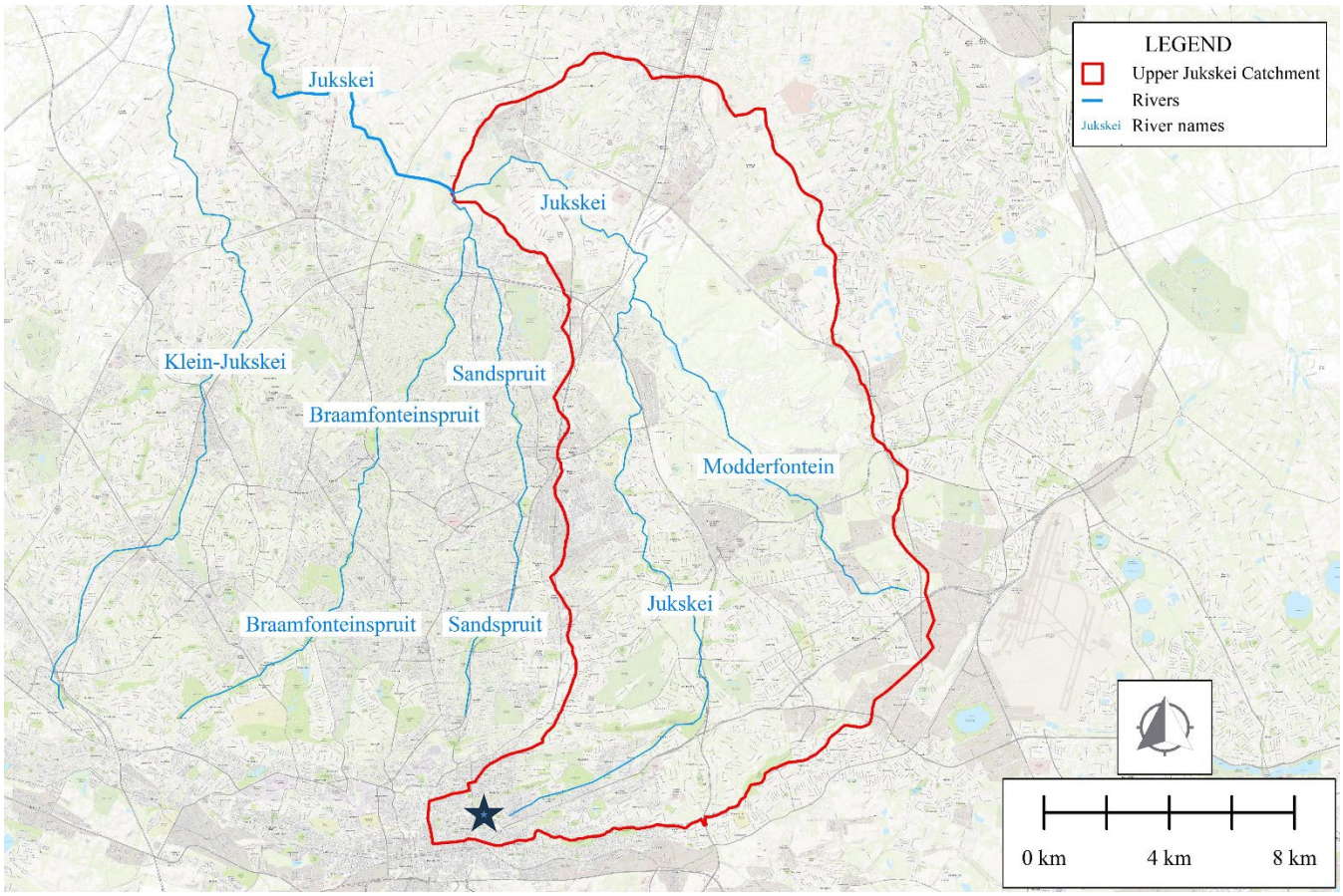

Figure 3-2: Upper Jukskei Catchment Area

3.2 Land Use & Land Cover

The land use and land cover has changed considerably in Johannesburg and the Jukskei catchment over the last few decades due to urbanisation. A Land Use Land Cover (LULC) change analysis of Johannesburg was performed from 2000 to 2016 by Verma et al. (2016) and they found that impervious surfaces had increased by 57.03%. Similarly, Mawasha & Britz (2022) conducted a land use and land cover change study of the Jukskei river catchment from 1987 to 2015 with Landsat 5 and Landsat 8 satellite data and found that the Jukskei river catchment has experienced considerable change in population and land use/land cover with an increase of built-up areas of 56.2% during this period.

The 2022 South African national land cover data of the upper Jukskei catchment is shown in **Figure 3-4**.

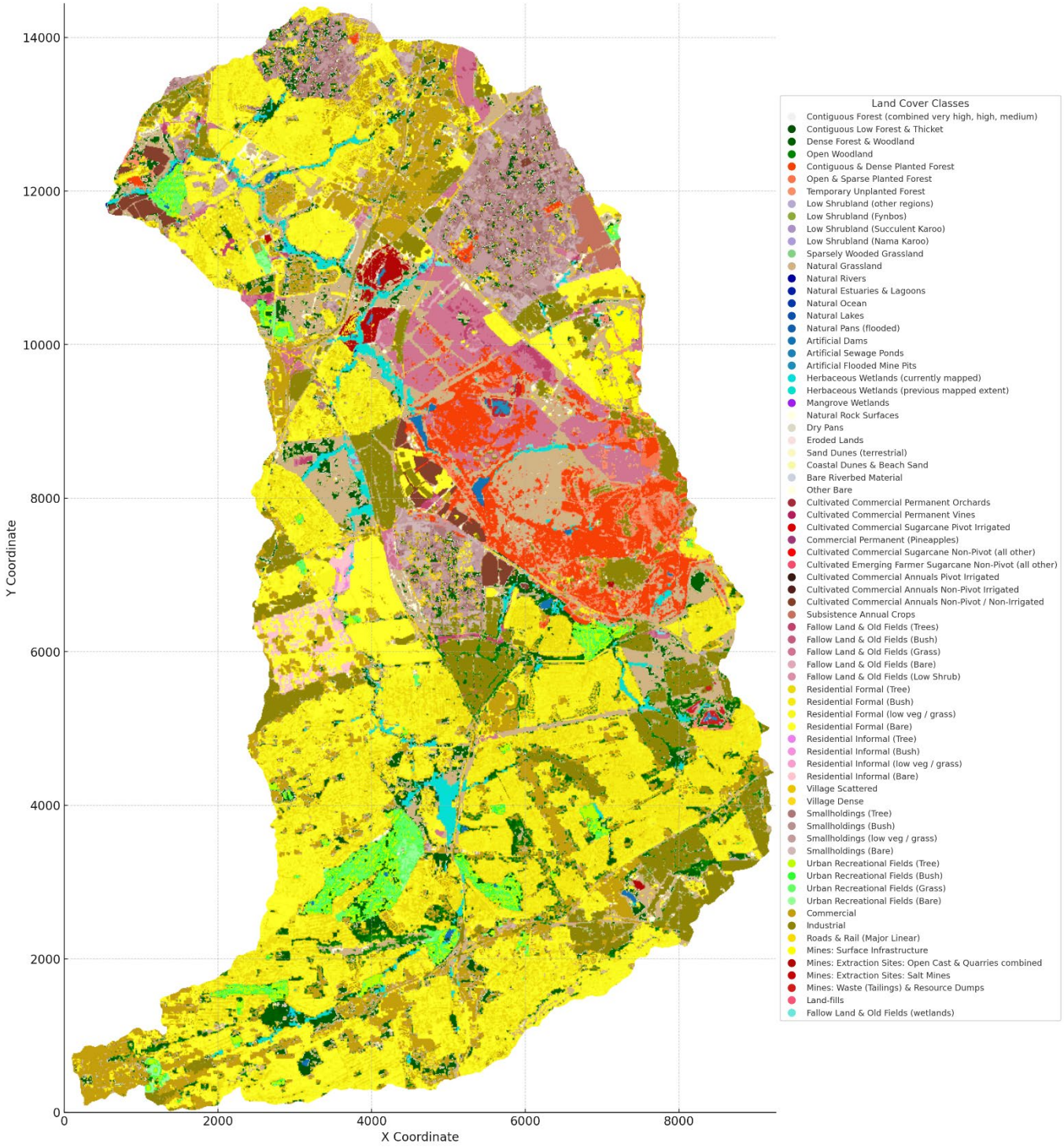

Figure 3-3: South Africa National Land-Cover Dataset 2022 – Upper Jukskei Catchment

A GIS analysis of the 2022 South African national land cover data shows that the catchment comprises of the following 10 largest land covers shown in **Figure 3-4**:

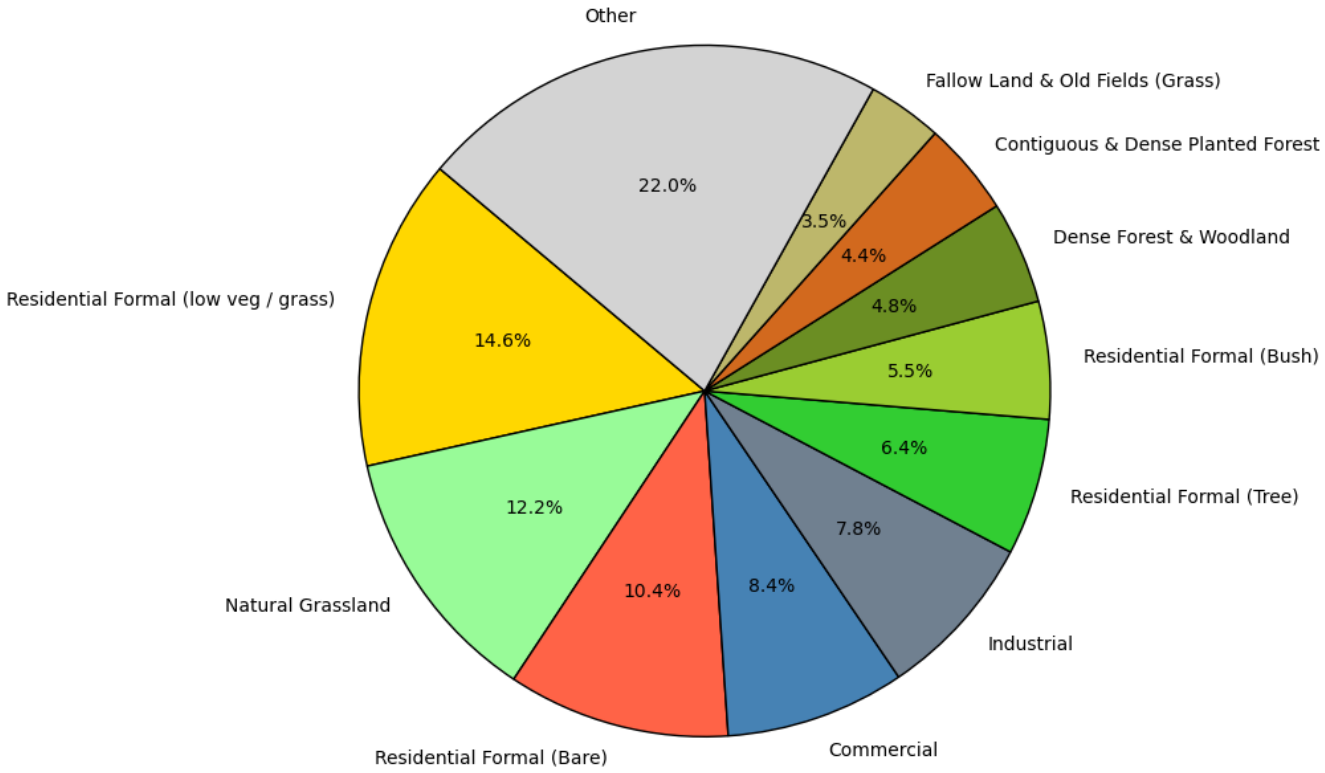

Figure 3-4: Dominant Land Cover Types in the Upper Jukskei Catchment

The increase in impervious surfaces and built-up areas in Johannesburg, as highlighted by Verma et al. (2016) and Mawasha & Britz (2022) leads to increased run-off volumes and higher peak flows. These hydrological changes create favourable conditions for SWH from a water quantity perspective as larger and more frequent run-off events make larger volumes of stormwater available for collection and re-use. **Figure 3-4** shows that 53.1% of the upper Jukskei catchment has land-uses that are associated with impervious surfaces and built-up areas (Residential, Commercial & Industrial) which indicates that the catchment has a high potential for stormwater harvesting.

3.3 Climate

Johannesburg is in a summer rainfall region that is characterised by a rainy season from October to March, with a Mean Annual Precipitation (MAP) in the order of 700mm with a typical number of 100 rain days annually (Dyson, 2009). The average daytime temperatures are 25 °C in summer and 17 °C in winter. The temperatures in winter occasionally drop below 0 °C and snow is a rare occurrence (Theeboom et al., 2009).

South Africa has been delineated into primary, secondary, tertiary and quaternary catchments that are part of a hierarchical structure of water management. The upper Jukskei catchment falls within quaternary catchment A21C with the following characteristics as per the South African Water Research Commission (Bailey & Pitman, 2015) :

- Mean Annual Precipitation (MAP): 682 mm
- Mean Annual Evaporation (MAE): 1700 mm
- Mean Annual Runoff (MAR): 59.11 mm

The upper Jukskei is therefore in negative water balance with the annual evaporation exceeding annual precipitation by 1018 mm, hence the need for alternative water supply options like SWH. Johannesburg has three main weather systems namely frontal cyclones, tropical cyclones and thunderstorm systems, with

thunderstorm systems being the most prevalent. Frontal systems are “cold fronts” that move up from the Western Cape in winter months and is characterised by low intensity rain over several days. Tropical cyclones from the Indian ocean seldomly push inland from the Eastern coast of South Africa and lead to rainfall events of 3 to 7 days which leads to severe flooding. Thunderstorms occur over the majority of South Africa and are characterised by a short duration in the order of minutes to hours and high intensity of rainfall, with storm cells often being accompanied by strong winds (Barnard et al., 2019).

3.4 Hydrology

The upper Jukskei catchment is a headwater subcatchment of the Crocodile River & Limpopo River catchments. The Jukskei river originates in the city centre of Johannesburg and ultimately discharges into the Hartebeespoort dam. The hydrology of the upper Jukskei catchment is highly influenced by urbanisation with the increased impervious surface area which typically leads to a reduction in infiltration and a flashier response to rainfall events (Kaur et al., 2019). Urbanisation has also led to the riverine system being highly modified with culverts, bridges & formalised canal sections evident when studying the Google Earth imagery.

A hydrological model study of the Jukskei river found that the effect of urban development has had 13 times increase in surface run-off from pre-development conditions and that in simplistic terms a flow of 2.9 million m^3/annum would be sufficient for ecological systems and river health and that ± 35.8 million m^3/annum could be available to other uses (Dunsmore, 2020).

4. METHODOLOGY

The methodology used in this assessment to identify the high-yielding Stormwater Harvesting (SWH) sites builds on the methodology used by Inamdar where a GIS based screening tool is used for locating and ranking of suitable stormwater harvesting sites in urban areas (Inamdar et al., 2013). This assessment builds on the work of Inamdar by defining the pervious and impervious areas on a finer resolution, by incorporating a hydrological and hydraulic model and by considering non-potable water demand.

The workflow of this assessment is shown in **Figure 4-1** and **Figure 4-2**. The methodology to setup the integrated model is shown in **Figure 4-1** and has 4 large blocks, namely, watershed delineation, hydrological model parameters, model forcing & water demand. The methodology for the collection models to determine the SWH rankings as well as the storage and distribution models is shown in **Figure 4-2.**

The methodology was executed in the software program PCSWMM which utilises the United States (US) Environmental Protection Agency (EPA) Surface Water Management Model (SWMM) to do the integrated hydrological & hydraulic modelling. SWMM is used primarily in urban areas and can model both single events and long-term continuous rainfall. SWMM is a dynamic rainfall-runoff modelling software that can model the hydrology, hydraulics and water quality (*SWMM | US EPA*, n.d.).

PCSWMM uses the SWMM engine and includes GIS tools and scripting functionality as part of an improved graphical user interface & post processing of SWMM. PCSWMM was chosen as the software to do the modelling for this research due to its strong capability in integrating GIS, scripting, hydrological & hydraulic modelling. The PCSWMM model can also be viewed in the freeware SWMM as provided by the US EPA. A detailed description of PCSWMM and the hydrology and hydraulic components are attached as **ANNEXURE A**. A detailed description of the methodology is attached as **Annexure B**.

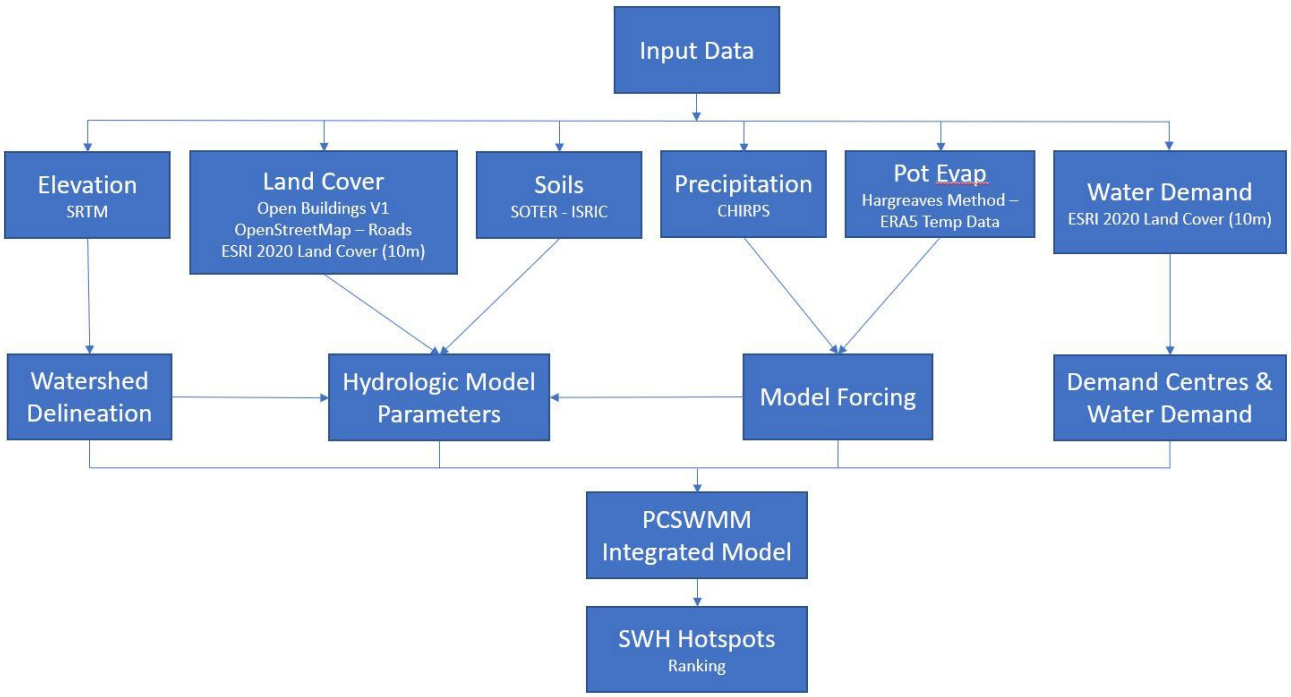

Figure 4-1: Workflow to Identify SWH Hotspots

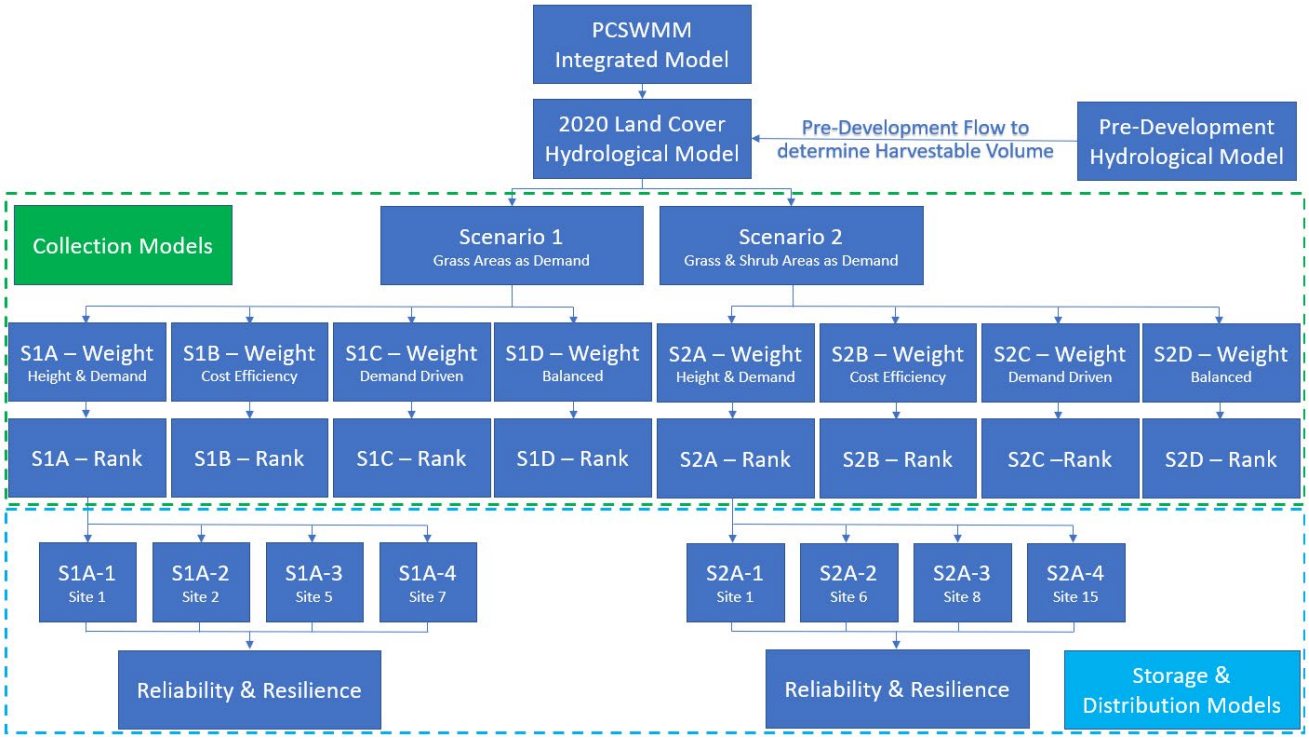

Figure 4-2: Workflow for Collection, Storage & Distribution Models

4.1 Watershed Delineation

The watershed delineation is done with the SRTM DEM data in PCSWMM with the Watershed Delineation Tool (WDT). The program then uses the D8 method to determine the subcatchments and generates a pit filled DEM, flow direction grid, flow accumulation grid, watershed areas and stream network. The subcatchments attributes of area, slope and flow length are calculated automatically from the created WDT layers. The conduits and their correct connectivity as well as the nodes and their invert elevations corresponding to the DEM are automatically defined in the program. The subcatchments are also automatically assigned to their outflow node. The watershed delineation of the upper Jukskei catchment is shown in **Figure 4-3** below.

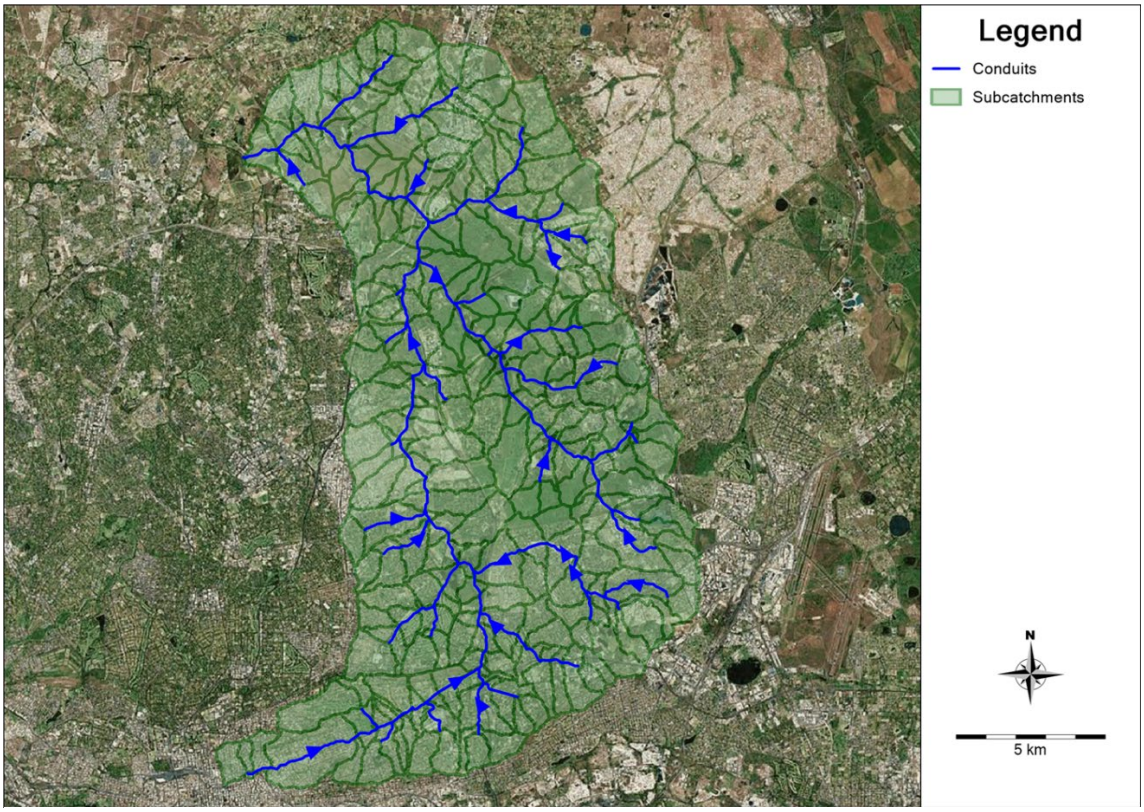

Figure 4-3: Upper Jukskei Catchment Watershed Delineation

4.2 Hydrological Parameters

The following hydrological parameters were determined for the model:

- Impervious Area (%)
- Impervious Area with No Depression Storage (%)
- Depression Storage for the Pervious Area (mm)
- Depression Storage for the Impervious Area (mm)
- Manning n for Pervious Area
- Manning n for Impervious Area
- Infiltration Parameters:
  - SCS Curve Number:
    - Curve Number (-)
    - Drying Time (Days)
- Area (Ha)
- Flow Length (m)
- Slope (%)

The Area, Flow Length & Slope were calculated as part of the watershed delineation as discussed in **Section 4.1**. The remaining SWMM hydrology input parameters were derived from the land-use and soils maps through spatial weighting (area weighting). The workflow for the hydrological parameter determination is shown below in **Figure 4-4.**

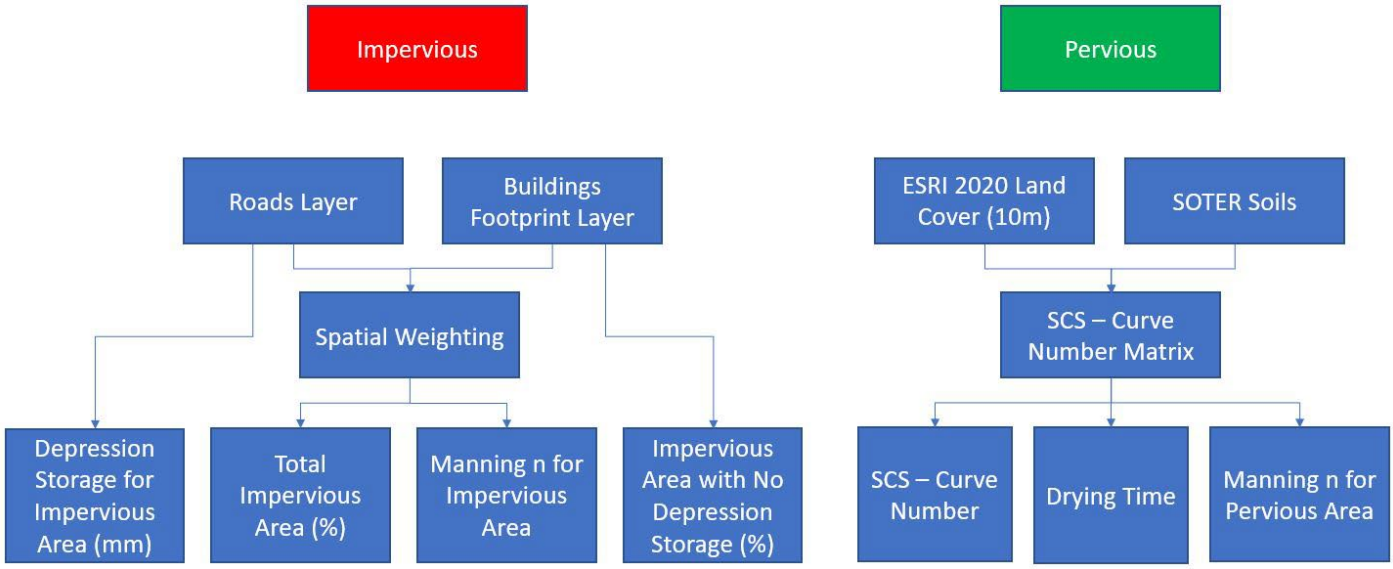

Figure 4-4: Hydrological Model Parameter Determination

4.2.1 Impervious Area

The impervious areas of the model were defined by the roads and the buildings footprint/roofs layers as is shown in **Figure 4-5** below for the Upper Jukskei Catchment. The impervious area of each subcatchment was calculated as the total area of roads and buildings within subcatchment and was calculated with spatial weighting. The pervious area was calculated as the remaining area within the subcatchment.

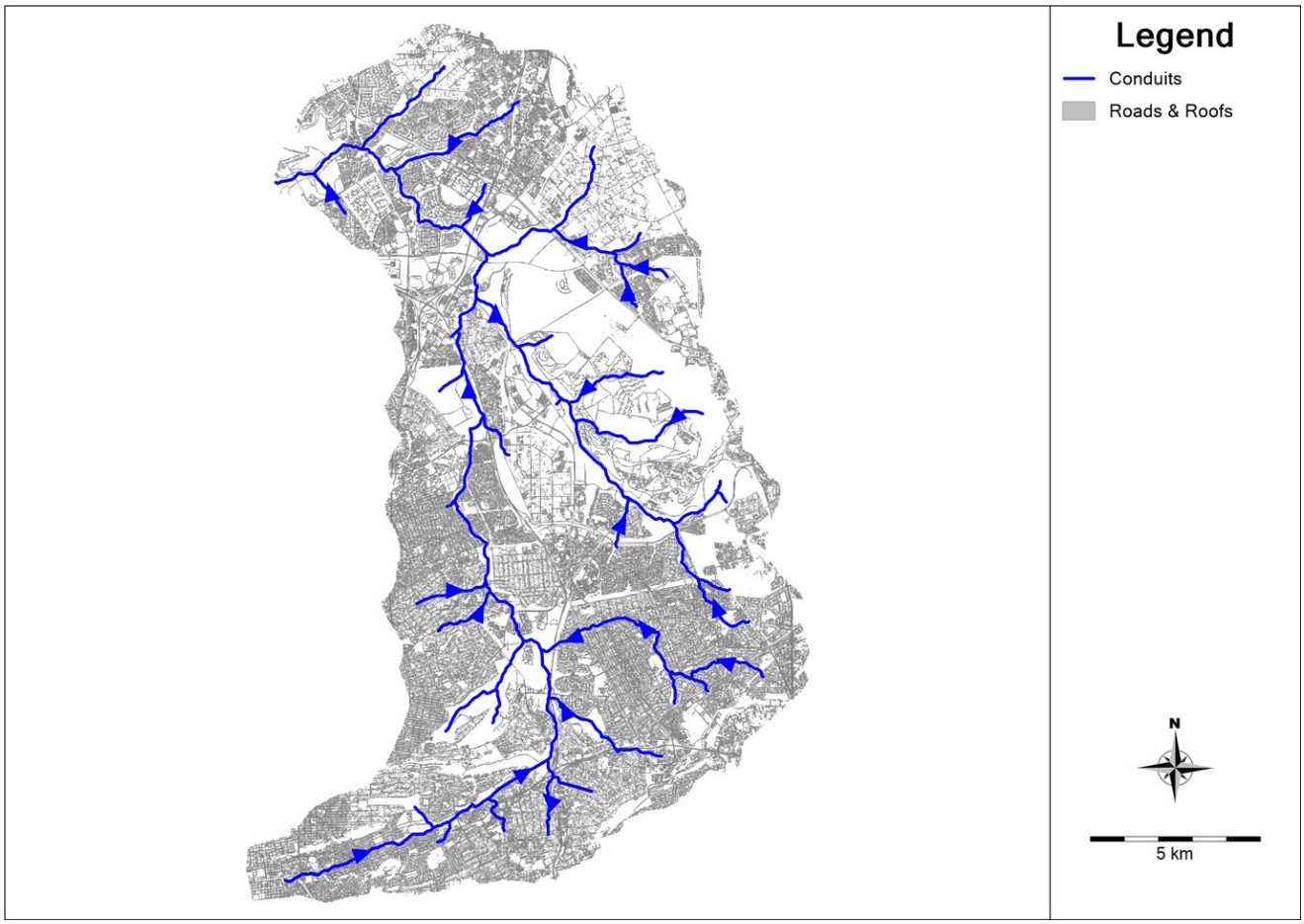

Figure 4-5: Roads & Roofs Layer

4.2.2 Depression storage

Depression storage can visually be observed in parking lots and on roads where localised puddles occur that need fill up before run-off can occur. Steep pitched roofs are an example of impervious areas with no depression storage. The impervious area with no depression storage was taken as 40% of the roofs in the subcatchment and was calculated with spatial weighting from the roofs/buildings layer. This is an assumption that was made based on visual observation from the satellite images. This can be further investigated in future studies. The depression storage figures used in the model are based on the 1992 ASCE paper "Design and construction of urban stormwater management systems" (ASCE, 1992). The depression storage values used in the model for the various land uses are:

- Impervious Areas:
  - Roads: 2 mm
  - Pitched Roofs: 1.25 mm
- Pervious Areas:
  - Water: 0 mm
  - Trees: 4 mm
  - Grass: 2.5 mm
  - Flooded Areas: 6 mm
  - Crops: 5 mm
  - Shrub: 5 mm
  - Built Up: 2.5mm
  - Bare Ground: 2 mm

4.2.3 Manning n – Overland Flow

The Manning n overland flow values for the pervious and impervious areas are based on the Table in **Annexure C** from SWMM hydrology manual (Rossman & Huber, 2016), which is based on studies done by Crawford & Lindsey (1966), Engman (1986) and Yen (2001). The Manning n overland flow values used in the model for the various land uses are:

- Impervious Areas:
  - Roads: 0.015
  - Roofs: 0.013
- Pervious Areas:
  - Water: 0.010
  - Trees: 0.090
  - Grass: 0.075
  - Flooded Areas: 0.150
  - Crops: 0.100
  - Shrub: 0.120
  - Built Up: 0.075
  - Bare Ground: 0.030

4.2.4 SCS Curve Number

The curve numbers typically given in the USDA manuals lump the pervious and impervious areas together for urban land cover situations. The curve number is therefore representative of both the impervious and pervious potions of the subcatchment.

SWMM does calculations for the pervious and impervious portions of the subcatchment separately before routing them both to the outlet of the subcatchment and determining the combined outflow hydrograph. Therefore, if the subcatchment is partitioned into impervious and pervious areas it is of particular importance to the modeller that the curve number assigned to the subcatchment must be representative of the pervious section of the subcatchment only, as SWMM uses the curve number for the infiltration calculations (Rossman & Huber, 2016).

The SCS curve numbers often found in curve number tables are for “normal” or “average” antecedent moisture conditions (AMC II). Adjustments can be made for AMC I (low moisture) and AMC III (high moisture) conditions. AMC I curve numbers were used in this assessment as recommended by the SWMM reference manual for continuous simulations.

The SCS curve numbers were determined from a ERSI 2020 land-cover and SOTER soils matrix. The SOTER soils FAO soil drainage classes, shown in **Figure 4-6,** were translated to SCS soil groups as shown below in **Table 4-1**.

Table 4-1: FAO Drainage Class to SCS Soil Group

FAO Soil Drainage Class	SCS Soil Group
Excessively Drained	A
Somewhat excessively drained	
Well drained	B
Moderately well drained	C
Imperfectly drained	
Poorly drained	D
Very Poorly Drained	

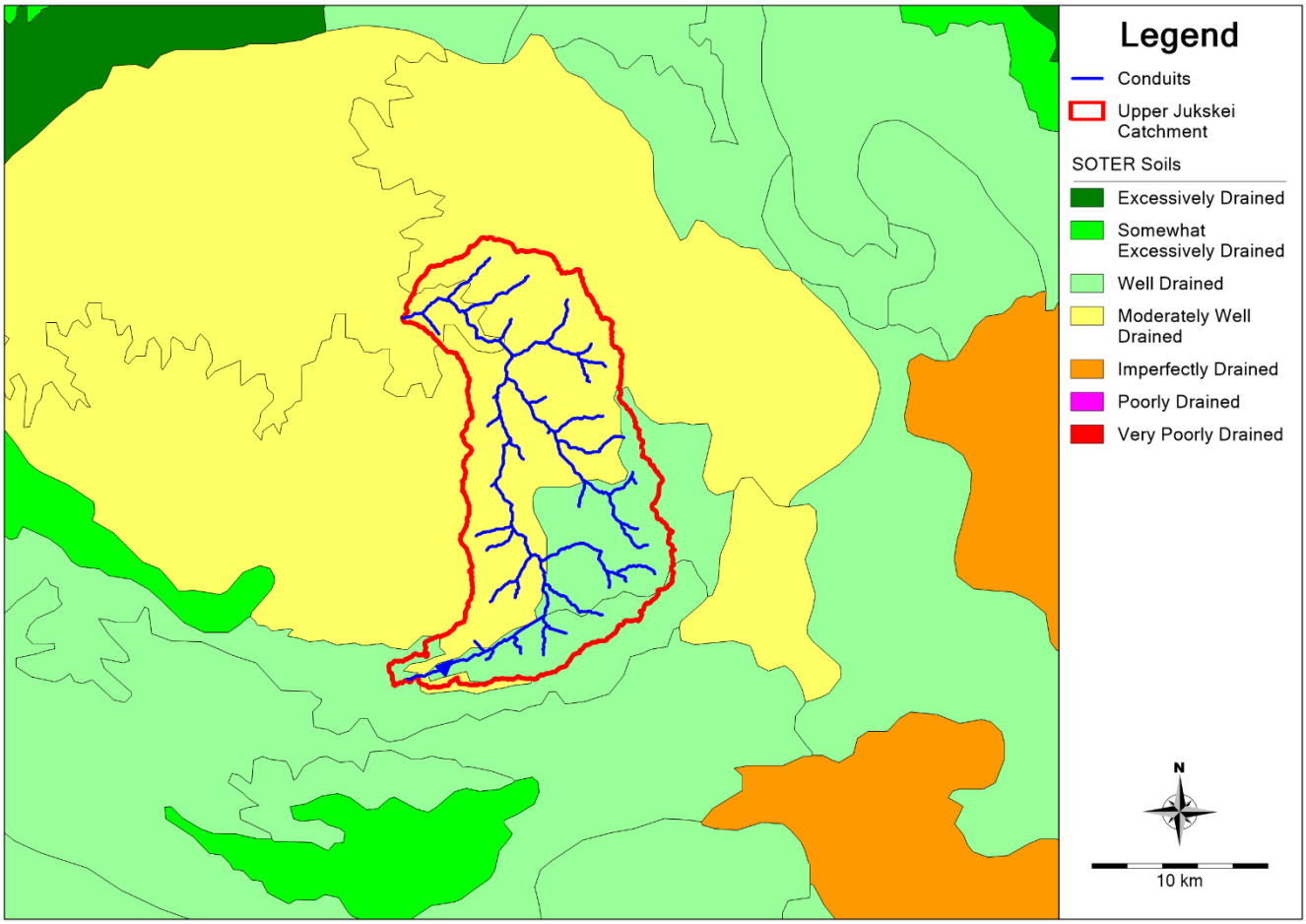

Figure 4-6: SOTER Soils - FAO Drainage Classes

The SCS-CN_I for the ESRI Land Cover classes is shown in **Table 4-2**. The SCS-CN_I values that were used in the model are shown in **Figure 4-7**.

Table 4-2: SCS-CNI for 2020 ESRI Land Cover Classes

ESRI Land Cover	Hydrological Soil Group			
	A	B	C	D
Water	95	95	95	95
Trees	18	38	48	56
Grass	29	48	61	69
Flooded Vegetation	15	35	45	52
Crops	42	54	66	70
Shrub	26	45	58	67
Built Up	35	52	63	74
Bare Ground	52	66	74	77

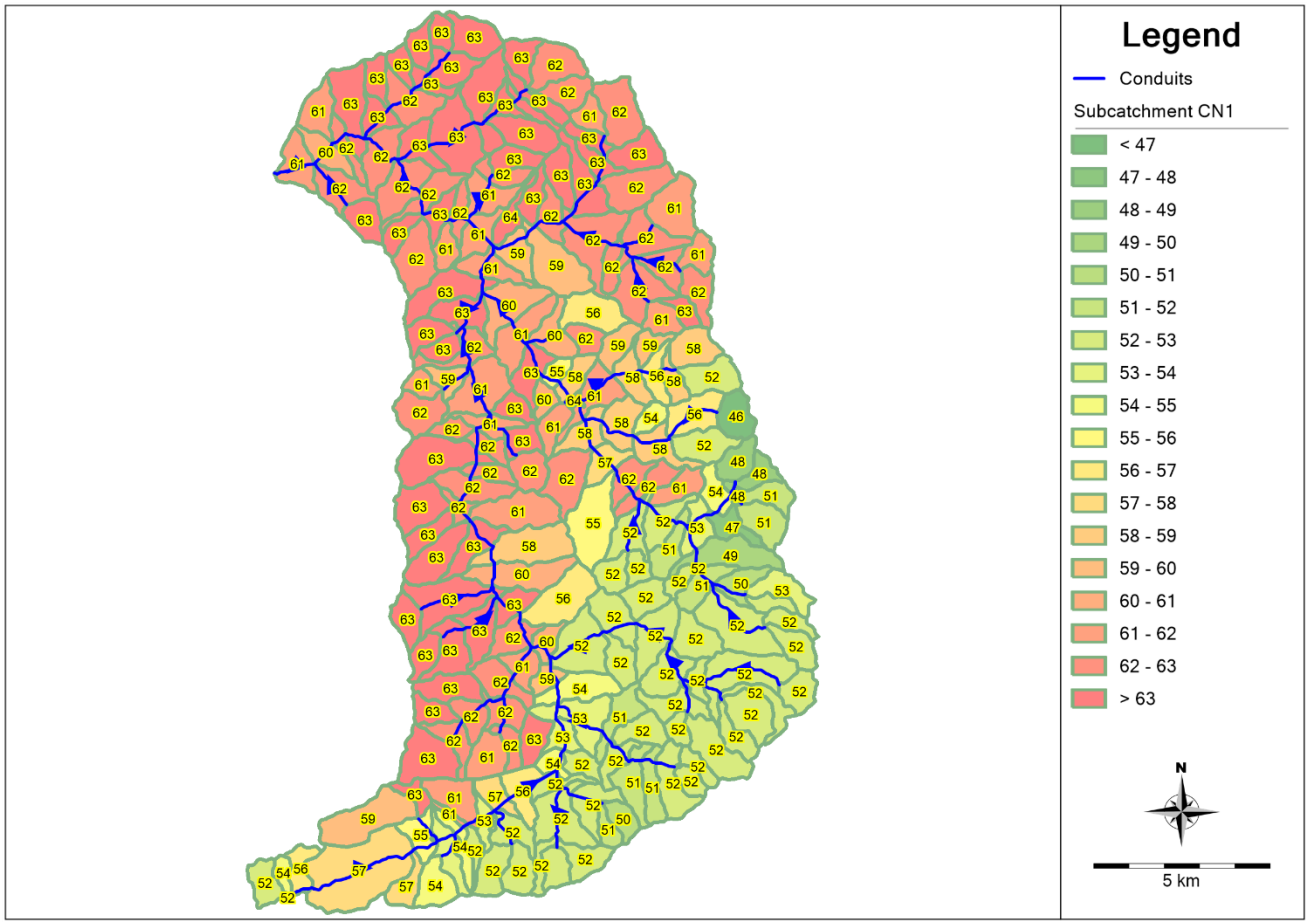

Figure 4-7: Upper Jukskei Catchment – SCS-CNI Curve Numbers

4.2.5 Drying Time

The drying time is related to the soil's saturated hydraulic conductivity Ks (mm/hr). The soil hydraulic conductivity was determined from the SANRAL permeability rates of the four hydrological soil groups and used to calculate the drying time of each soil group as follows:

- Soil Group A: 5.71 days
- Soil Group B: 6.60 days
- Soil Group C: 9.86 days
- Soil Group D: 13.81 days

4.3 Model Forcing

4.3.1 CHIRPS Rainfall

The CHIRPS rainfall has a gridded spatial resolution of 0.05° where the data is available from 1981 to present and produces daily precipitation estimates. The rainfall record used in this study is from 1981 to 2021 (41 years) where the rainfall from each of the 0.05° grids is assigned to the subcatchment below it. The 0.05° grids over the Upper Jukskei Catchment are shown in **Figure 4-8**.

4.3.2 Hargreaves Potential Evaporation

The Hargreaves Potential Evaporation is calculated by PCSWMM based on the method set out in Hargreaves et al., 1998. The method utilises the daily maximum and minimum temperatures as well as the study site latitude, to determine the extra-terrestrial radiation, in the calculation of the potential evaporation. ERA5 reanalysis data with a spatial resolution of 0.25° was used to determine the daily maximum and minimum temperatures.

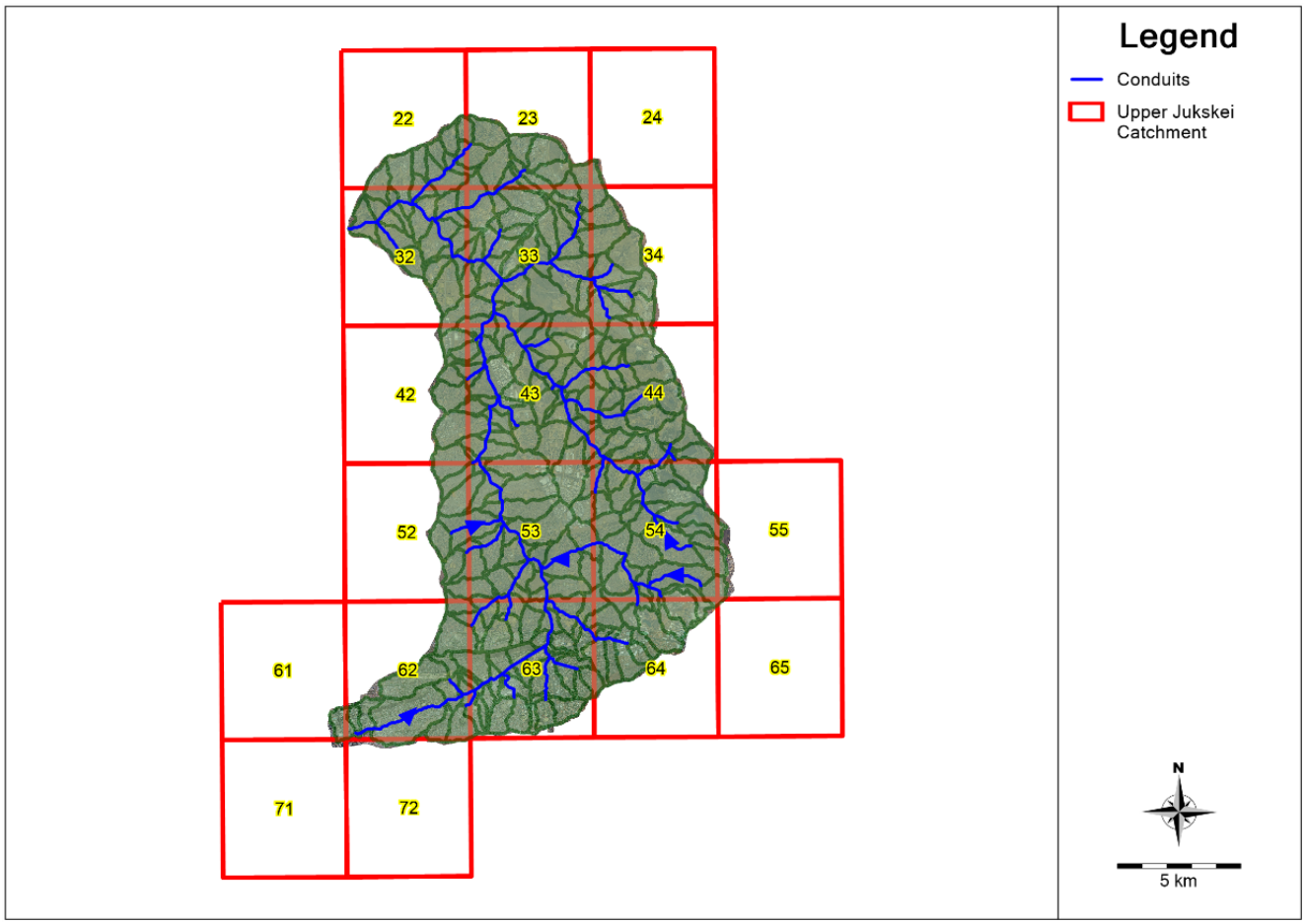

Figure 4-8: CHIRPS Rainfall 0.05° Grids

4.4 Harvestable Inflow

The harvestable volume is determined by simulating the flows of the 2020 land cover hydrological model and subtracting the pre-development flows from the pre-development hydrological model. The pre-development flow (environmental flow) is determined by taking the 2020 land cover hydrological model and converting all the subcatchments to be 100% pervious to represent the pre-development situation, where no built-up areas and impervious surfaces are present. This is represented visually in **Figure 4-9.** The harvestable volume is visually represented by the difference in the run-off arrows of the two subcatchments shown in **Figure 4-9.**

The harvestable volume is then determined by taking the total runoff over the simulation for the 2020 land cover hydrological model and subtracting the total runoff from the pre-development model. This gives a broad understanding of the harvestable volume although it does not take into considerations the time dynamics of the harvestable volume.

The total harvestable volume is then divided by the total number of simulation years to determine the average annual harvestable volume in Mℓ/annum.

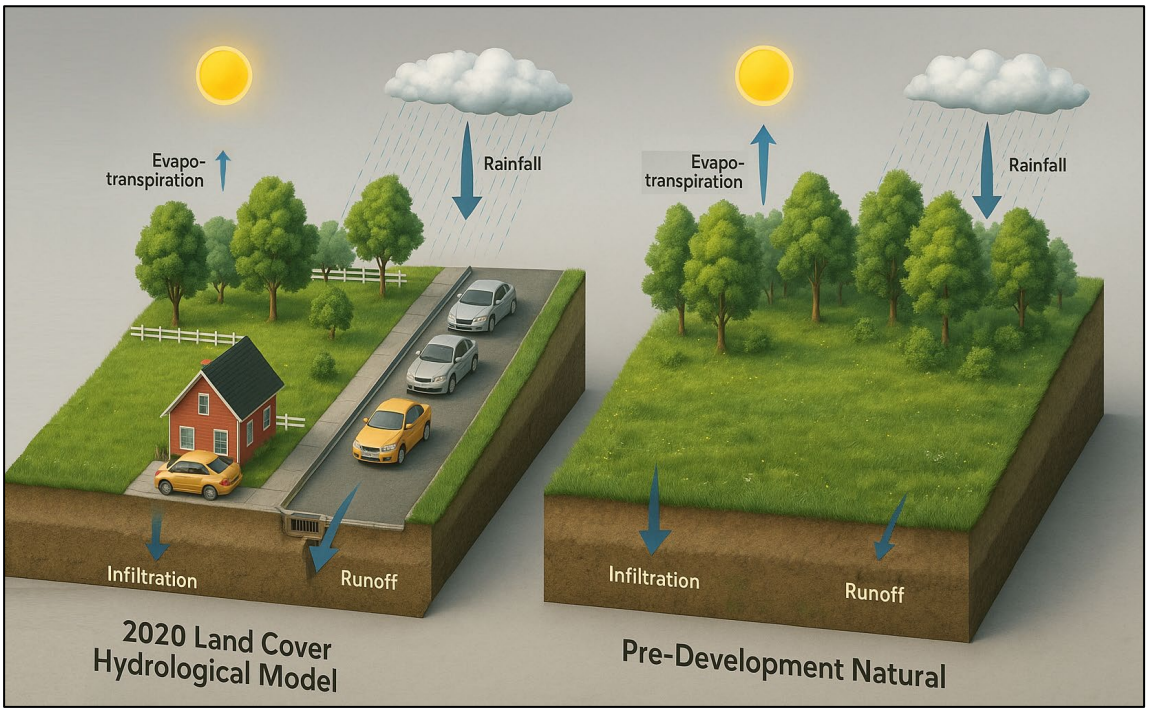

Figure 4-9: Visual Representation of 2020 Hydrological Model & Pre-Development Hydrological Model (Adapted (Computational Hydraulics International (CHI), n.d.-b).

4.5 Demand Areas

Two sperate analyses were done in terms of demand areas. One where the Grass Land Cover was considered as the only applicable demand area (**Scenario 1**). The second where Grass and Shrub Land Cover Areas were considered as demand areas (**Scenario 2**). The demand areas were disregarded if they were outside of a 500m radius from the SWH junction and if they were higher than 10m above the SWH junction.

The demand areas are visually shown as the blue highlighted areas in **Figure 4-10** and **Figure 4-11** for scenario 1 and scenario 2 respectively. The grass areas are shown by the green polygons, and the shrub areas are shown by the orange polygons. The areas that are outside of the 500m radius are not considered as demand areas. If the demand areas have a minimum elevation that is higher than 10m above (>=1654.02 m) the elevation of the SWH junction (1644.02 m in the below example) then the demand areas are also disregarded. In the examples shown in **Figure 4-10** and **Figure 4-11** all of the demand areas that where within 500m had minimum elevations within the 10m threshold.

The shrub areas are more prevalent in the Eastern part of the Jukskei Catchment, and correspond with undeveloped land, with one very large shrub area centrally located within the catchment with a total size of 18 059 986m². The grass areas correspond to golf courses, public parks & sports fields.

4.6 SWH Sites

The minimum area needed for a stormwater harvesting plant was determined from various SWH facilities that have been built in Australia. It was found that the minimum area needed is roughly 2500m². The larger the area that is available, the larger the storage and re-use facilities can be and subsequently more of the demand can be satisfied. A larger available area could also lend itself towards on-surface storage whereas with limited space, below surface options might need to be considered which in turn increases costs. The grass and shrub areas within a 500m radius were used to determine the area available for a SWH plant.

Figure 4-10: Grass Demand Areas within 500m Radius shown as blue highlighted polygons (Scenario 1)

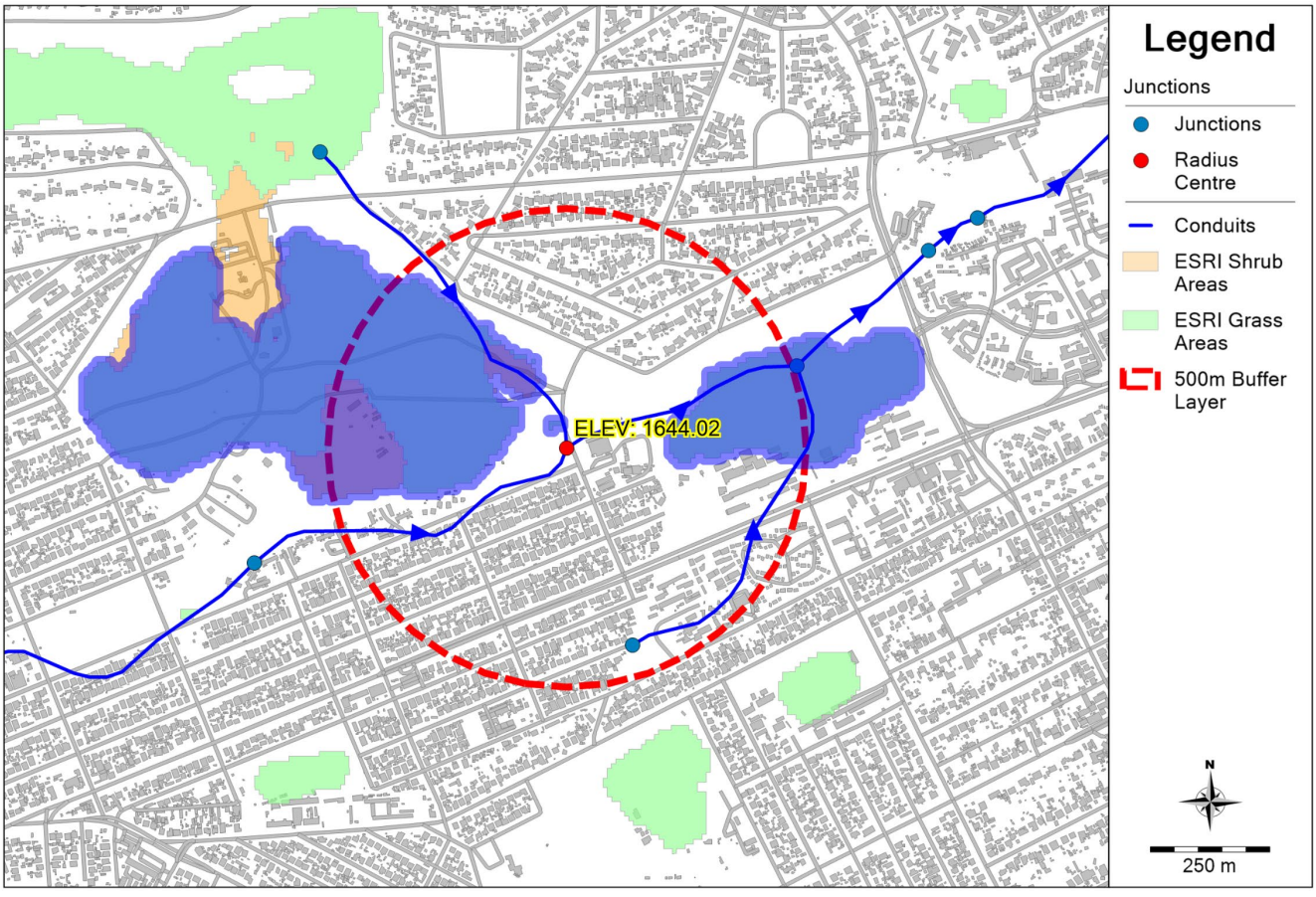

Figure 4-11: Grass and Shrub Areas within 500m Radius shown as blue highlighted polygons (Scenario 2)

4.7 Collection Models - SWH Site Metrics

Several metrics were determined and given weightings towards determining the best potential stormwater harvesting sites. The metrics that were included are shown below:

- Weighted Horizontal Distance (ΔX)
- Weighted Vertical Distance (ΔZ)
- Non-Potable Water Demand
- Ratio of Harvestable Volume to Demand
- Largest Area available for SWH Plant

The above metrics were adapted from Inamdar (2013) and the vertical distance and largest area available for a SWH plant were added after consultation with several stormwater academia and industry professionals. Inamdar (2013) used the following metrics in his assessment:

- Radius of Influence
- Harvestable Run-Off
- Demand
- Ration Run-off to Demand
- Weighted Distance

The weightings of Variation A were discussed with several academics and industry professionals, and a balance of inputs was used as the final weighting. The weighting of variations B to D were added by the researcher to find a balance for each objective stated in **Table 4-3** and to gauge if the SWH site locations would change considerably from Variation A.

Table 4-3: Collection Model Site Metric Weightings

Criteria	Variation A: Height & Demand	Variation B: Cost Efficiency	Variation C: Demand Driven	Variation D: Balanced
Weighted Horizontal Distance (ΔX)	15%	30%	10%	25%
Weighted Vertical Distance (ΔZ)	40%	40%	15%	25%
Non-Potable Water Demand	30%	15%	40%	20%
Ratio of Harvestable Volume to Demand	10%	10%	30%	20%
Largest Area Available for SWH Plant	5%	5%	5%	10%

Variation A: Emphasis is given to the height and demand with 70% of the weighting. This places and emphasis on possible gravity feed schemes and towards larger demand areas.

Variation B: Construction and Operations and Maintenance costs rise sharply with pipe lengths and pumping head. This led to the 70% weighting of Weighted Horizontal Distance and Weighted Vertical Distance.

Variation C: Demand and the Ratio of Harvestable Volume to Demand have a combined weighting of 70%. This puts the emphasis on supplying the largest demand and also having sufficient volumes of water available to supply the demand.

Variation D: A balanced mixture of weightings to remove any subjectivity and to balance costs and demand.

4.7.1 Weighted Horizontal Distance (ΔX)

The weighted horizontal distance is an indication of the horizontal distance from the SWH site to the demand areas and represents the cost practicalities of conveying the water horizontally across the landscape. The weighted horizontal distance is calculated as shown below in **Equation 1**:

$$\Delta X = \frac{\sum_{i=1}^{n}(xi.\,Ai)}{\sum_{i=1}^{n} A\,i} \qquad [1]$$

- ΔX = Weighted Horizontal Distance (m)
- xi = Horizontal Distance to Demand Area (m)
- Ai = Surface Area of Demand Area (m²)

The weighted horizontal distance is therefore a proxy for the pipe lengths that will need to be installed from the SWH site to the demand areas. The closer the SWH site is to the demand area the more economically advantageous it is, as shorter pipe lengths will need to be installed to the demand area.

Longer horizontal distances increase the infrastructure requirements and may introduce complexities in system design. By minimising the horizontal distance between the SWH site and the demand areas, material costs, land disruption and maintenance is reduced.

4.7.2 Weighted Vertical Distance (ΔZ)

The weighted vertical distance is an indication of the vertical distance from the SWH site to the demand areas and represents the cost practicalities of conveying the water vertically across the topography. The weighted vertical distance is calculated as shown below in **Equation 2**:

$$\Delta Z = \frac{\sum_{i=1}^{n}(zi.\,Ai)}{\sum_{i=1}^{n} A\,i} \qquad [2]$$

- ΔX = Weighted Vertical Distance (m)
- zi = Vertical Distance to Demand Area (m)
- Ai = Surface Area of Demand Area (m²)

The vertical distance determines whether the system can be gravity fed or if pumping is required. The weighted vertical distance is therefore a proxy for the energy that will be needed to transfer the water from the SWH site to the demand area. The higher the demand area is above the SWH site the higher the capital cost for pumps and the higher the ongoing operational cost of electricity. The ideal situation is where the demand area can be supplied under gravity feed conditions, and no energy is needed.

The vertical distance has a significantly higher feasibility and operational cost than the weighted horizontal distance as is illustrated below for a pumping system:

Pumping System:

- Ø315ND HDPE Class PN16 Pipe
- Flow: 50 l/s
- 263m of Horizontal Distance equals 1m in Dynamic Head Loss
- 10m of Vertical Distance (Static Head) is therefore equal to 2630m of Horizontal Pipe in the system.

4.7.3 Non-Potable Water Demand

The non-potable water demand for this assessment was determined in CROPWAT by considering a grass that is planted in loamy soil in Johannesburg and its water demand during the warmer months of October to March as it assumed that irrigation is not applied during the colder winter months. The evaporation and rainfall data were used from the pre-defined station available for Johannesburg in CROPWAT. It is recommended that for each assessment the water demand be calculated for local conditions with CROPWAT as the rainfall period and irrigation period could have a mismatch. The total gross irrigation demand that was calculated is 290.1mm as is shown in **Figure 4-12.** This equates to 2.917 Mℓ/Ha/annum and was rounded up to 3 Mℓ/Ha/annum. Inamdar (2013) used a non-potable water demand of 2 Mℓ/Ha/annum for the demand of the city parks in Melbourne, Australia.

The total water demand was therefore calculated by calculating the total area of all the applicable demand areas and then multiplying the area with 3 Mℓ/Ha/annum to determine the annual water demand.

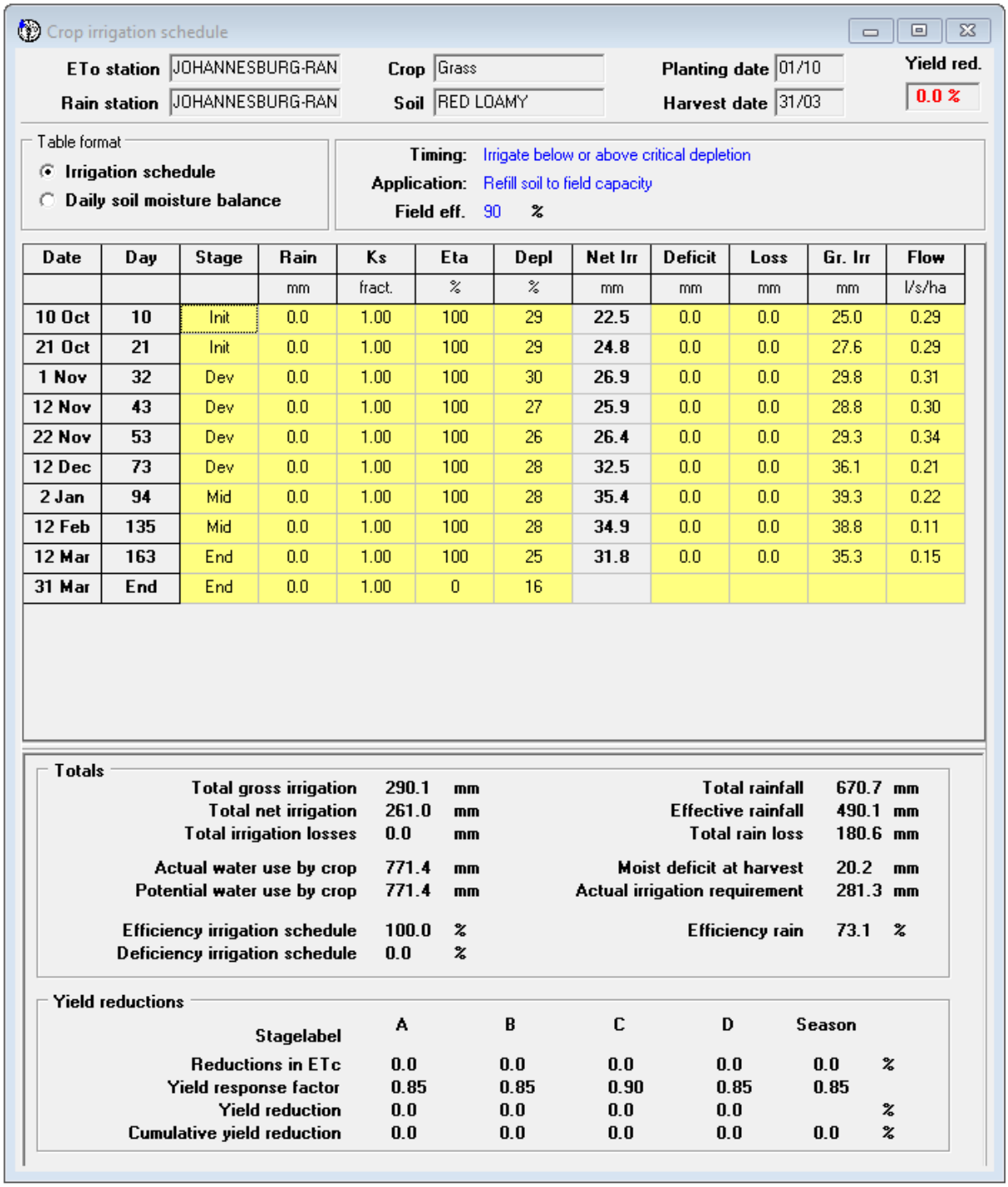

Crop irrigation schedule

ETo station: JOHANNESBURG-RAN | Crop: Grass | Planting date: 01/10 | Yield red.: 0.0 %

Rain station: JOHANNESBURG-RAN | Soil: RED LOAMY | Harvest date: 31/03

Table format: (•) Irrigation schedule ( ) Daily soil moisture balance

Timing: Irrigate below or above critical depletion

Application: Refill soil to field capacity

Field eff.: 90 %

Date	Day	Stage	Rain	Ks	Eta	Depl	Net Irr	Deficit	Loss	Gr. Irr	Flow
			mm	fract.	%	%	mm	mm	mm	mm	l/s/ha
10 Oct	10	Init	0.0	1.00	100	29	22.5	0.0	0.0	25.0	0.29
21 Oct	21	Init	0.0	1.00	100	29	24.8	0.0	0.0	27.6	0.29
1 Nov	32	Dev	0.0	1.00	100	30	26.9	0.0	0.0	29.8	0.31
12 Nov	43	Dev	0.0	1.00	100	27	25.9	0.0	0.0	28.8	0.30
22 Nov	53	Dev	0.0	1.00	100	26	26.4	0.0	0.0	29.3	0.34
12 Dec	73	Dev	0.0	1.00	100	28	32.5	0.0	0.0	36.1	0.21
2 Jan	94	Mid	0.0	1.00	100	28	35.4	0.0	0.0	39.3	0.22
12 Feb	135	Mid	0.0	1.00	100	28	34.9	0.0	0.0	38.8	0.11
12 Mar	163	End	0.0	1.00	100	25	31.8	0.0	0.0	35.3	0.15
31 Mar	End	End	0.0	1.00	0	16					

Totals

Total gross irrigation	290.1	mm	Total rainfall	670.7	mm
Total net irrigation	261.0	mm	Effective rainfall	490.1	mm
Total irrigation losses	0.0	mm	Total rain loss	180.6	mm
Actual water use by crop	771.4	mm	Moist deficit at harvest	20.2	mm
Potential water use by crop	771.4	mm	Actual irrigation requirement	281.3	mm
Efficiency irrigation schedule	100.0	%	Efficiency rain	73.1	%
Deficiency irrigation schedule	0.0	%			

Yield reductions

Stagelabel	A	B	C	D	Season	
Reductions in ETc	0.0	0.0	0.0	0.0	0.0	%
Yield response factor	0.85	0.85	0.90	0.85	0.85	
Yield reduction	0.0	0.0	0.0	0.0		%
Cumulative yield reduction	0.0	0.0	0.0	0.0	0.0	%

Figure 4-12: CROPWAT Gross Water Requirement for Grass in Johannesburg

4.7.4 Ratio - Harvestable Runoff to Demand

The harvestable inflow calculations are explained in **Section 4.4**. The average annual harvestable volume is divided by the total demand that is calculated as described in Section 4.7.3 above to determine the ratio of harvestable run-off to demand.

This ratio represents how much of the demand can be satisfied from the run-off that can be harvested at the stormwater harvesting site. A ratio of 1 or above shows that the total demand can be satisfied whereas a ratio of below 1 shows that the total demand cannot be satisfied from the SWH site. A ratio of above 1 indicates that the total demand can be satisfied and that excess stormwater is available to supply alternative demands. A run-off to demand ratio of 1 was used as a threshold for sites to be deemed as a potential stormwater harvesting site. If the run-off to demand ratio was below 1 the site would not be considered as a potential SWH site.

4.7.5 Area Available for SWH Plant

The minimum area needed for a stormwater harvesting plant was determined as roughly 2500m². The grass and shrub areas were used to determine the area available for a SWH plant. The output metric is the largest area of all the areas within a 500m radius that are larger than 2500 m² and are less than 10m higher than the SWH junction.

4.7.6 Min-Max Normalisation

In order to develop an effective ranking system, it was necessary to develop normalised metrics before applying the weights, especially since the Weighted Vertical Distance has some negative values. This was done with a Min-Max Normalisation which transforms all values to a scale by using the following equations:

$$\text{Higher is Better} = \frac{(Value - Minimum)}{(Maximum - Minimum)} \qquad [3]$$

$$\text{Lower is Better} = \frac{(Maximum - Value)}{(Maximum - Minimum)} \qquad [4]$$

The normalisation ensures that the best possible value receive a score of 1 whilst the worst receives a 0. The normalisation was done with the Weighted Horizontal Distance & Weighted Vertical Distance being the best when smallest and the rest of the metrics being best when being the largest.

4.8 Storage & Distribution Models

In order to further investigate the reliability of the potential SWH sites in delivering the required non-potable water demand it was decided to model the time dynamics of four SWH sites from Scenario 1 and Scenario 2. The SWH sites that were modelled are shown below:

- **Scenario 1:**
  - Site 1
  - Site 2
  - Site 5
  - Site 7
- **Scenario 2:**
  - Site 1
  - Site 6
  - Site 8
  - Site 15

4.8.1 Storage and Distribution Models - SWH Scheme Setup

The storage and distribution model scheme setup are shown graphically in **Figure 4-13** and consists of a storage pond, biofilter and re-use pond. The setup for the detailed models assumes that the storage and re-

use facilities are on-surface ponds and that the entire system is gravity fed. The on-surface ponds included evaporation losses but did not include infiltration losses as it was assumed that the permeability of the ponds would be decreased with soil modifications or geosynthetic clay liner products. No gross-pollutant trap, sedimentation chamber and UV disinfection was modelled as this was deemed to have minor losses. The storage pond was also given a spillway to safely discharge excess water inf the storage pond is full.

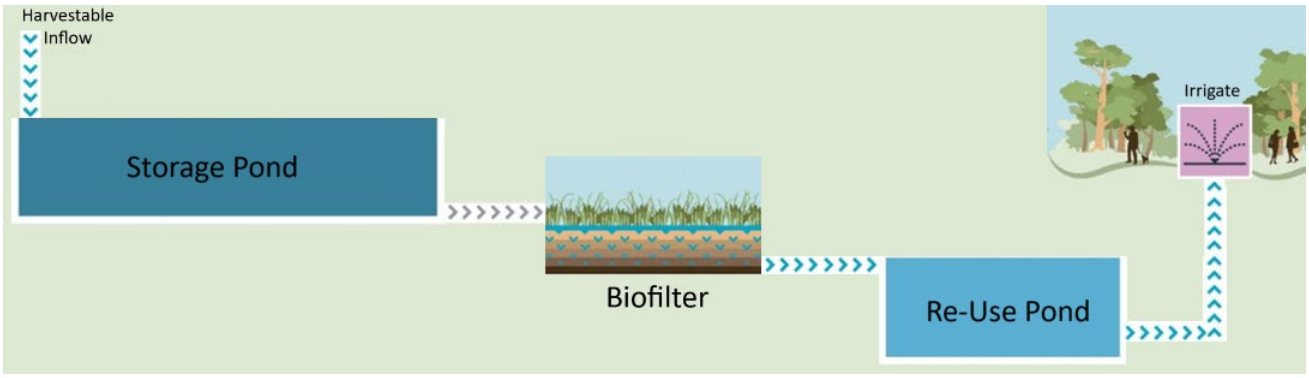

Figure 4-13: Storage and distribution model System (Adapted from City of Melbourne, n.d)

4.8.2 Harvestable Inflow

The harvestable inflow of the collection models was determined by taking the total inflow from the 2020 land cover hydrological model and subtracting the total inflow for the pre-development model. This difference was then annualised by simply dividing the total harvestable inflow over the simulation by the total number of years of the simulation to get a Mℓ/annum of harvestable inflow. This was kept as simplistic as possible to ease the determination of potential SWH sites.

The storage and distribution models explicitly subtracted the pre-development inflow from the 2020 land cover hydrological model to determine the harvestable inflow hydrograph as is shown in **Figure 4-14**. The red line shows the hydrograph for the 2020 land cover hydrological model and the blue line shows the pre-development hydrograph. The difference between the two hydrographs is the total harvestable inflow and is shown by the green hydrograph. This harvestable inflow hydrograph was introduced into the storage and distribution models to determine the reliability of the SWH sites.

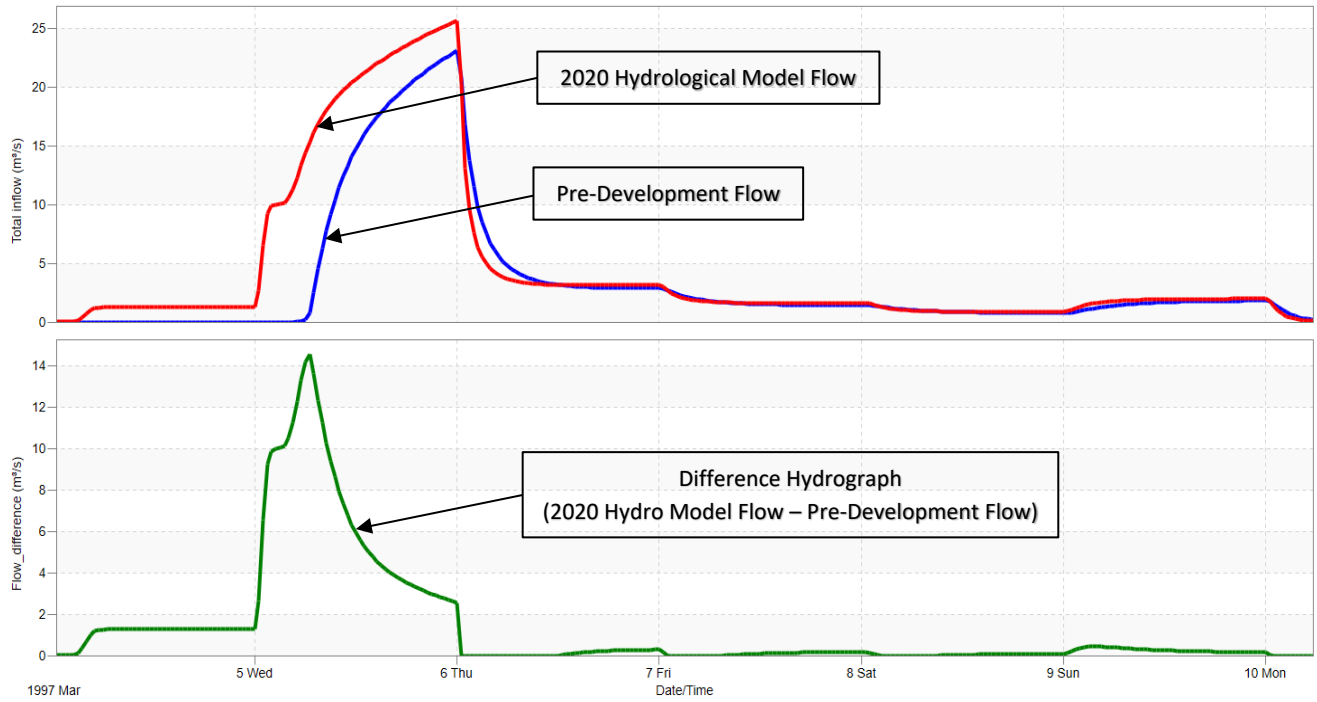

Figure 4-14: Time Dynamic Harvestable Inflow

4.8.3 Demand

The demand time series was calculated in CROPWAT by considering a grass that is planted in loamy soil in Johannesburg during the warmer months of October to March. It is assumed that no irrigation is done during the colder winter months due to frost. The irrigation schedule from October to March shown in **Figure 4-15** and was used for every simulation year. CROPWAT calculates the plant water demand needs based on the climatic conditions and the plant growth stage. To ensure reproducibility for future assessments no changes were made to the demand time series calculated by CROPWAT.

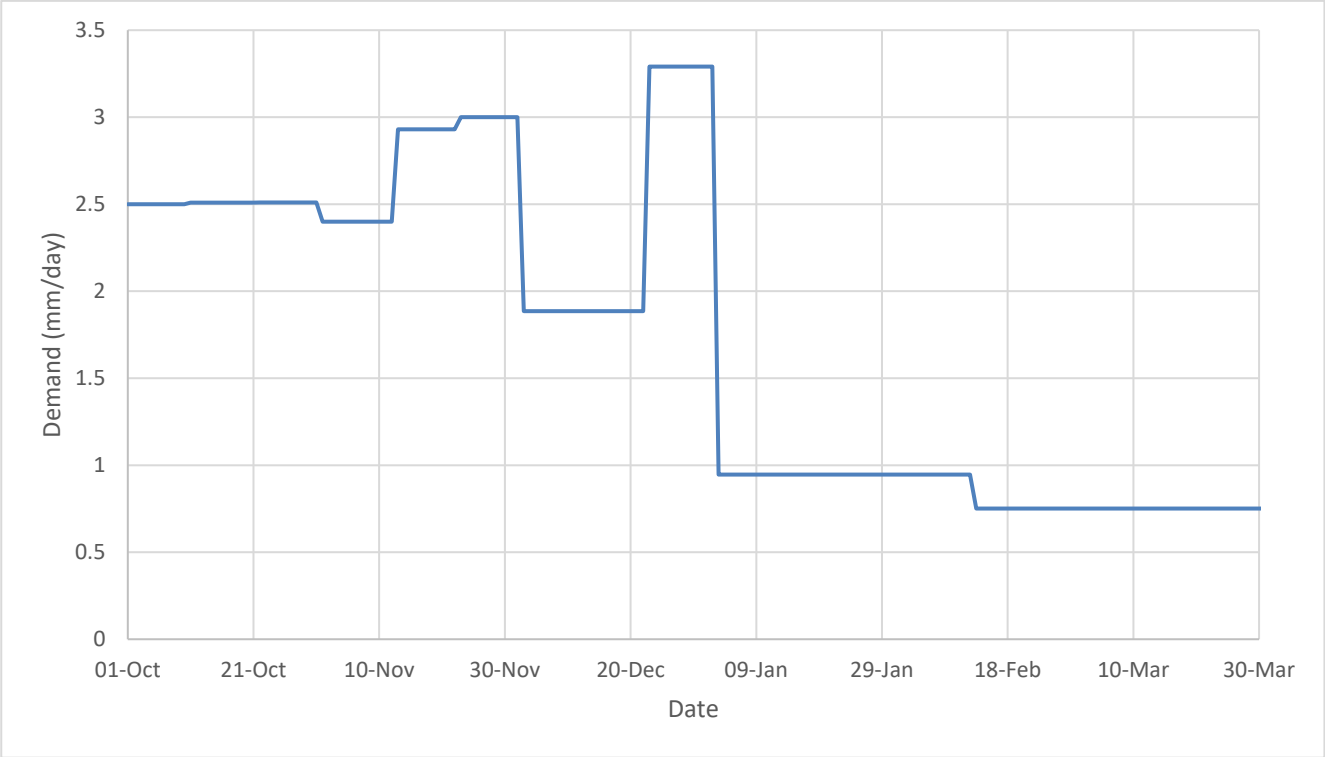

Figure 4-15: Demand - Irrigation Schedule

4.8.4 Volumetric Reliability

The volumetric reliability is the total volume of supply (yield) divided by the total demand during the simulation(V. G. Mitchell et al., 2008). The volumetric reliability is therefore an indication of the water supply efficiency of a SWH system by quantifying the total water demand that can successfully be supplied over the entire simulation period. A volumetric reliability of 1 (100%) shows that the total demand can be met over the simulation period.

$$\mathrm{RV} = \frac{\sum_{t=1}^{T} Yt}{\sum_{t=1}^{T} Dt} \qquad [5]$$

- RV = Volumetric Reliability
- Yt = Yield per timestep (m^3)
- Dt = Demand per timestep (m^3)

4.8.5 Time Based Reliability

The time based reliability shows the fraction of time steps that the demand could be totally satisfied during the simulation (Mcmahon et al., 2008). The time base reliability is therefore the temporal performance of the SWH system. The time based reliability was calculated on the daily time step at which the models where run.

$$\mathrm{RT} = \frac{N}{T} \qquad [6]$$

- RT = Time based reliability
- N = Number of timestep where demand was fully met
- T = Total number of timesteps

4.8.6 Resilience

The resilience of the SWH system is an indication of how quickly the system will recover after a "failure" where demand could not be met (Hashimoto et al., 1982). According to Hashimoto (1982) the resilience is equivalent to the average probability that the unit will recover in its next simulation time step. Mcmahon (2008) states that resilience is the inverse of the average failure duration.

$$\emptyset = \frac{fs}{fd} \text{ for fd} \neq 0 \qquad [7]$$

- $\emptyset$ = Resilience
- fs = number of continuous failures
- fd = total number of days where the system failed to meet demand

Resilience is illustrated in the example of **Table 4-4 below**. The system has three continuous failures as illustrated by the red boxes. The system failed to deliver the target demand on 6 days. The resilience is therefore

$$\emptyset = \frac{fs}{fd} = \frac{3}{6} = 0.5$$

Table 4-4: Resilience Example

Time Step (day)	1	2	3	4	5	6	7	8	9	10	11	12
Target Demand (Mℓ)	5	2	2	3	3	4	4	5	7	9	5	5
Supplied Demand (Mℓ)	5	2	0	0	3	4	0	5	0	0	0	5

Mcmahon (2008) states that the average failure duration is the inverse of the resilience of the system and is therefore:

$$Avg\ Failure\ Duration = \frac{1}{\emptyset} = \frac{1}{0.5} = 2\ Days$$

4.8.7 Overflow Ratio

The overflow ratio is the volume of water that overflows from the storage unit to the volume of water that flows into the storage unit (Rohrer, 2017).

$$\mathrm{OR} = \frac{\sum_{t=1}^{T} St}{\sum_{t=1}^{T} It} \qquad [8]$$

- OR = Overflow Ratio
- St = Volume of water spilled by storage unit (m^3)
- It = Volume of Water entering the storage unit (m^3)

5. MATERIALS

5.1 Climate

5.1.1 CHIRPS Rainfall

The Climate Hazards Group InfraRed Precipitation with Stations (CHIRPS) uses 0.05° resolution satellite imagery with in-situ station data to create a gridded rainfall time series. The data is available from 1981 to present and produces daily precipitation estimates. The CHIRPS dataset integrates data from the Climate Hazards group Precipitation climatology (CHPclim), the Cold Cloud Duration (CCD) and observed rain gauge data (du Plessis & Kibii, 2021). The integration of the in-situ station data and the CCD rainfall estimates makes CHIRPS a reliable dataset for sparsely gauged locations (Funk et al., 2015).

5.1.2 Hargreaves Evaporation

The Hargreaves method can be used to compute the potential evaporation rates from the daily minimum and maximum temperatures and the study area latitude. The Hargreaves method utilises an average daily temperature as well as an average daily temperature range over a period of 5 or more days to provide satisfactory results (Hargreaves et al., 1998). The Hargreaves method also utilises the extra-terrestrial radiation to compute the evaporation rate based on the study site latitude (Rossman & Huber, 2016). The temperature data used to provide the daily maximum and minimum temperatures is the ERA5 reanalysis data with a spatial resolution of 0.25°.

5.2 Land Cover

Publicly available Land Cover datasets are very useful to derive hydrological input parameters through spatial weighting GIS functionalities. Impervious areas such as roads and buildings are a major driver of run-off volume in urban areas and a finer resolution land cover map of the impervious areas could potentially assist in better representing the impervious area representation of the hydrological model. A roads layer (OpenStreetMap) and a buildings footprint layer (Open Buildings V1 Polygons) were utilized to improve the spatial representation of the impervious areas of the land cover dataset that was used (ESRI 2020 Land Cover).

5.2.1 OpenStreetMap Roads

OpenStreetMap (OSM) is a Volunteered Geographic Information (VGI) project that aims to map the entire world as a crowdsourcing project. Volunteers can contribute data such as GPS and vector data that adds to the publicly available dataset. The dataset consists primarily of nodes, ways, tags and relations (Siebritz, 2014). OpenStreetMap was created in 2004 due to the legal restrictions on available maps and subsequently it is distributed under the open access Open Database License (ODbL) which makes the data available for free use (Minghini & Frassinelli, 2019).

The OpenStreetMap roads dataset was utilised in this study to explicitly define the impervious area contributions from roads in the subcatchment. The OpenstreetMap roads data shapefile is a line vector and therefore only has a length attribute. The area of the roads was calculated by creating a 3.5m buffer around the line layer to define the road width of 7m that is commonly used in South Africa.

5.2.2 Open Buildings V1

The Open Buildings V1 Polygons dataset was created by Google Research and derives the outlines of buildings from 50cm high resolution satellite imagery. The dataset contains 516 million building detections and maps 64% of the African Continent. Each building footprint has attributes on its footprint size, a Plus Code for the centre of the building and a confidence score where three bands are used: 60 to 65%, 65 to 70% and larger than 70% (Sirko et al., 2021). Shown in **Figure 5-1** is the Buildings Polygons for an area in the Upper Jukskei catchment where the green polygons have a confidence score of larger than 70%, the orange polygons have a confidence score of 65 to 70% and the red polygons have a confidence score of 60 to 65%. The data is licensed under the open access Open Database License (ODbL) and the Creative Commons Attribution 4.0 International License (CC BY-4.0) to enable the use of the data for free.

The buildings footprint dataset was utilised in this study to explicitly define the impervious area contributions from buildings in the subcatchment. The buildings footprint is a polygon shapefile that has the area of the building's footprint as an attribute of the polygon.

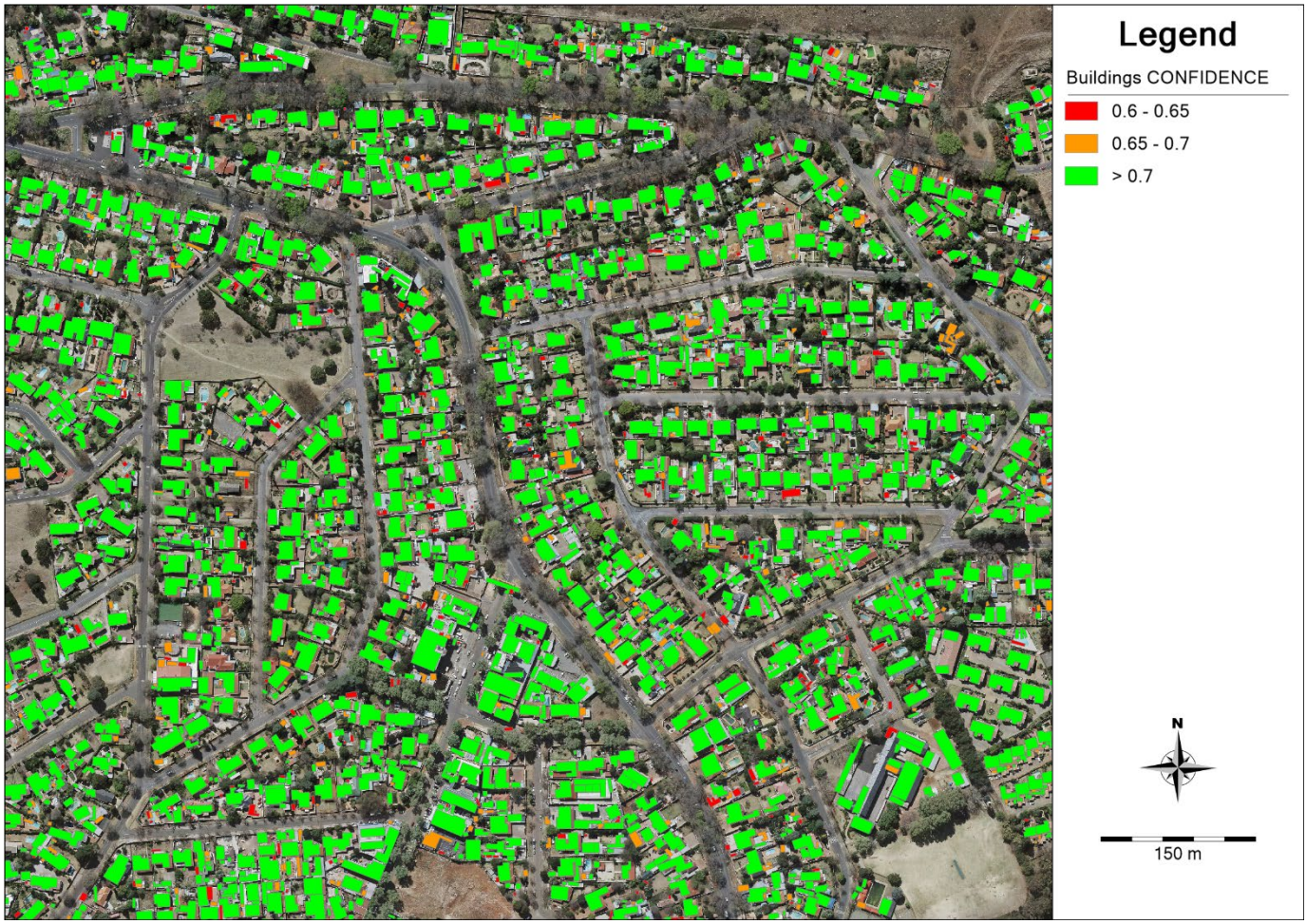

Figure 5-1: Buildings Polygons in the Upper Jukskei

5.2.3 ESRI 2020 Land Cover (10m)

The ESRI 2020 Global Land Cover dataset is derived from the ESA Sentinel 2 imagery at a 10m resolution. The dataset makes use of the National Geographic Society Dynamic World training dataset and was produced for the Dynamic World Project by National Geographic Society in partnership with Google and the World Resource Institute (Roy, 2021). The ESRI Global Land Cover dataset has 10 land cover classes as listed below:

- Water
- Trees
- Grass
- Flooded Vegetation
- Crops
- Shrub
- Built area
- Bare Ground
- Snow/Ice
- Clouds

The ESRI Global Land Cover product is available free of charge and is licenced under the Creative Commons Attribution 4.0 International License (CC BY-4.0).

The ESRI 2020 Global Land Cover dataset was used to determine the Soil Conservation Services (SCS) curve numbers and the areas where stormwater harvesting facilities can be installed based on the areas available for in the Grass & Shrub defined areas of the dataset.

5.3 SOTER Soils

The World Soils and Terrain Database (SOTER) is an update of the 1:5 Million Soil Map of the World that is being done by ISRIC, the FAO and UNEP. The SOTER units are defined by a geographic delineation with associated attributes of the soil that have been estimated from 9600 measured soil profiles in the ISRIC-WISE database and gap filled with taxotransfer rules. The taxotransfer relies primarily on the soils physical and chemical data in the ISRIC-WISE database (Batjes, 2004).

Attributes associated with SOTER units include:

- FAO Soil Drainage Class
- Layer Depth
- Coarse Fragments (> 2mm)
- Sand (mass %)
- Silt (mass %)
- Clay (mass %)
- FAO Texture Class
- Bulk Density (kg/dm^3)
- Available Water Capacity

The SOTER Soil Drainage Class was used in the assessment to determine the SCS curve number for each subcatchment.

5.4 SRTM Digital Elevation Model (DEM)

The Shuttle Radar Topography Mission (SRTM) was launched on 11 February 2000. The SRTM provided a digital elevation model (DEM) of the earth between 54 degrees South and 60 degrees North and was obtained using radar interferometry (van Zyl, 2001). The SRTM data has a spatial resolution of 1 arc second which is approximately 30m and was updated for the Version 3.0 SRTM to a void filled DEM using data from the Advanced Spaceborne Thermal Emission and Reflection Radiometer (ASTER) Global Digital Elevation Model 2 (GDEM2), USGS Global Multi-resolution Terrain Elevation Data (GMTED) and USGS National Elevation Dataset (NED) (*SRTM Version 3.0*, 2021).

The SRTM DEM data was used to do a watershed delineation of the catchment in order to determine the subcatchment geometries as well as the conduit flow paths and slopes.

5.5 Water Demand

The non-potable water demand was calculated from the ESRI 2020 Land Cover data where the areas of grass & shrubs was utilised to calculate the non-potable water demand with CROPWAT.

6. RESULTS

6.1 Runoff

The runoff for the 2020 hydrological model was calculated on a daily time step from January 1981 to December 2021. The daily time step was chosen due to the precipitation data being daily data. The quantity of runoff produced by a subcatchment from a precipitation event or events can be evaluated through the runoff coefficient. The run-off coefficient is the ratio of total runoff to total precipitation for a subcatchment (Rossman & Huber, 2016). The runoff coefficient for the entire simulation from 1981 to 2001 is shown below in **Figure 6-1.**

The runoff coefficient shows a strong correlation to the % imperviousness where the subcatchments with high percentages of imperviousness have a higher run-off coefficient than those subcatchments with smaller percentages of imperviousness. This is due to there being no infiltration losses from the impervious parts of the subcatchment. The impervious parts do however have small losses in the order of 1.25mm to 2mm from depression storage and the evaporation that occurs from the depression storage. The total amount of precipitation that therefore falls on impervious surfaces is almost totally converted into run-off. The pervious parts of the subcatchment are subjected to infiltration losses from the curve number methodology as well as losses from depression storage and evaporation. Subsequently the quantity of precipitation that is converted into run-off is much less for a pervious area than for an impervious area.

The North-Eastern part of the study area therefore has lower runoff coefficients due to the area being predominantly pervious (>90% pervious), as opposed to the Southern and Western parts of the study area that exhibit higher runoff coefficients due to higher density and population and subsequently higher percentages of imperviousness. The four subcatchments with the highest runoff coefficients (0.238 to 0.266) are situated in the Western part of the study area and cover the Alexandra township that is very densely populated with the % imperviousness ranging between 37% and 42% for the four subcatchments.

The runoff coefficients for the driest and wettest year are shown in **Figure 6-2** and **Figure 6-3** respectively. The wettest year is the year 2000 with 920mm of precipitation. The driest year is 1999 with 498mm of precipitation. **Figure 6-2** and **Figure 6-3** have been rendered with a different scale than that of **Figure 6-1** to better accentuate the difference in runoff coefficient for each figure. **Figure 6-1** has a scale from 0 to 0.25, whereas **Figure 6-2** has a scale from 0 to 0.2 and **Figure 6-3** has a scale from 0 to 0.3.

As expected, the runoff coefficients are less for the driest year (**Figure 6-2**) compared to the wettest year (**Figure 6-3**), as more runoff is generated in the wet year compared to the dry year. This is due to the depression storage having to fill up before runoff can occur and the effect of antecedent moisture conditions. The run-off coefficient for the driest year (1999) is 0.11 and the run-off coefficient for the wettest year (2000) is 0.18.

The WR2012 data of South Africa shows that the upper Jukskei is situated in quaternary catchment A21C with a Mean Annual Precipitation (MAP) of 682mm and a Mean Annual Run-off of 59.11mm giving an average annual runoff coefficient of 0.0866 (59.11/682 = 0.0866) (Bailey & Pitman, 2015). The total simulated rainfall in the Upper Jukskei from 1981 to 2021 is 29 650mm and the total simulated run-off depth for this period is 3 899mm giving a total simulated run-off coefficient of 0.131 (3 899mm/29 650mm = 0.131). The run-off coefficient of the upper Jukskei catchment simulation is slightly higher than that of the WR2012 quaternary catchment. This can potentially be attributed to the increased amount of urbanisation in the upper Jukskei catchment as opposed to the entire quaternary catchment A21C, where the lower portions of A21C have large areas of grasslands and agriculture.

The simulated run-off coefficient is however not orders of magnitude higher than the WR2012 data and gives a relative amount of confidence that the hydrological modelling is a good representation of reality, especially considering that the model is not calibrated. The higher simulated run-off coefficient could however point towards over-estimation of the run-off volumes and therefore an overestimation of harvestable volumes at the various stormwater harvesting sites. The objective of this assessment is however not to conclusively determine the best stormwater harvesting sites but is to serve as a screening tool for determining the locations of the potential best sites.

The run-off coefficient of the entire upper Jukskei for the pre-development scenario is 0.016. An indication of the harvestable volume is therefore the difference between the current scenario run-off coefficient of 0.131 and the pre-development run-off coefficient of 0.016 which is 0.115. The harvestable run-off depth can therefore be estimated as 83.49mm from the mean annual precipitation of 726mm (726mm x 0.115 = 83.49mm) and the annual harvestable run-off volume can therefore be estimated as 20 013 481.83m³ (0.08349m x 239 711 125m²).

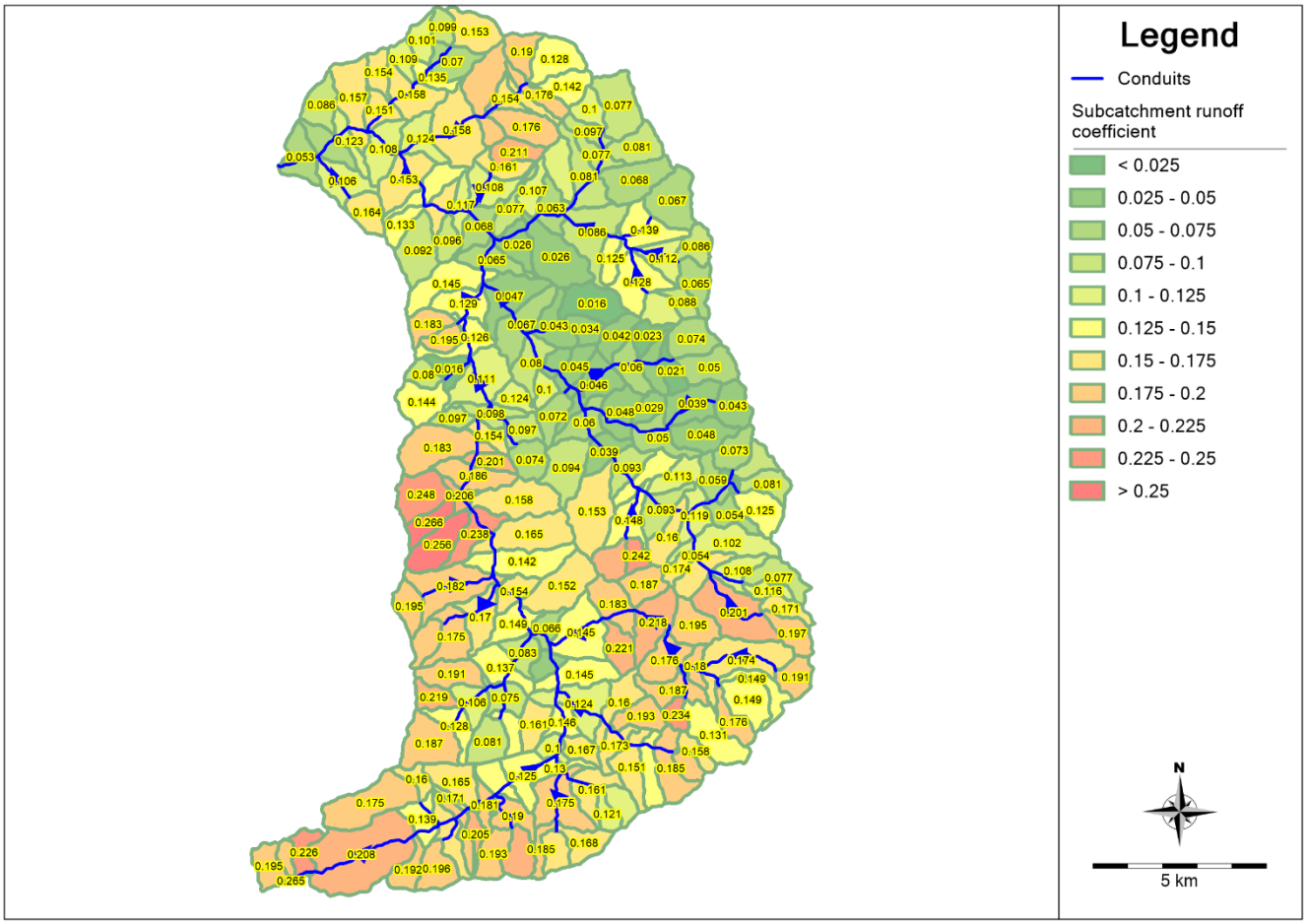

Figure 6-1: Runoff coefficients for the entire simulation

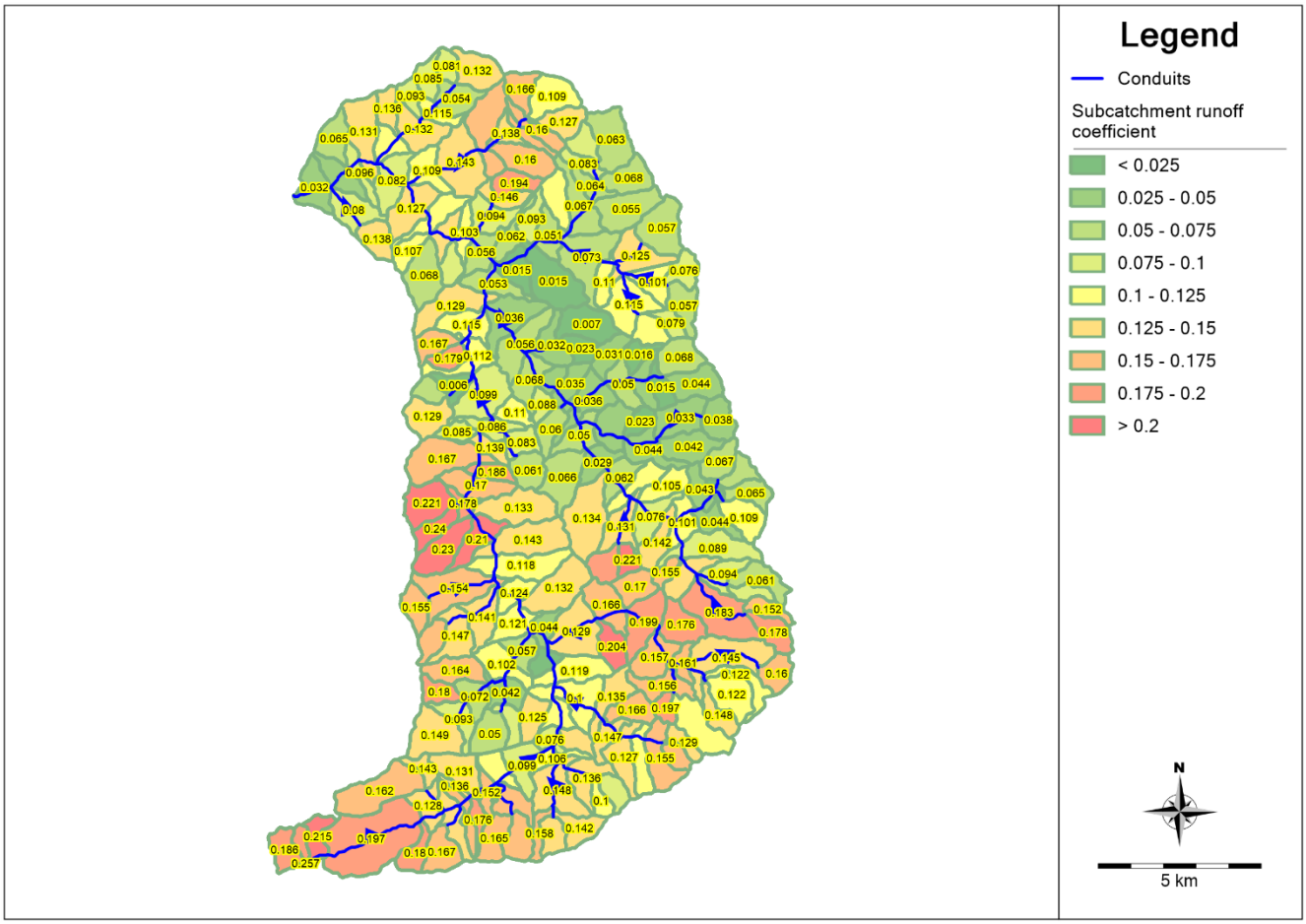

Figure 6-2: Runoff coefficients for the driest year (1999 – 498mm of Precipitation)

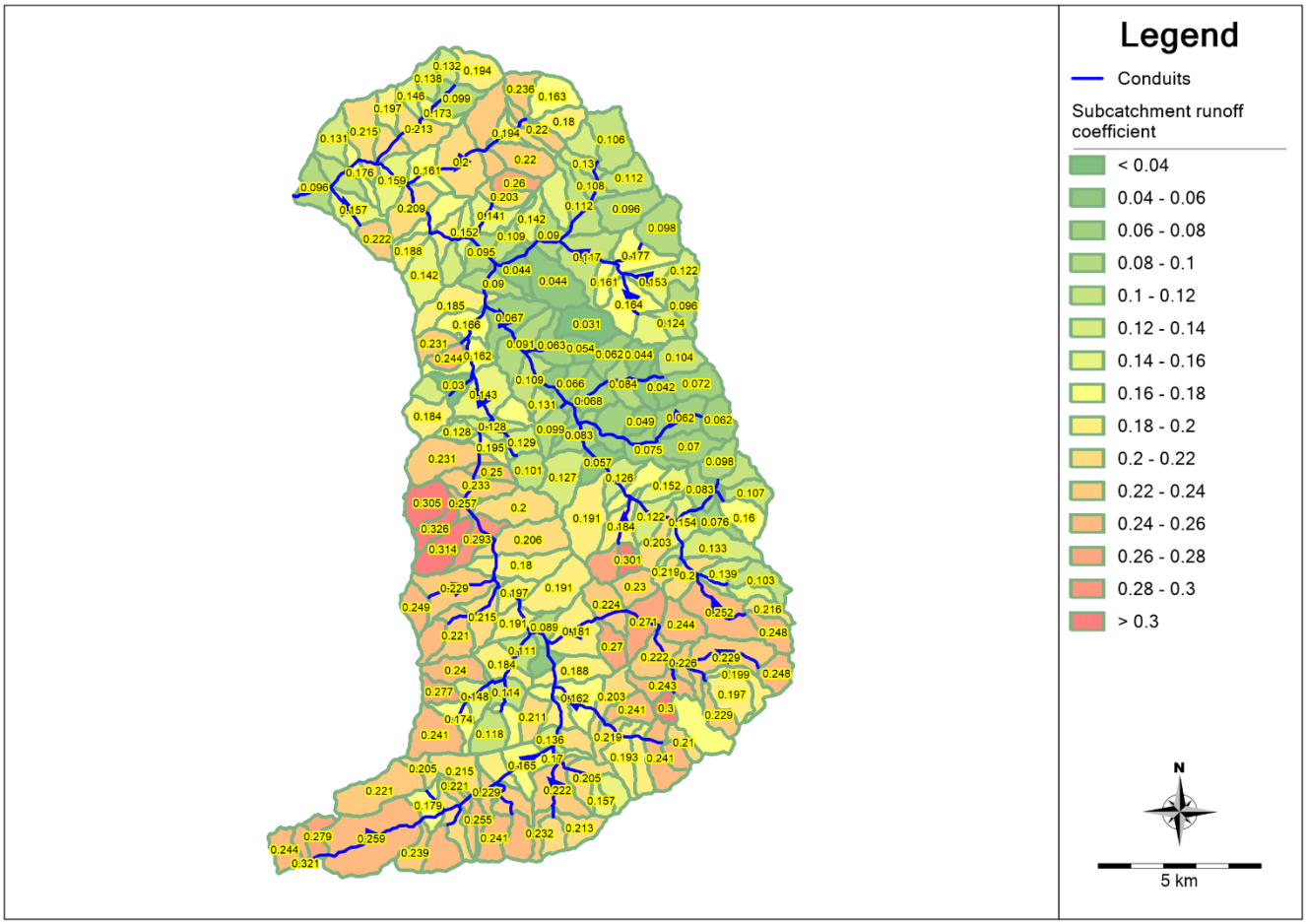

Figure 6-3: Runoff coefficients for the wettest year (2000 – 920mm of Precipitation)

6.2 Watershed Delineation Size

The watershed delineation target discretization level (target subcatchment size) determines the number of subcatchments that are created, which in turn determines the number of junctions that are created in the model. The junctions are used to determine the stormwater harvesting sites and subsequently the number of and the location of the junctions are critical in the overall determination of the best stormwater harvesting sites.

The analysis was done with a target discretization level (target subcatchment size) of 100Ha. The watersheds were created to be roughly 100Ha, but the size and orientation is dependent on the topography. The subcatchment area distribution for the analysis is shown in **Figure 6-4.** A total of 222 subcatchments were created with the mean area of the catchments being 108Ha and the median being 96Ha. The largest subcatchment is 491Ha and the smallest is 1.4Ha. 149 junctions were created that receive the inflows from the subcatchments. The junctions are used to determine the distance and height metrics to the demand areas. If there are too few junctions the risk exists that a good stormwater harvesting location could be missed due to a drainage junction not being located in close proximity to the demand centres and an open area to establish a stormwater harvesting plant.

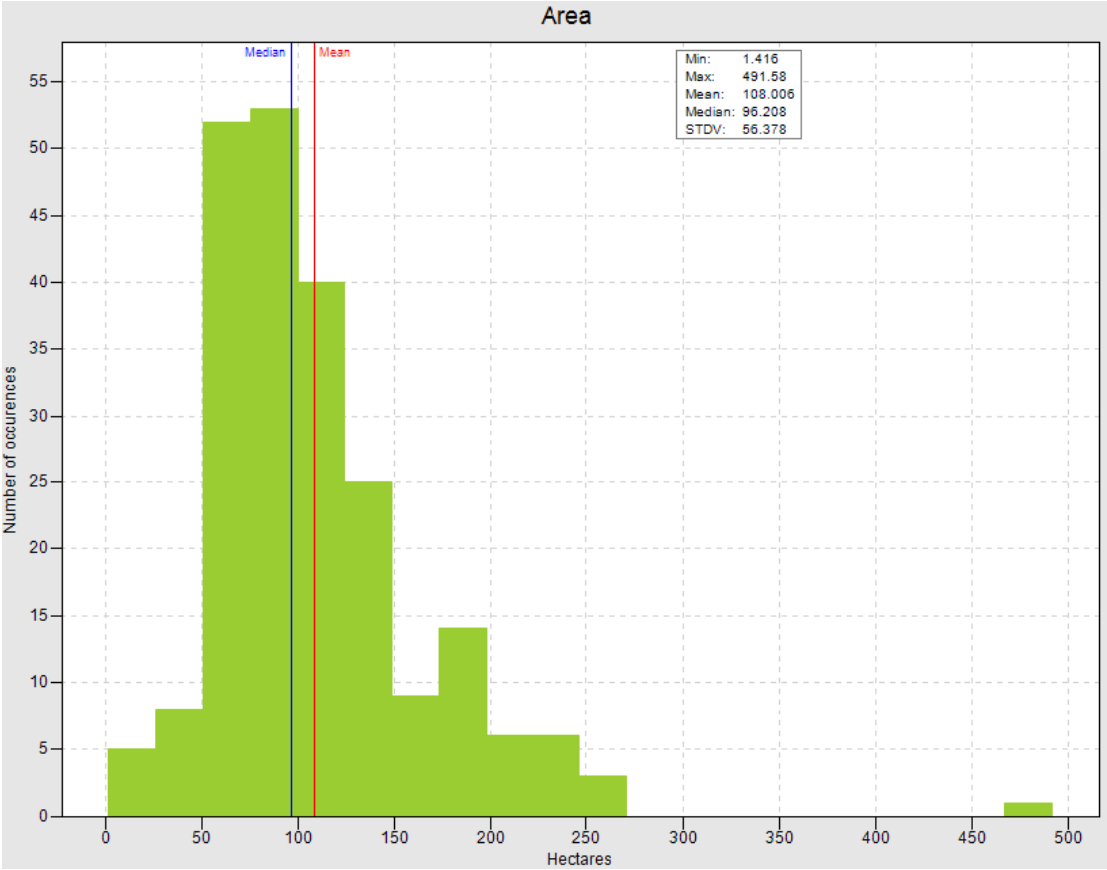

Figure 6-4: Analysis Subcatchment Area Distribution

In order to test if the 100Ha target discretization level is sufficient in terms of the spatial coverage of junctions, a test was done where a model was setup and run with a target discretization level of 50Ha. The 50Ha model subcatchment area distribution is shown **Figure 6-5**. A total of 463 subcatchments were created with the mean area of the catchments being 51Ha and the median being 46Ha. The largest subcatchment is 248Ha and the smallest is 0.991Ha. 330 junctions were created, which is more than double the number of junctions for the 100Ha target discretization level model.

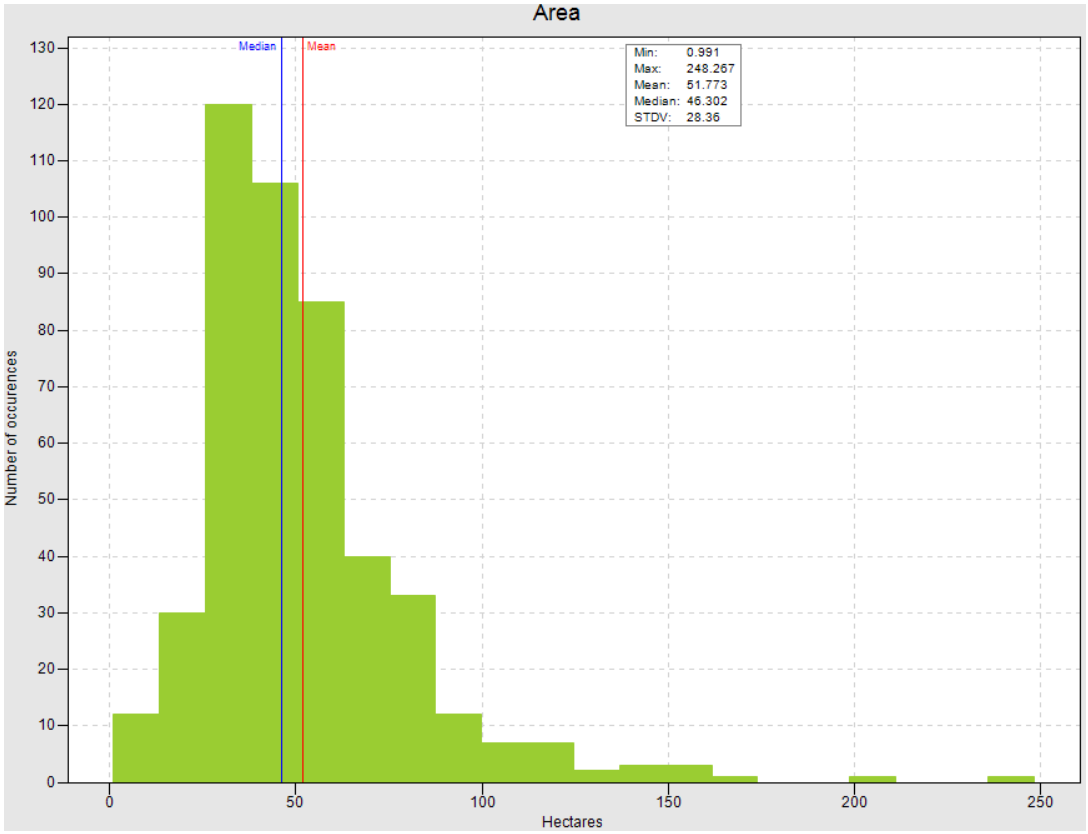

Figure 6-5: 50Ha Model Subcatchment Area Distribution

The comparison of results between the 100Ha model and 50Ha model for the top 20 stormwater harvesting sites is shown visually in **Figure 6-6 below**. The top 20 stormwater harvesting sites are still concentrated around the 5 golf courses for the 50Ha model, similar to the 100Ha model**.** The exceptions are locations 11,12, 14,15, 16 and 18 for the 100Ha model that are not shown in the 50Ha model. The 50Ha model shows a clearer grouping around the three golf courses in the upper reaches of the catchment and shows a new site, site 20, that was not shown on the 100Ha model. The models show a good amount of overlap for the high-ranking areas. The tool was not developed as an absolute indication of the best stormwater harvesting sites but was rather developed as a screening tool to identify areas for more detailed analysis of stormwater harvesting. The results of both the 100Ha model and the 50Ha model show that the main target areas remain quite consistent in terms of where the detailed analysis needs to be done. The advantage of the 100Ha model is lower data storage requirements and shorter model run time, whereas the advantage of the 50Ha model is a clearer grouping of best sites but at the cost of larger data storage requirements and longer model run times.

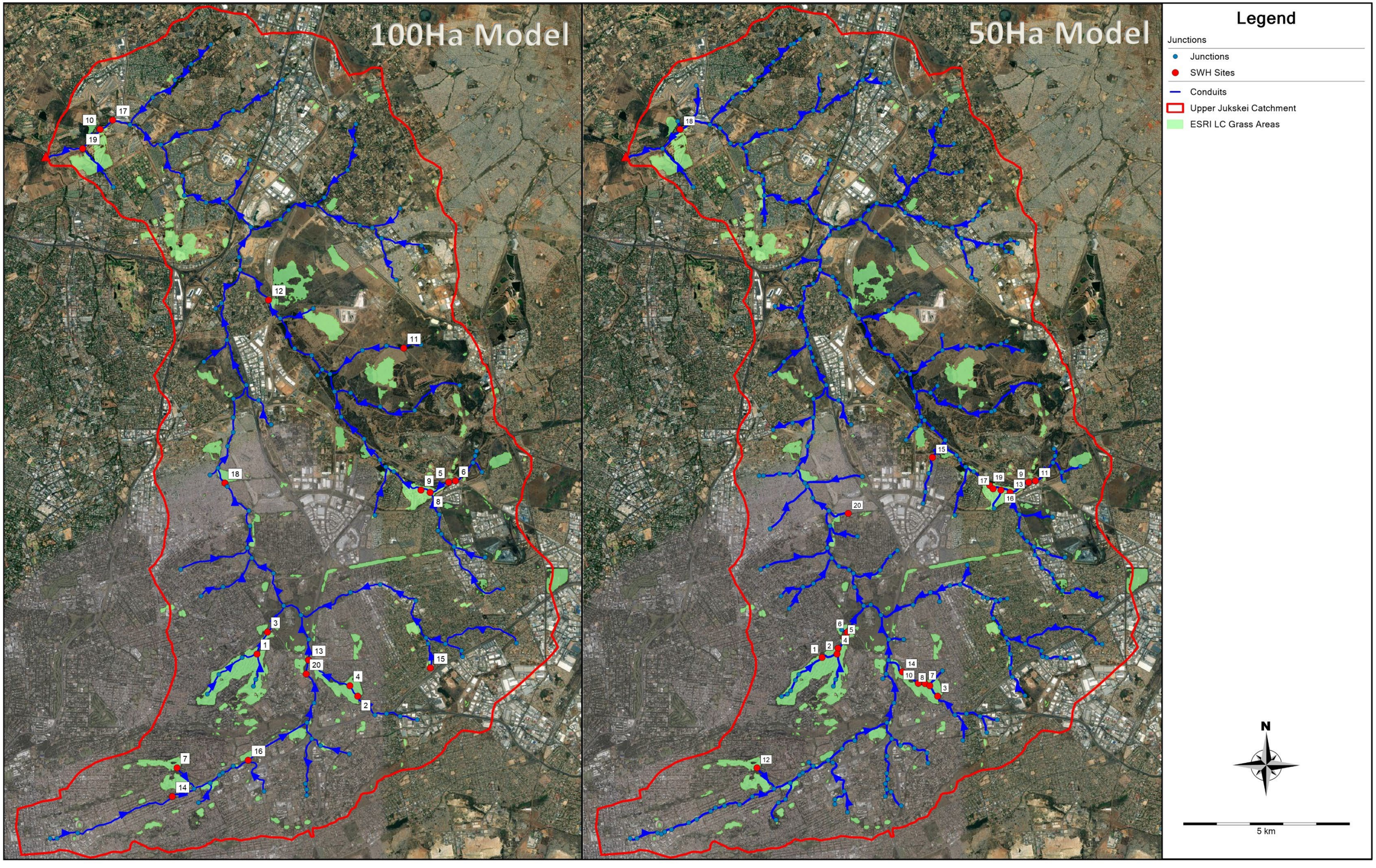

Figure 6-6: 100Ha Model vs 50Ha Model - Top 20 SWH Sites for Grass Areas as Demand

6.3 Hydrological Model Sensitivity

A sensitivity analysis was done for a mean annual precipitation year of the model. This was done to determine what parameters the hydrological model is most sensitive towards in terms of run-off generation and ultimately harvestable run-off volume. The sensitivity analysis was only done for a mean annual precipitation year due to the significant run time needed to run the 72 sensitivity analysis models. The mean annual precipitation for all the CHIRPS grids from 1981 to 2022 was determined as 715mm. The year with average rainfall closest to 715mm is 1981 with 720mm. The 1981 data was therefore used to do the sensitivity analysis.

The sensitivity analysis was done by assigning uncertainty ranges to the various hydrological input parameters based on the recommendations in the publication "Rules for Responsible Modelling" by James, (2003). The sensitivity analysis was done for the following hydrological parameters with the uncertainty shown in brackets:

- Curve Number (100%)
- Impervious % (50%)
- Zero Impervious % (25%)
- Depression Storage Pervious Areas (100%)
- Depression Storage Impervious Areas (50%)
- Drying time (50%)
- Subcatchment Flow Length (100%)
- Manning n for Pervious Areas (100%)
- Manning n for Impervious Areas (25%)

Due to the non-linear response of hydrology, a total of 8 sensitivity points was used in the sensitivity analysis. This resulted in 72 models (9 Hydrology Parameters x 8 sensitivity points = 72 Models). The sensitivity points indicate the number of models that will be run with a range of values within the uncertainty percentage assigned. For example, the uncertainty value of the curve number was set to 100% and 8 sensitivity points were chosen which results in 8 models that are created where the curve number is changed by -100%, -75%, -50%, -25%, +25%, +50%, +75% and +100% from the original value.

The ranked sensitivity graphs and sensitivity gradient graphs for the total flow are shown in **Figure 6-7** and Error! Reference source not found.. The mean normalised sensitivity is calculated by dividing the difference between the max and min of the functions with the objective function value. In this case the objective function is the total flow at the outlet of the Upper Jukskei Catchment. The figures below clearly show that the hydrology is the most sensitive to the curve number parameter, followed by the impervious percentage of the catchments. The sensitivity of the hydrology to the remaining parameters is quite low. **Figure 6-7** is ranked from left to right as the most sensitive to the least sensitive. The bars below zero in **Figure 6-7** show that for an increase in the parameter the total outflow (objective function) decreases.

Figure 6-8 shows that as the curve number increases, the total flow increases drastically. The curve number controls the amount of infiltration that can occur from the subcatchments. As the curve number increases, so the infiltration decreases, and the run-off increases. **Figure 6-8** shows that for a decrease in the curve number the total flow does not decrease as drastically as the increase in flow for an increase in the curve number.

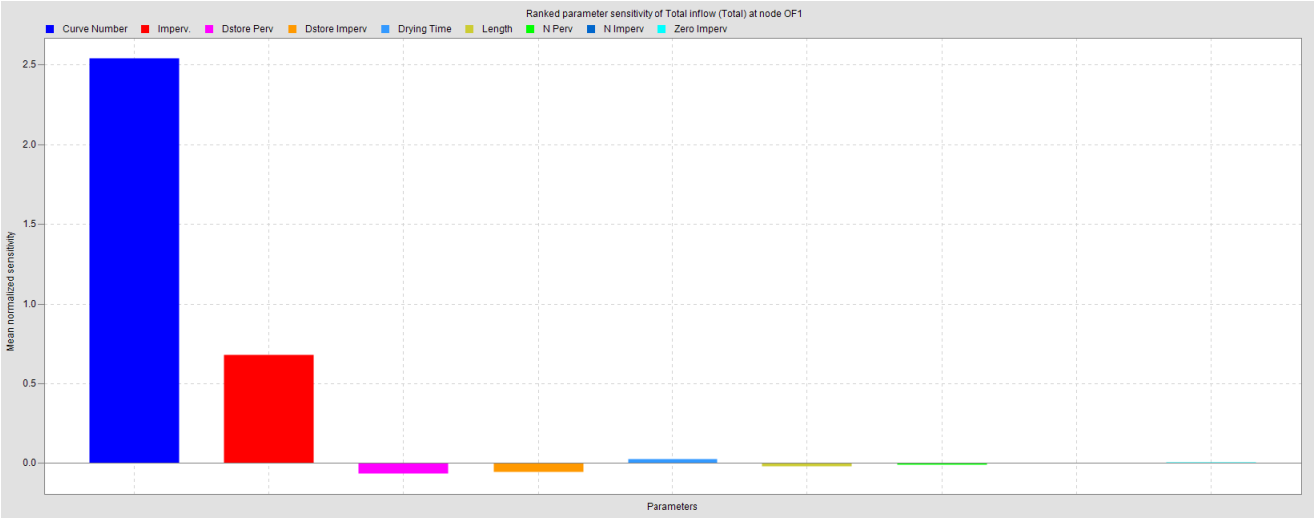

Figure 6-7: Ranked Sensitivity Graph (Total Flow)

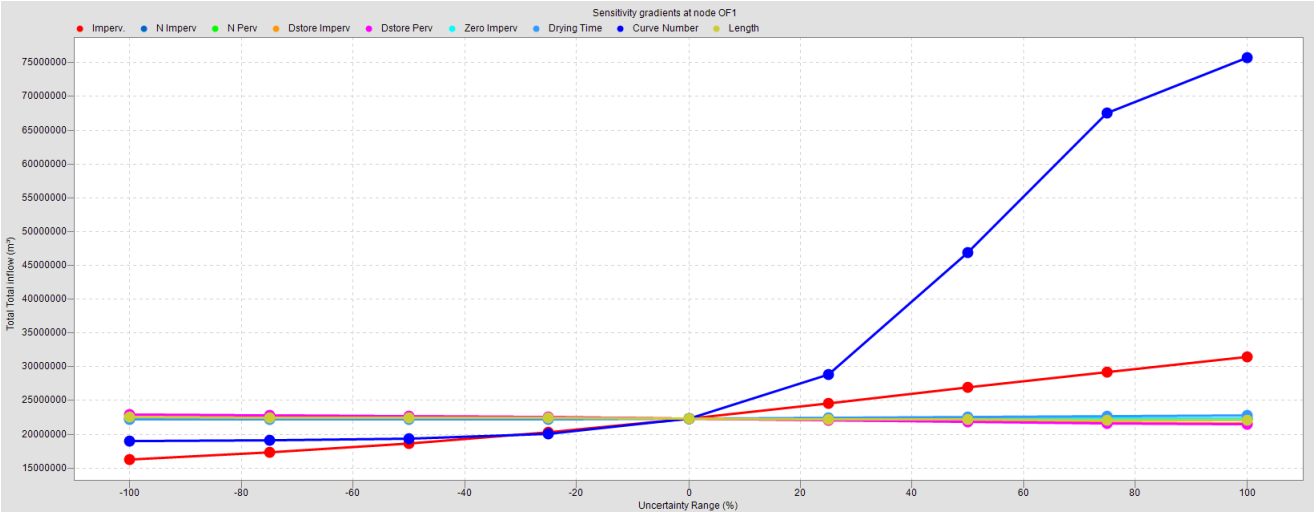

Figure 6-8: Sensitivity Gradient Graph (Total Flow)

6.4 Results of Collection Models

The Scenario 1A and Scenario 2A models were used as the primary models to determine the locations of the ideal SWH sites where the weightings were determined from discussions with several academics and industry professionals. Scenarios 1B to 1D and Scenarios 2B to 2D were used to determine if different weightings and project objectives considerably changes the locations of the ideal SWH sites.

6.4.1 Results of Scenario 1A and Scenario 2A

6.4.1.1 Scenario 1A Results

The results of the top 20 SWH sites for Scenario 1A is shown in **Figure 6-9** as the red junctions with their corresponding ranking shown as the number adjacent to the junction. The majority of the high-ranking areas are located in close proximity to golf courses. SWH sites 1 to 10 are all located on, or immediately upstream of a golf course. Sites 1 to 9 are in the upper areas of the Upper Jukskei catchment and site 10 is in the lower portion.

The results of the top 20 SWH sites for Scenario 1A is shown in **Table 6-1.**

The scatter plots of each metric and the SWH Score is shown as the red dots in **Figure 6-11 to Figure 6-15** for all of the junctions in the model that met the thresholds (70 Junctions in total)**.**

The weighted horizontal distance shows a negative correlation of -0.51, showing that the further away the demand sites the lower the SWH Score. The data shows a strong negative correlation (-0.77) to weighted vertical distance, indicating that as the vertical distance becomes smaller, so the score increases. Negative values for weighted vertical distance indicate that the demand area can be supplied under gravity feed conditions. As the weighted vertical distance becomes more negative so the gravitational head increases under which the gravity feed demand can be supplied.

The non-potable water demand shows a strong positive correlation of 0.72, showing that as the demand increases the SHW Score increases. The ratio of run-off to demand has a negative correlation of -0.11 with the majority of the junctions with a ratio between 1 to 5 showing high SWH scores. Interestingly as the ratio increases above 5 so the SWH score tends to decrease.

The largest available area shows a weak correlation of 0.003 to the SWH Score showing that once the minimum area of 2500 m² has been met an increase in available are does not improve the score much. The correlations are inherent to the weightings given for each metric and as such are reflected in the correlations.

Table 6-1: Results – Top 20 SWH Sites for Scenario 1A

SWH Rank	Weighted Horizontal Distance (ΔX - m)	Weighted Vertical Distance (ΔZ - m)	Non-potable Demand (Ml/annum)	Ratio - Harvestable Run-off to Demand	Largest Available Area for SWH Site (m^2)	SWH Score
1	0.00	-15.00	524.80	1.20	1 774 864.97	0.66
2	0.00	-34.52	179.03	3.63	596 773.56	0.65
3	2.42	-0.84	541.72	1.31	1 774 864.97	0.54
4	23.84	-22.75	179.03	4.26	596 773.56	0.53
5	138.69	-26.83	156.17	2.07	2 277 103.43	0.53
6	330.17	-27.80	156.17	1.92	2 277 103.43	0.48
7	89.38	-16.83	158.46	1.81	277 318.75	0.45
8	0.00	-11.42	151.72	8.19	505 723.13	0.42
9	0.00	-4.75	151.72	8.95	505 723.13	0.36
10	105.08	-2.08	247.36	69.64	1 140 893.16	0.36
11	453.76	-11.21	148.46	1.20	18 059 986.97	0.33
12	16.37	-2.30	24.88	118.56	18 059 986.97	0.31
13	85.64	2.46	218.70	18.86	1 774 864.97	0.31
14	238.77	-10.52	83.20	11.33	277 318.75	0.30
15	25.30	-7.96	6.33	32.71	21 097.39	0.30
16	41.50	-6.89	21.40	103.17	67 479.35	0.29
17	466.56	-7.02	247.36	69.13	1 140 893.16	0.29
18	64.16	-5.89	37.91	236.74	126 368.87	0.29
19	182.01	2.82	245.73	71.01	1 140 893.16	0.29
20	227.12	-1.12	205.74	15.80	596 773.56	0.29

Table 6-2: Scenario 1A – Correlation of All Junctions to SWH Score

Metric	Correlation
Weighted Horizontal Distance (ΔX - m)	-0.51
Weighted Vertical Distance (ΔZ - m)	-0.77
Non-potable Demand (Ml/annum)	0.72
Ratio - Harvestable Run-off to Demand	-0.11
Largest Available Area for SWH Site (m^2)	0.003

The results from Scenario 1A shows the following summarised results:

- Keep SWH Demand areas close and downhill of the SWH site.
- Aim for a run-off to demand ration of near unity, where once the ratio exceeds 5 the excess water does not significantly increase the SWH Score.
- The largest available area does not increase the SWH Score once the minimum area of 2500m^2 has been satisfied.

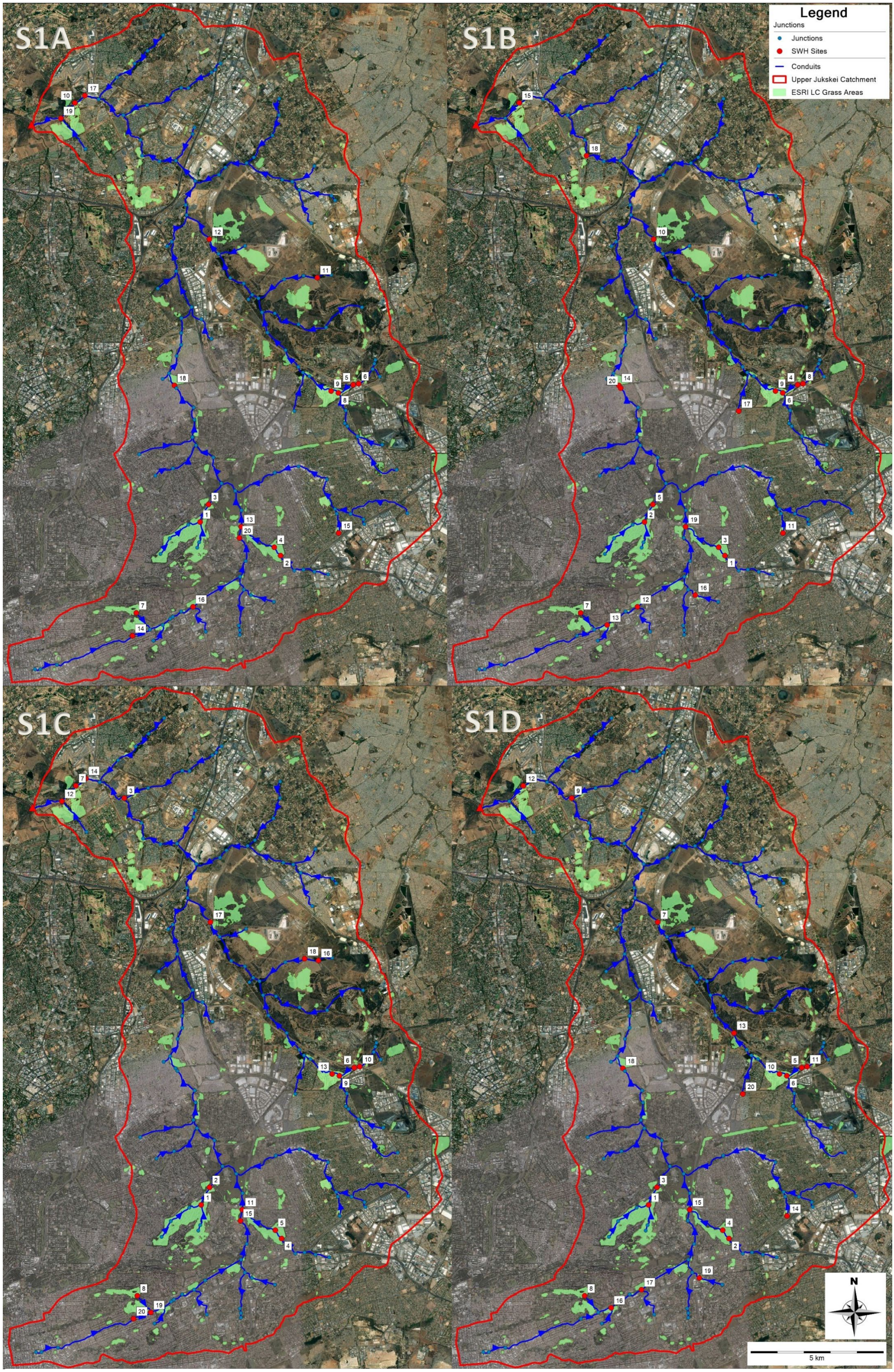

Figure 6-9: Top 20 SWH Sites for Scenario 1A to Scenario 1D

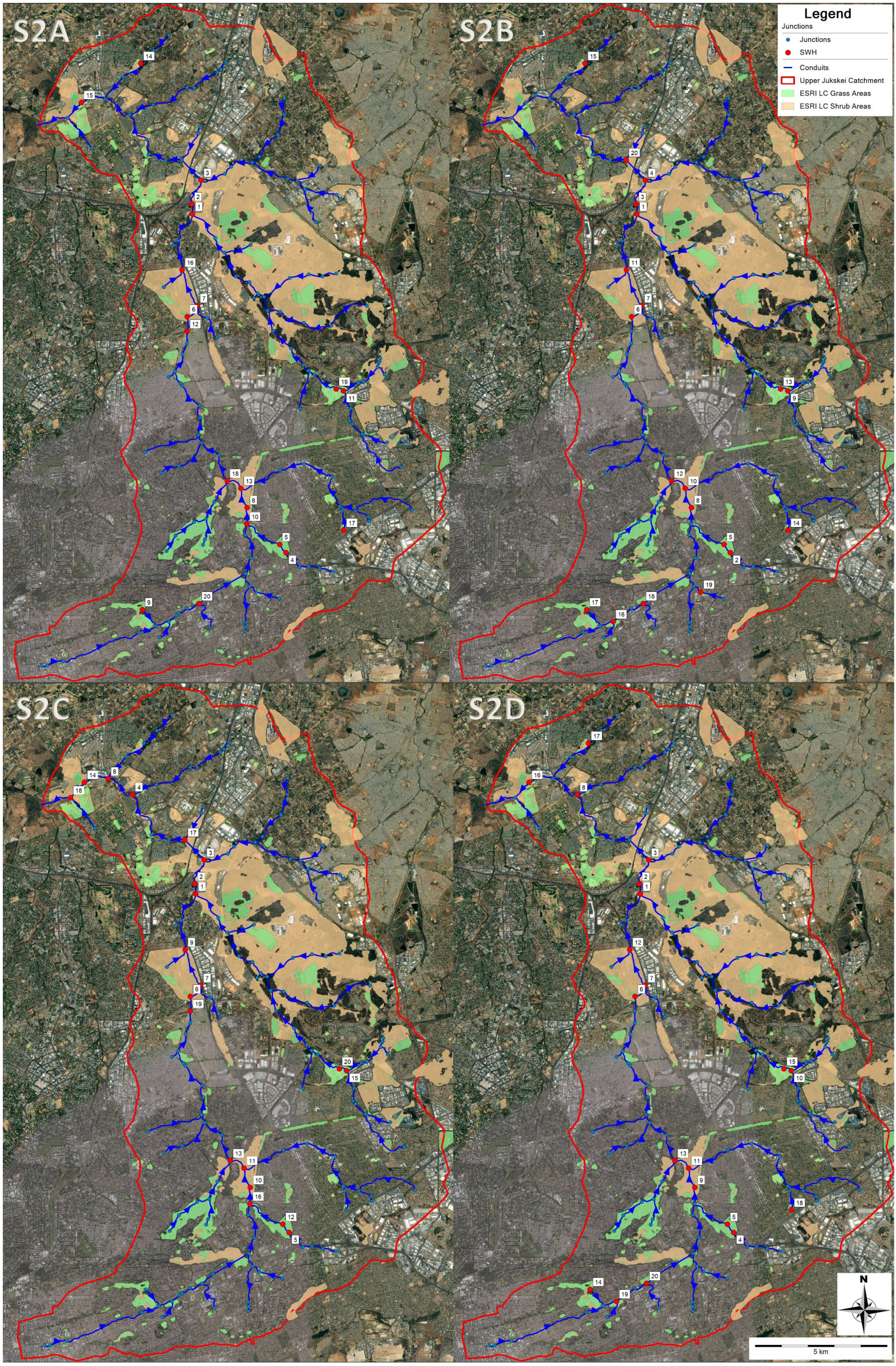

Figure 6-10: Top 20 SWH Sites for Scenario 2A to Scenario 2D

6.4.1.2 Scenario 2A Results

The results of the top 20 SWH sites for Scenario 2A is shown in **Figure 6-10** as the red junctions with their corresponding ranking shown as the number adjacent to the junction. The majority of the high-ranking areas are located in in the central parts of the Upper Jukskei Catchment. SWH sites 1 to 3 are all located immediately downstream of the very large shrub area that is centrally located with a total size of 18 059 986m². Sites 4, 5 and 9 are in the upper areas of the Upper Jukskei catchment on golf courses. Sites 6, 7 and 8 are located in the upper areas of large shrub areas in the central parts of the upper Jukskei catchment.

The results of the top 20 SWH sites for Scenario 2A is shown in **Table 6-3 below**.

The scatter plots of each metric and the SWH Score is shown as the blue dots in **Figure 6-11 to Figure 6-15** for all of the junctions in the model that met the thresholds (71 Junctions in total). The correlation of each metric to the SWH Score is shown in **Table 6-4 below**.

The correlations show the same trend and similar values to Scenario 1A with one large exception of the largest available area for SWH site that has a correlation of 0.76. The correlation of the Largest Available Area for SWH Site of Scenario 1A is 0.003. The strong correlation is due to the very large areas that the shrub areas cover. The area in turn drives the demand metric that has weight of 30%.

Table 6-3: Results – Top 20 SWH Sites for Scenario 2A

SWH Rank	Weighted Horizontal Distance (ΔX - m)	Weighted Vertical Distance (ΔZ - m)	Non-potable Demand (Ml/annum)	Ratio - Harvestable Run-off to Demand	Largest Available Area for SWH Site (m^2)	SWH Score
1	0.00	-17.23	5418.00	2.48	18 059 986.97	0.74
2	89.76	-16.24	5418.00	2.51	18 059 986.97	0.70
3	84.48	-8.02	5418.00	2.73	18 059 986.97	0.63
4	0.00	-34.52	179.03	3.63	596 773.56	0.56
5	23.84	-22.75	179.03	4.26	596 773.56	0.45
6	0.65	-12.00	797.79	12.35	2 637 389.37	0.39
7	3.98	-10.80	797.79	12.50	2 637 389.37	0.38
8	8.28	-11.72	554.40	7.67	1 774 864.97	0.37
9	114.19	-16.09	180.34	1.59	277 318.75	0.36
10	214.47	-15.18	751.16	5.49	1 774 864.97	0.35
11	0.00	-11.42	151.72	8.19	505 723.13	0.35
12	239.32	-14.70	791.22	12.35	2 637 389.37	0.34
13	1.46	-7.67	536.08	11.80	1 774 864.97	0.34
14	63.10	-11.38	33.08	7.63	75 905.77	0.32
15	61.74	-6.55	596.24	28.89	1 140 893.16	0.31
16	0.00	-2.54	791.22	12.92	2 637 389.37	0.31
17	25.30	-7.96	6.33	32.71	21 097.39	0.30
18	0.00	-2.84	532.46	13.29	1 774 864.97	0.29
19	0.00	-4.75	151.72	8.95	505 723.13	0.28
20	41.50	-6.89	21.40	103.17	67 479.35	0.28

Table 6-4: Scenario 2A – Correlation of All Junctions to SWH Score

Metric	Correlation
Weighted Horizontal Distance (ΔX - m)	-0.53
Weighted Vertical Distance (ΔZ - m)	-0.73
Non-potable Demand (Ml/annum)	0.76
Ratio - Harvestable Run-off to Demand	-0.14
Largest Available Area for SWH Site (m^2)	0.76

The results from Scenario 2A shows the following summarised results:

- Keep SWH Demand areas close and downhill of the SWH site.
- Aim for a run-off to demand ration of near unity, where once the ratio exceeds 5 the excess water does not significantly increase the SWH Score.
- The largest available area does increase the SWH Score due to the area also being part of the demand calculations.

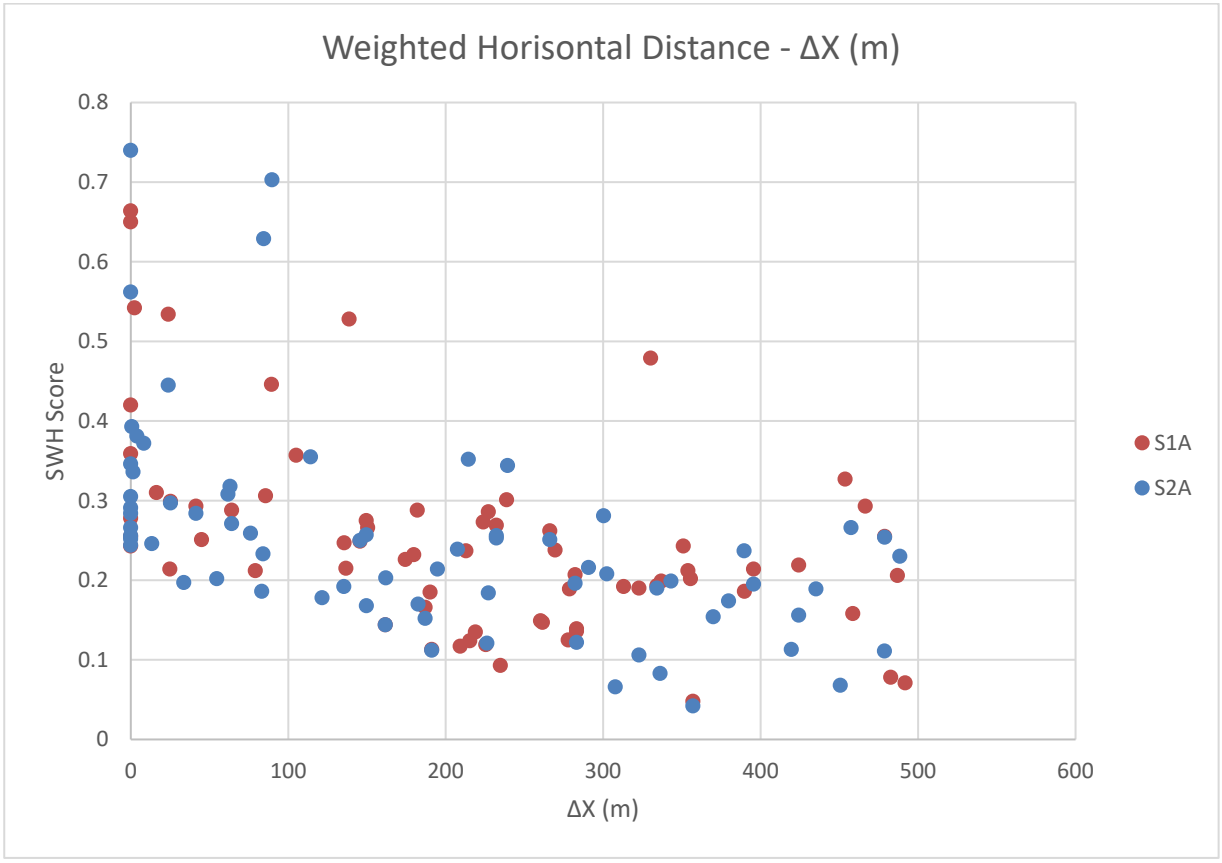

Figure 6-11: Scatter Plot - Weighted Horizontal Distance - ΔX

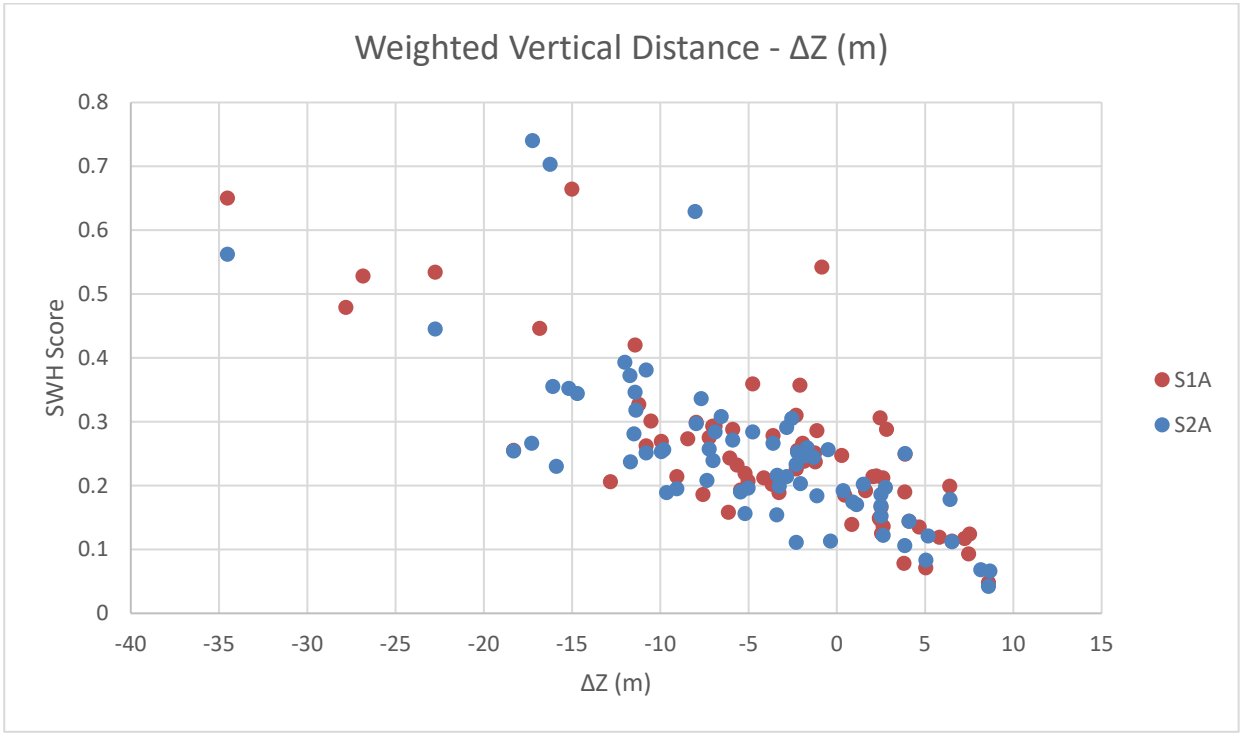

Figure 6-12: Scatter Plot - Weighted Vertical Distance - ΔZ

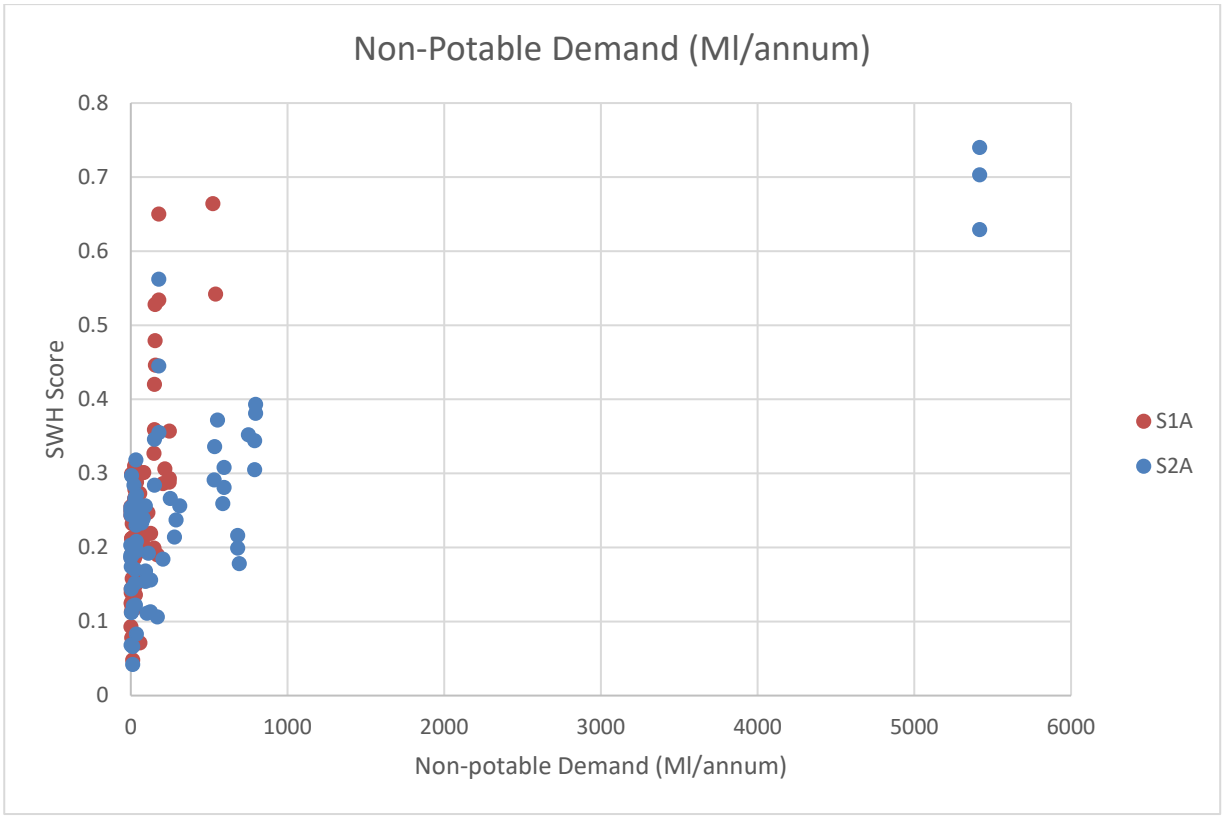

Figure 6-13: Scatter Plot - Non-Potable Demand (Ml/annum)

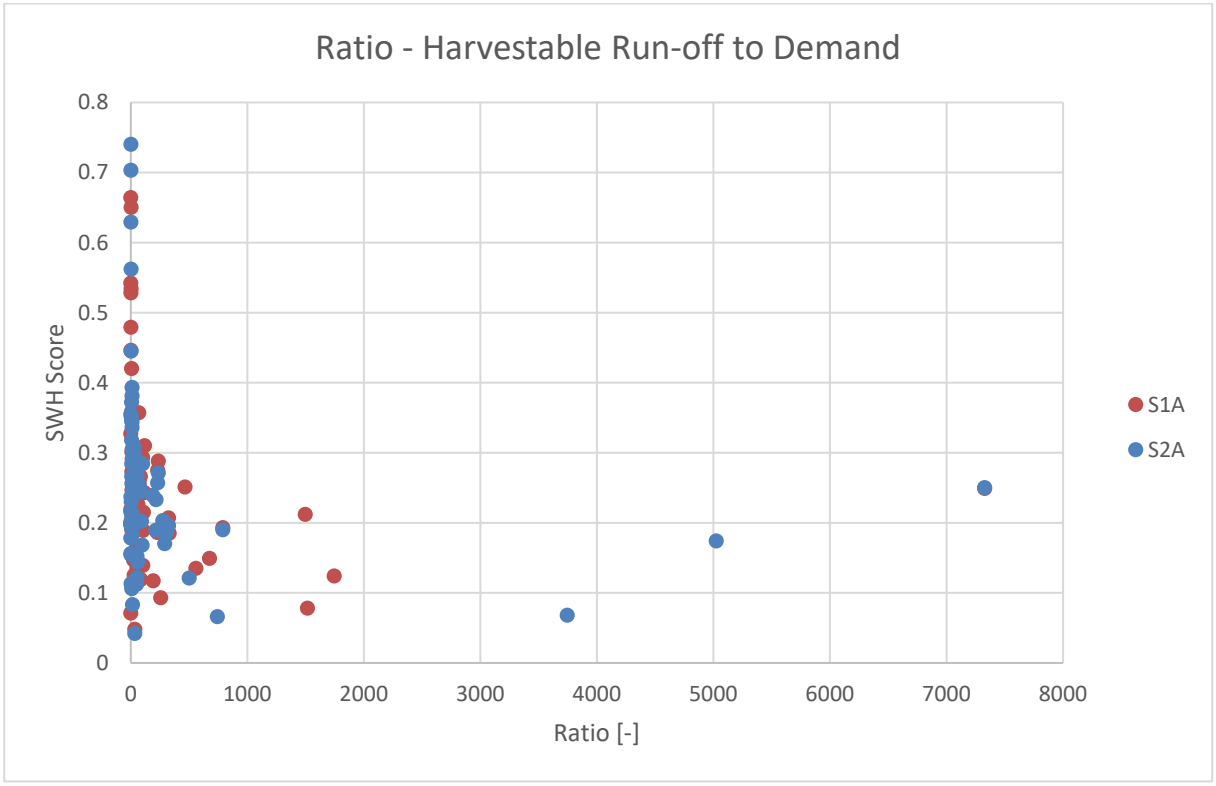

Figure 6-14: Scatter Plot - Ratio - Harvestable Run-off to Demand

Figure 6-15: Scatter Plot – Largest Available Area for SWH Site (m²)

6.4.2 Results of Scenario 1B to 1D & Scenario 2B to 2D

Variations B to D were added to gauge different objectives through changes in the weighting and to gauge if the SWH site locations would change considerably from the Variation A locations.

6.4.2.1 Results of Scenario 1B-1D

The scatter plots for all the Scenario 1 Variations (Scenario 1A to Scenario 1D) are attached in **Annexure D.** The correlations for all the scenario 1 variations are shown in **Table 6-5.** The correlations show that the horizontal, vertical and demand metrics have the highest correlation to the SWH score across all 4 variations showing the importance of these metrics in the overall ranking of the SWH site.

The ratio harvestable run-off to demand maintains a low correlation, even for Scenario 1C (Demand Driven) where it was assigned a weight of 30% (second highest after Demand with 40%). The available area shows near zero correlations for all four variations and adds little additional distinguishment value when considering only the grass areas as demand centres. Future studies should consider redefining this metric (e.g. cost per m^2) or leaving it out.

Table 6-5: Scenario 1 Variations (1A to 1D) Correlations

Metric	Correlation			
	S1A	S1B	S1C	S1D
Weighted Horizontal Distance (ΔX - m)	-0.51	-0.74	-0.49	-0.75
Weighted Vertical Distance (ΔZ - m)	-0.77	-0.69	-0.45	-0.54
Non-potable Demand (Ml/annum)	0.72	0.53	0.85	0.60
Ratio - Harvestable Run-off to Demand	-0.11	-0.06	0.17	0.07
Available Area for SWH Site (m^2)	0.0003	-0.04	0.03	0.12

The visual positions of the Top 20 SWH sites for each Scenarios 1A to 1D are shown **Figure 6-9.** Scenario 1A was used as the base case with each variation change shown relative to it in **Table 6-6.**

Example usage of Table 6-6:

- The Junction that has a SWH Rank 6 for Scenario 1A has a SWH Rank of 8 for Scenario 1B, a SWH Rank of 10 for Scenario 1C and a SWH Rank of 11 for Scenario 1D.
- The Junction that has a SWH Rank 11 for Scenario 1A did not show up as one of the top 20 SWH sites in Scenario 1B and Scenario 1D.
- Scenario 1C has 3 junctions that have SWH Ranks within the Top 20 that were not part of the Top 20 SWH sites in Scenario 1A. Scenario 1C therefore has 3 New SWH sites with SWH Rank 3, 18 and 19 shown at the bottom of the table.

Table 6-6: Changes in SWH Rank relative to Scenario 1A

SWH Rank			
S1A	**S1B**	**S1C**	**S1D**
1	2	1	1
2	1	4	2
3	5	2	3
4	3	5	4
5	4	6	5
6	8	10	11
7	7	8	8
8	6	9	6
9	9	13	10
10	15	7	12
11	N/A	16	N/A
12	10	17	7
13	19	11	15
14	N/A	20	N/A
15	11	N/A	14
16	12	N/A	17
17	N/A	14	N/A
18	14	N/A	18
19	N/A	12	N/A
20	N/A	15	N/A
New SWH Sites			
	13	3	9
	16	18	13
	17	19	16
	18		19
	20		20

It is evident that the first 5 SWH Rank sites of Scenario 1A rank very high for the remaining 3 Scenarios. SWH Rank 7 and SWH Rank 8 of Scenario 1A also have high ranks for the remaining Scenarios. The variability in ranks across the various Scenarios becomes evident as the Scenario 1 SWH ranks increase. The new sites that show up in Scenario 1B, 1C and 1D show that SWH Rank 3 of Scenario 1C (also the junction for SWH Rank 9 for Scenario 1D) is worthwhile for further investigation as was not picked up by Scenario 1A.

The SWH Rankings from all four scenarios show that the methodology is fairly successful in consistently pointing out the top 10 SWH sites. The results from Scenario 1A, Scenario 1C and Scenario 1D are very similar for the first 10 SWH Rank junctions.

Scenario 1A did however miss out on the junction that shows up as SHW Rank 3 in Scenario 1C and SWH Rank 9 in Scenario 1D. In Scenario 1A this junction has SWH Rank of 30. The junction in Scenario 1C is shown below in **Figure 6-16** with the 500m buffer. Only the smaller of the two grass areas in the 500m buffer would serve as a demand area due to the larger grass area being 20.873m higher than the junction.

The junction has a weighted horizontal distance of 145.67m, a weighted vertical distance of 2.26m, an annual demand of 2.26 Mℓ, a ratio of harvestable run-off to demand of 7328.16 and an available area for a SWH plant of 7517.97 m². This shows that it might be worthwhile to adopt the Scenario 1C or 1D weighting for future assessments where only the grass areas are considered as demand areas as the weighting used in Scenario 1A missed this junction as part of the top 20 SWH sites.

Figure 6-16: Scenario 1C - SWH Rank 3 Junction

6.4.2.2 Results of Scenario 2B-2D

The scatter plots for all the Scenario 2 variations (Scenario 2A to Scenario 2D) are attached in **Annexure E**. The correlations for all the scenario 1 variations are shown in **Table 6-7.** Similar to the Scenario 1 results, the correlations show of the horizontal, vertical and demand metrics are among the highest once again underpinning the importance of these metrics in the overall ranking of the SWH site.

Similar to Scenario 1, the ratio harvestable run-off to demand maintains a low correlation, even for variation C (Demand Driven) where it was assigned a weight of 30% (second highest after Demand with 40%). The available area shows a very strong correlation which is completely different to the results in Scenario 1 that had an almost zero correlation. The large areas that the shrub areas contribute to the overall demand area and demand in Mℓ/annum could be a reason for the large correlation in Scenario 2 as opposed to Scenario 1.

Table 6-7: Scenario 1 Variations (2A to 2D) Correlations

Metric	Correlation			
	S2A	S2B	S2C	S2D
Weighted Horizontal Distance (ΔX - m)	-0.53	-0.88	-0.53	-0.74
Weighted Vertical Distance (ΔZ - m)	-0.73	-0.48	-0.31	-0.51
Non-potable Demand (Ml/annum)	0.76	0.52	0.86	0.70
Ratio - Harvestable Run-off to Demand	-0.14	-0.14	0.21	0.003
Available Area for SWH Site (m^2)	0.76	0.52	0.86	0.70

The visual positions of the Top 20 SWH sites for each Scenarios 2A to 2D are shown Error! Reference source not found.. Scenario 2A was used as the base case with each variation change shown relative to it in **Table 6-8.**

Example usage of Table 6-8:

- The Junction that has a SWH Rank 11 for Scenario 2A has a SWH Rank of 9 for Scenario 2B, a SWH Rank of 15 for Scenario 2C and a SWH Rank of 10 for Scenario 2D.
- The Junction that has a SWH Rank 10 for Scenario 2A did not show up as one of the top 20 SWH sites in Scenario 2B and Scenario 2D.
- Scenario 2B has 3 junctions that have SWH Ranks within the Top 20 that were not part of the Top 20 SWH sites in Scenario 2A. Scenario 2B therefore has 3 New SWH sites with SWH Rank 16, 19 and 20 shown at the bottom of the table.

Table 6-8: Changes in SWH Rank relative to Scenario 1A

SWH Rank			
S2A	**S2B**	**S2C**	**S2D**
1	1	1	1
2	3	2	2
3	4	3	3
4	2	5	4
5	5	12	5
6	6	6	6
7	7	7	7
8	8	10	9
9	17	N/A	14
10	N/A	16	N/A
11	9	15	10
12	N/A	19	N/A
13	10	11	11
14	15	N/A	17
15	N/A	14	16
16	11	9	12
17	14	N/A	18
18	12	13	13
19	13	20	15
20	18	N/A	20
New SWH Sites			
	16	4	8
	19	8	19
	20	17	
		18	

It is evident that the first 4 SWH Rank sites of Scenario 2A rank very high for the remaining 3 Scenarios. SWH Rank 5, 6, 7 & 8 of Scenario 2A also have high ranks for the remaining Scenarios. The variability in ranks across the various Scenarios becomes evident as the Scenario 2 SWH ranks increase. The new sites that show up in Scenario 2B, 2C and 2D show that SWH Rank 4 of Scenario 2C (also the junction for SWH Rank 8 for Scenario 2D) is worthwhile for further investigation as was not picked up by Scenario 2A.

Similar to Scenario 1 the SWH Rankings from all four scenarios show that the methodology is fairly successful in consistently pointing out the top 8 SWH sites. The results from Scenario 2A, Scenario 2C and Scenario 2D are very similar for the first 8 SWH Rank junctions.

Scenario 2A did however miss out on the junction that shows up as SHW Rank 4 in Scenario 2C and SWH Rank 8 in Scenario 2D. In Scenario 2A this junction has SWH Rank of 33. The junction in Scenario 2C is shown below in **Figure 6-17** with the 500m buffer. This is the same junction that was missed in the Scenario 1A analysis. Only the smaller of the two grass areas in the 500m buffer would serve as a demand area due to the larger

grass area being 20.873m higher than the junction. None of the shrub areas within the 500m buffer would serve as demand areas. The large shrub area to the North of the junction is more than 10m above the junction and the small shrub areas close to the junction are both smaller than 2500m² and where therefore disregarded. In retrospect this is a slight flaw of the determination of the demand areas as areas larger than 2500m² also contribute to the total demand, and in cases such as shown in **Figure 6-17,** the small shrub areas together with the grass area should be seen as a whole in terms of demand area. This should be addressed in future research and assessments.

Similar to the Scenario 1 example this shows that it might be worthwhile to adopt the Scenario 2C or 2D weighting for future assessments when the grass areas and shrub areas are considered as demand areas, as the weighting used in Scenario 2A missed this junction as part of the top 20 SWH sites.

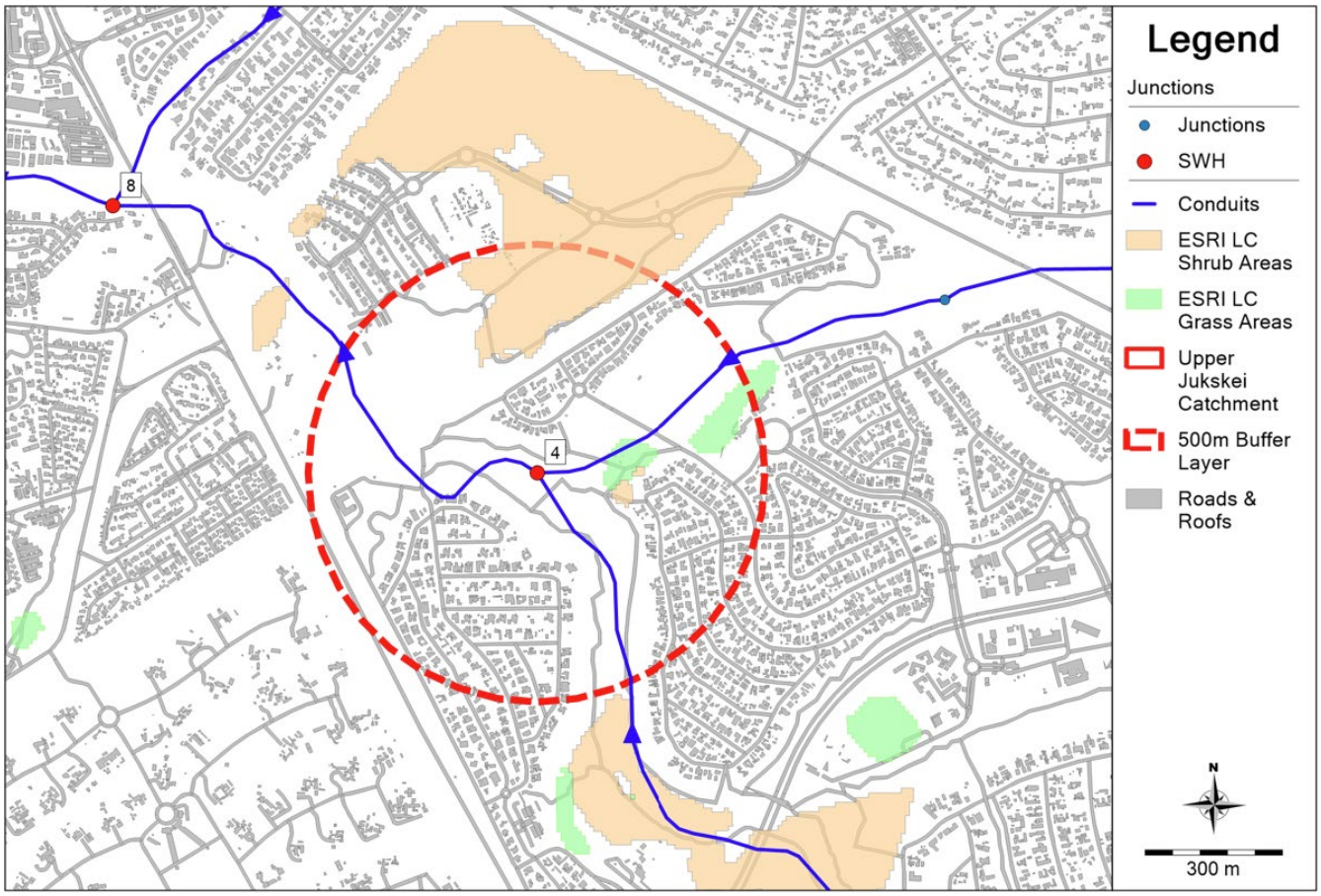

Figure 6-17: Scenario 2C - SWH Rank 4 Junction

6.5 Results of Storage and Distribution Models

6.5.1 Results of Scenario S1A-1 to Scenario S1A-4

The 4 SWH sites form Scenario 1A for which the storage and distribution models where analysed are shown in **Figure 6-18.** Interestingly all 4 SWH sites are located on or adjacent to golf courses. SWH sites 1 and 7 are located in the downstream parts of the golf courses whereas SWH sites 2 and 5 are located close to the upstream parts of the golf courses.

The results for the 4 SWH sites from the Scenario 1A simulation, are shown in **Table 6-9 below**. The water demand for SWH sites 2, 5 & 7 is very similar, whereas SWH site 1 has a significantly larger demand which is driven by the large the surface area of the two golf courses adjacent to one another. The ratio of harvestable volume to demand is close to unity for SWH site 1, around 2 for SWH sites 2 and 5 and almost 4 for SWH Site 2. SWH Sites 1 and 5 have the largest area available to build a SWH plant.

Figure 6-18: Scenario 1A – Locations for Storage and Distribution Models

Table 6-9: Scenario 1A - Results from Collection Model for Storage and Distribution Models

Scenario	SWH Rank	Weighted Horizontal Distance (ΔX - m)	Weighted Vertical Distance (ΔZ - m)	Non-potable Demand (Ml/annum)	Ratio - Harvestable Run-off to Demand	Largest Available Area for SWH Site (m^2)	SWH Score
S1A-1	1	0	-15.003	524.798	1.196	1 774 865	0.664
S1A-2	2	0	-34.521	179.032	3.631	596 773	0.650
S1A-3	5	138.69	-26.8329	156.171	2.065	2 277 103	0.528
S1A-4	7	89.381	-16.8288	158.458	1.814	277 318	0.446

The storage-, bio-filtration - and re-use facilities where iteratively sized to optimise reliability and increase resilience. The maximum daily demand for each scenario together with scaling factors were used to the determine the sizing of the various facilities. The scaling factors that were used are shown in **Table 6-10**. The volumes of the storage facilities are shown for a scaling factor of 10.

Table 6-10: Scaling Factors used for Storage Sizing of Scenario 1A Storage & Distribution Models

SWH Site Attribute	Factor	Scenario			
		S1A-1	S1A-2	S1A-3	S1A-4
Max Demand (m^3/day)	-	5 757	1 964	1 713	1 738
Rounded Up Max Demand (m^3/d)	-	5 800	2 000	1 800	1 800
Storage Facility (m^3)	**10**/15/20	**58 000**	**20 000**	**18 000**	**18 000**
Bio-filter Facility (m^3)	4	23 200	8 000	7 200	7 200
Re-Use Facility (m^3)	3	17 400	6 000	5 400	5 400

The sizing factor of the storage unit was adjusted to see how it affects the resilience and reliability of the SWH system. The storage unit is the 1st part of the SWH plant and governs the volume of water that is routed to the bio-filtration unit and the re-use facility. The Storage unit is also where the excess water that cannot be stored is spilled. The increase in the storage unit capacity increases the reliability and resilience of the SWH system by enabling the system to bridge longer dry periods. The reliability and resilience results of the 4 scenarios are shown in **Table 6-11** where 3 different storage unit scaling factors where considered.

Table 6-11: Reliability and Resilience of Scenario 1A Storage & Distribution Models

Metric	Scenario											
	S1A-1 (SWH 1)			S1A-2 (SWH 2)			S1A-3 (SWH 5)			S1A-4 (SWH 7)		
Storage Scaling Factor	10	15	20	10	15	20	10	15	20	10	15	20
Volumetric Reliability	0.774	0.818	0.851	0.925	0.958	0.975	0.842	0.881	0.909	0.858	0.899	0.927
Time Based Reliability	0.916	0.932	0.945	0.974	0.986	0.991	0.945	0.959	0.968	0.952	0.966	0.975
Resilience	0.165	0.169	0.176	0.165	0.177	0.189	0.194	0.191	0.210	0.175	0.178	0.204
Avg Failure Duration (days)	6.048	5.918	5.690	6.047	5.658	5.280	5.145	5.222	4.760	5.714	5.615	4.893
Overflow Ratio	0.380	0.336	0.299	0.743	0.727	0.717	0.398	0.358	0.327	0.568	0.533	0.505

It is clear to see that as the storage size increases from a factor of 10x the maximum daily demand to 20 x times the maximum daily demand each one of the reliability and resilience metrics improves. The volumetric reliability increases to above 85% and the time-based reliability increases to above 90% for all 4 SWH sites. The average failure duration also comes down to below 6 days for all 4 SWH sites. It is clear that the two sites with the higher ratio of harvestable run-off to demand achieve better reliability and resilience metrics than the two sites that have a ratio of close to unity.

The overflow ratio also becomes smaller due to the large storage volume and the utilisation of more of the harvestable run-off. Scenario S1A-1 and Scenario S1A-3 show that SWH Site 1 and SWH Site 5 utilise close to 70% of the harvestable inflow with an overflow factor of ±30%. The overflow factor of 71.7% shows that scenario S1A-2 (SWH Site 2) can further increase its reliability by increasing the storage size and could most likely give 100% time based and volumetric reliability if the storage size is big enough.

The increase in the reliability and resilience comes at the cost of increasing the storage capacity. A trade-off therefore exists between capital cost for storage and the reliability of the system. The larger the storage, the higher the capital cost, the more reliable the system is. Smaller storage leads to a lower capital investment but also to a lower overall reliability and resilience of the system. The above results are encouraging and show that the SWH sites can potentially be used to excellent effect to satisfy the demand with quite a high confidence in the reliability of the system.

6.5.2 Results of Scenario S2A-1 to Scenario S2A-4

The 4 SWH sites form Scenario 2A for which the storage and distribution models where analysed are shown in **Figure 6-19.** SHW Sites 1, 6 & 8 are located in open shrub areas and SWH Site is located just upstream of a gold course.

The results for the 4 SWH sites from the Scenario 2A simulation, are shown in **Table 6-12**. The water demand for SWH sites 6, 8 & 15 is very similar, whereas SWH site 1 has a significantly larger demand which is driven by the large the surface area of the large shrub area located in the centre of **Figure 6-19**. The ratio of harvestable volume to demand is almost 2.5 for SWH site 1. The other sites have a ratio in excess of 7. All 4 SWH plants have a substantial area, in excess of 1 000 000m², on which to build the SWH plant .

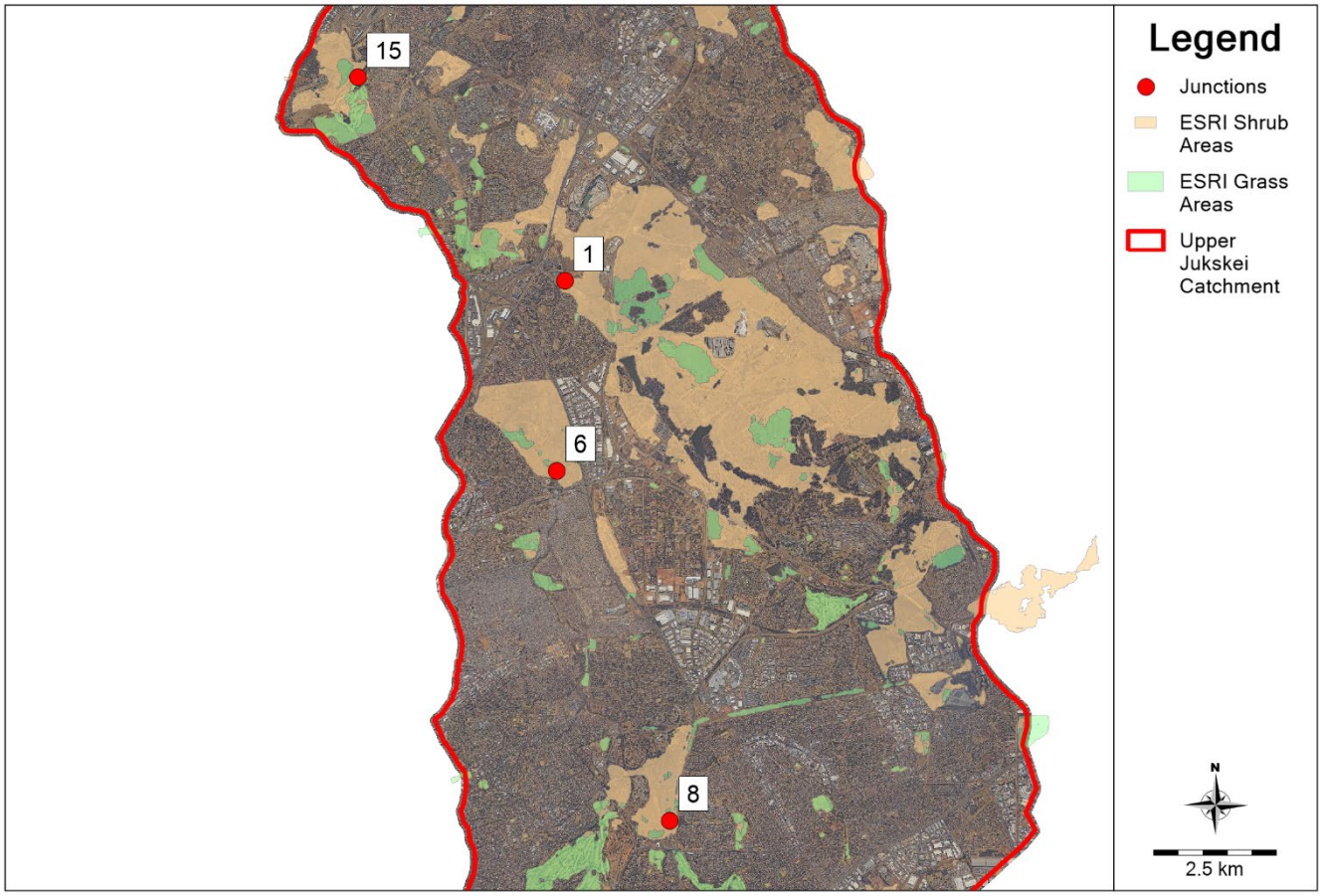

Figure 6-19: Scenario 2A – Locations for Storage and Distribution Models

Table 6-12: Scenario 2A - Results from Collection Model for Storage and Distribution Models

Scenario	SWH Rank	Weighted Horizontal Distance (ΔX - m)	Weighted Vertical Distance (ΔZ - m)	Non-potable Demand (Ml/annum)	Ratio - Harvestable Run-off to Demand	Largest Available Area for SWH Site (m^2)	SWH Score
S2A-1	1	0.00	-17.23	5418.00	2.48	18 059 986.97	0.74
S2A-2	6	0.65	-12.00	797.79	12.35	2 637 389.37	0.39
S2A-3	8	8.28	-11.72	554.40	7.67	1 774 864.97	0.37
S2A-4	15	61.74	-6.55	596.24	28.89	1 140 893.16	0.31

The storage-, bio-filtration - and re-use facilities were sized similarly to the storage and distribution models for Scenario 1A with scaling factors based on the maximum daily demand. The scaling factors that were used are shown in **Table 6-13**. The volumes of the storage facilities are shown for a scaling factor of 10.

Table 6-13: Scaling Factors used for Storage Sizing of Scenario 1A Storage & Distribution Models

SWH Site Attribute	Factor	Scenario			
		S1A-1	S1A-2	S1A-3	S1A-4
Max Demand (m^3/day)	-	59 434	8 752	6 082	6 541
Rounded Up Max Demand (m^3/d)	-	59 500	8 800	6 100	6 600
Storage Facility (m^3)	**10**/15/20	**595 000**	**88 000**	**61 000**	**66 000**
Bio-filter Facility (m^3)	4	238 000	35 200	24 400	26 400
Re-Use Facility (m^3)	3	178 500	26 400	18 300	19 800

Similar to the Scenario 1A Storage & Distribution models, the sizing factor of the storage unit was adjusted to see how it affects the resilience and reliability of the SWH system. The reliability and resilience results of the 4 scenarios are shown in **Table 6-14** where 3 different storage unit scaling factors where considered.

Table 6-14: Reliability and Resilience of Scenario 1A Storage & Distribution Models

Metric	Scenario											
	S2A-1 (SWH 1)			S2A-2 (SWH 6)			S2A-3 (SWH 8)			S2A-4 (SWH 15)		
Storage Scaling Factor	10	15	20	10	15	20	10	15	20	10	15	20
Volumetric Reliability	0.881	0.923	0.952	0.973	0.989	0.995	0.955	0.979	0.989	0.984	0.994	0.997
Time Based Reliability	0.958	0.972	0.983	0.990	0.996	0.998	0.985	0.993	0.996	0.994	0.998	0.999
Resilience	0.151	0.159	0.179	0.191	0.180	0.120	0.185	0.128	0.161	0.202	0.147	0.188
Avg Failure Duration	6.604	6.288	5.574	5.241	5.545	8.333	5.395	7.786	6.222	4.944	6.800	5.333
Overflow Ratio	0.594	0.570	0.551	0.925	0.921	0.919	0.882	0.877	0.873	0.961	0.959	0.958

The trend is similar to the Storage & Distribution models of Scenario S1A where with an increase in the storage volume, so the reliability and resilience metrics improves. The volumetric reliability increases to above 95% and the time-based reliability increases to above 98% for all 4 SWH sites.

Interestingly the failure duration increases in few cases as the storage capacity increases. This is due to there being less failures and the ratio of continuous failures over total days of failure increasing. This is illustrated for the factor 10 model of Scenario S2A-2 that has a resilience of 0.191 and an average failure duration of 5.241 (1/0.191 = 5.241), where this model has 152 days of failure and 29 continuous failures (29/152 = 0.191). The factor 15 model of Scenario S2A-2 that has a resilience of 0.18 and an average failure duration of 5.545 (1/0.18 = 5.545), where this model has 61 days of failure and 11 continuous failures (11/61 = 0.18). The factor 20 model of Scenario S2A-2 that has a resilience of 0.12 and an average failure duration of 8.333 (1/0.12 = 8.333) where this model has 25 days of failure and 3 continuous failures (3/25 = 0.12). This shows that careful interpretation of the resilience and average failure duration is needed in conjunction with the total number of failures and the number of continuous failures.

The overflow ratio for all 4 scenarios is quite considerable, especially the three sites lower down in the catchment. This is due to the large upstream area that contributes to a significant volume of harvestable run-off. The ration of harvestable run-off to demand for the three lower sites is higher than 7, indicating that there are significant volumes that can be harvested more than the demand.

The trade-off between capital cost for storage and the reliability of the system is an integral part of the final solution, although not addressed in this research. Future studies could look to include the economics of the SWH sites in the final scoring. The above results are encouraging and show that the SWH sites can potentially be used to excellent effect to satisfy the demand with quite a high confidence in the reliability of the system.

7. CONCLUSION

This study developed an integrated GIS-based hydrological screening tool that uses publicly available spatial datasets to identify and rank the suitable stormwater harvesting sites in the Upper Jukskei Catchment of Johannesburg. The approach combined GIS analysis, remote sensing data and hydrological modelling to determine the high-yielding stormwater harvesting sites as a screening tool for more detailed analysis. The use of publicly available datasets ensured that this tool is applicable and can be utilised and reproduced in various African urban areas, especially where local data availability and data quality is a problem. The top ranked sites were typically those in close proximity to a large non-potable water demand areas that had favourable topographic conditions and could allow for a gravity feed system or pumping with a minimal head.

The analysis clearly demonstrates the potential of stormwater harvesting in sustainably supplying non-potable water uses such as irrigation of parks, golf courses, sports fields and the establishment of grass areas/parks in the shrub areas. The study also shows how stormwater harvesting could enhance urban resilience in the face of growing water demand and climate change.

This study did not consider potable water demand, nor did it consider water quality. This tool can easily be adapted to include potable water demand, but a much larger focus would need to be placed on the water quality. The tool can also be used and adjusted for managed aquifer recharge.

The non-potable water demand was calculated with the pre-defined weather station data available for Johannesburg within CROPWAT. Johannesburg has a clear rainfall period which coincides with the warmer summer months which are beneficial for the growth of grass. If the tool is used in other parts of Africa the alignment of the rainfall period and the demand for water could be somewhat skewed. It is recommended that for each assessment the rainfall patterns and the chosen grass or “crop” to irrigate are adjusted based on the local conditions and need. The local need might not be for the irrigation of grass areas, but for rural or urban farming. It is recommended for ease of use that the weather station data is used that is available in CROPWAT. Alternatively, an assessment of the water demand can be made with alternative calculations or software.

The research has considered two research questions:

1) *Can high yielding (hotspot) stormwater harvesting sites be identified with publicly available data?*
2) *How reliable are these stormwater harvesting sites at supplying demand?*

The collection models showed that high yielding stormwater harvesting sites can be identified with publicly available data. The sites are however dependent on the weights that were allocated to the 5 metrics used to score the sites. It is recommended that the weights be adjusted to suit the needs of the project being considered, such as a demand driven need or an economic need. All 4 weightings showed to be very consistent in pointing out the top 8 stormwater harvesting sites.

Future assessments should also consider if the grass areas as demand (Scenario 1) or a grass and shrub areas as demand (Scenario 2) should be used. The grass areas as demand is ideal if existing water uses need to be replaced or supplemented with an alternative water source, such as golf courses using potable water for irrigation and being able to utilise stormwater harvesting to supply the majority of their irrigation needs. The grass and shrub areas as demand showed that the large shrub areas dominated the demand. These shrub areas can be repurposed into amendable areas for the public such as parks or sports fields. This assessment did not consider alternative crops to growing grass, but future assessments could look at urban and rural farming.

The storage and distribution models showed that with a storage facility that has a capacity of 10x the maximum daily demand, high reliability figures can be achieved in excess of 80% in terms of volume and time-based reliability. The storage and distribution models also showed that if the storage capacity can be increased, the reliability and resilience of the facility can also be increased. Future assessments might also be more space constrained than the Upper Jukskei river catchment and might prohibit the installation of storage facilities as large as 10 times the maximum daily demand. The space constraints can factored into future assessments with the available area metric.

The study does also have some limitations and intrinsic uncertainties due to the use of publicly available data and by using an uncalibrated hydrological model. The uncertainties and limitations are however why this tool was meant only as a screening tool and not be used as an absolute guide on where the best stormwater harvesting site is. The tool has been developed to rather point out good potential sites that can be used as a starting point for a much more thorough and detailed analysis.

Recommendations on future research that can be done in this field is summarised below:

- Incorporating water quality aspects into the identification of the best stormwater harvesting sites.
- Incorporating reliability and resilience into the ranking of the best stormwater harvesting sites.
- Model calibration using remote sensing and satellite products to enhance the reliability of the hydrological model.
- Policy and stakeholder analysis in the adoption of stormwater harvesting into guidelines, standards and water management policies.
- Environmental and ecological assessments of the downstream influence of stormwater harvesting.
- Economic and life cycle cost analysis of how to attract investment into stormwater harvesting schemes.
- Treatment of harvested stormwater to non-potable and potable water standards.

This study places focus on stormwater harvesting as an integral part of sustainable management of urban water and presents a robust, adaptable and scalable tool that can support urban areas across Africa to address the growing water demand challenges.

REFERENCES

Ali, M. (2021). Urbanisation and energy consumption in Sub-Saharan Africa. *The Electricity Journal*, *34*(10), 107045. https://doi.org/10.1016/J.TEJ.2021.107045

Armitage, N., Lloyd, F.-J., Winter, K., & Vice, M. (2013). *South African Guidelines for Sustainable Drainage Systems*. https://www.researchgate.net/publication/274076390

ASCE. (1992). Design and construction of urban stormwater management systems. In *American Society of Civil Engineers, Manuals and Reports on Engineering Practice* (Issue 77).

Bailey, A. K., & Pitman, W. V. (2015). *WATER RESOURCES OF SOUTH AFRICA 2012 STUDY (WR2012) EXECUTIVE SUMMARY Version 1*.

Barnard, J., Brooker, C., Dunsmore, S., & Fitchett, A. (2019). *Stormwater Design Manual for the City of Johannesburg*.

Batjes, N. H. (2004). *SOTER-based soil parameter estimates for Southern Africa*.

Bega, S. (2021, August 15). *Climate crisis: "Day Zero" drought risk for Gauteng - The Mail & Guardian*. https://mg.co.za/environment/2021-08-15-climate-crisis-day-zero-drought-risk-for-gauteng/

Carden, K., & Fisher-Jeffes, L. (2017, March 21). *Stormwater harvesting could help South Africa manage its water shortages*. https://theconversation.com/stormwater-harvesting-could-help-south-africa-manage-its-water-shortages-74377

Chitonge, H. (2020). Urbanisation and the water challenge in Africa: Mapping out orders of water scarcity. *Https://Doi-Org.Tudelft.Idm.Oclc.Org/10.1080/00020184.2020.1793662*, *79*(2), 192–211. https://doi.org/10.1080/00020184.2020.1793662

City of Melbourne. (n.d.). *Fitzroy Gardens Stormwater Harvesting System | City of Melbourne Urban Water*. Retrieved December 15, 2022, from https://urbanwater.melbourne.vic.gov.au/projects/water-capture-and-reuse/fitzroy-gardens-stormwater-harvesting-project/

COGTA - JHB Profile. (2020).

Computational Hydraulics International (CHI). (n.d.-a). *Introduction to SWMM Hydraulics*.

Computational Hydraulics International (CHI). (n.d.-b). *SWMM Hydrology Quantity Modeling*.

CRC. (2018). *Waterproofing the West - CRC for Water sensitive cities*. https://watersensitivecities.org.au/solutions/case-studies/waterproofing-the-west/

CRC - Kalkallo. (2018). *Kalkallo stormwater harvesting and reuse*. https://watersensitivecities.org.au/solutions/case-studies/kallakallo-stormwater-harvesting-and-reuse/

Dandy, G. C., Marchi, A., Maier, H. R., Kandulu, J., MacDonald, D. H., & Ganji, A. (2019). An integrated framework for selecting and evaluating the performance of stormwater harvesting options to supplement existing water supply systems. *Environmental Modelling & Software*, *122*, 104554. https://doi.org/10.1016/J.ENVSOFT.2019.104554

Dillon, P. (2005). Future management of aquifer recharge. *Hydrogeology Journal*, *13*(1), 313–316. https://doi.org/10.1007/s10040-004-0413-6

Du, G., & de Villiers, T. (1996). South Africa's Water Resources and the Lesotho Highlands Water Scheme: A Partial Solution to the Country's Water Problems. *International Journal of Water Resources Development*, *12*(1), 65–77. https://doi.org/10.1080/713672193

du Plessis, K., & Kibii, J. (2021). Applicability of CHIRPS-based satellite rainfall estimates for South Africa. *Journal of the South African Institution of Civil Engineering*, *63*(3), 43–54. https://doi.org/10.17159/2309-8775/2021/v63n3a4

Dunsmore, S. (2020). *UPPER JUKSKEI CATCHMENT MANAGEMENT PLAN HYDROLOGICAL MODEL PHASE 1: STATUS QUO MODEL*.

DWAF. (2010). *The Atlantis Water Resource Management Scheme: 30 years of Artificial Groundwater Recharge*.

Dyson, L. (2009). Heavy daily-rainfall characteristics over the Gauteng Province. *Water SA*, *35*(5). http://www.wrc.org.za

Echols, S., & Pennypacker, E. (2015). The History of Stormwater Management and Background for Artful Rainwater Design. *Artful Rainwater Design*, 7–22. https://doi.org/10.5822/978-1-61091-318-8_2

European Investment Bank. (2002, November 26). *Lesotho Highlands Water Project*. https://www.eib.org/en/press/news/lesotho-highlands-water-project

Fisher-Jeffes, L. (2015). *The viability of rainwater and stormwater harvesting in the residential areas of the Liesbeek River Catchment, Cape Town*. University of Cape Town.

Fisher-Jeffes, L. N., Armitage, N. P., & Carden, K. (2017). The viability of domestic rainwater harvesting in the residential areas of the liesbeek river catchment, Cape Town. *Water SA*, *43*(1), 81–90. https://doi.org/10.4314/wsa.v43i1.11

Foster, S., Eichholz, M., Nlend, B., & Gathu, J. (2020). Securing the critical role of groundwater for the resilient water-supply of urban Africa. *Water Policy*, *22*, 121–132. https://doi.org/10.2166/wp.2020.177

Funk, C., Peterson, P., Landsfeld, M., Pedreros, D., Verdin, J., Shukla, S., Husak, G., Rowland, J., Harrison, L., Hoell, A., & Michaelsen, J. (2015). The climate hazards infrared precipitation with stations—a new environmental record for monitoring extremes. *Scientific Data 2015 2:1*, *2*(1), 1–21. https://doi.org/10.1038/SDATA.2015.66

Hargreaves, G. H., Asce, F., & Allen, R. G. (1998). *History and Evaluation of Hargreaves Evapotranspiration Equation*. https://doi.org/10.1061/ASCE0733-94372003129:153

Hashimoto, T., Stedinger, J. R., & Loucks, D. P. (1982). Reliability, Resiliency, and Vulnerability Criteria For Water Resource System Performance Evaluation. *WATER RESOURCES RESEARCH*, *18*(1), 14–20.

Hatt, B. E., Deletic, A., & Fletcher, T. D. (2006). Integrated treatment and recycling of stormwater: a review of Australian practice. *Journal of Environmental Management*, *79*(1), 102–113. https://doi.org/10.1016/J.JENVMAN.2005.06.003

Heggie, J. (2020). *Day Zero: Where next?* https://www.nationalgeographic.com/science/article/partner-content-south-africa-danger-of-running-out-of-water

Inamdar, P. M., Cook, S., Sharma, A. K., Corby, N., O'Connor, J., & Perera, B. J. C. (2013). A GIS based screening tool for locating and ranking of suitable stormwater harvesting sites in urban areas. *Journal of Environmental Management*, *128*, 363–370. https://doi.org/10.1016/j.jenvman.2013.05.023

Innovyze. (n.d.). *Swale - InfoDrainage*. Retrieved December 15, 2022, from https://help.innovyze.com/display/infodrainage2021v3/Swale

James, William. (2003). *Rules for responsible modeling*. CHI.

Kaur, L., Rishi, M. S., Sharma, S., & Khosla, A. (2019). *Impervious Surfaces an Indicator of Hydrological Changes in Urban Watershed: A Review*. https://doi.org/10.32474/OAJESS.2019.04.000180

Kumar, T., & Jhariya, D. C. (2017). Identification of rainwater harvesting sites using SCS-CN methodology, remote sensing and Geographical Information System techniques. *Geocarto International*, *32*(12), 1367–1388. https://doi.org/10.1080/10106049.2016.1213772

LHDA. (2022). http://www.lhda.org.ls/lhdaweb

Liesbeek River Life Plan | Urban Water Management. (2014, October 21). http://www.uwm.uct.ac.za/news/liesbeek-river-life-plan

Lim, M. H., Leong, Y. H., & Tiew, K. N. (2011). Urban stormwater harvesting: a valuable water resource of Singapore. *Water Practice & Technology*, *6*(4). https://doi.org/10.2166/wpt.2011.067

Mahlasela, P., Oke, A., & Madonsela, N. S. (2020). Household's Satisfaction with Water Supply in Johannesburg Metropolitan Municipality, South Africa. *Procedia Manufacturing*, *43*, 183–192. https://doi.org/10.1016/J.PROMFG.2020.02.133

Makelane, H., & Roodbol, A. (2020, February 5). *South Africa approaching physical water scarcity by 2025 - ESI-Africa.com*. https://www.esi-africa.com/event-news/south-africa-approaching-physical-water-scarcity-by-2025/

Mawasha, T., & Britz, W. (2022). Detecting land use and land cover change for a 28-year period using multi-temporal Landsat satellite images in the Jukskei River catchment, Gauteng, South Africa. *South African Journal of Geomatics*, *11*(1). https://doi.org/10.4314/sajg.v11i1.2

Mcardle, P., Gleeson, J., Hammond, T., Heslop, E., Holden, R., & Kuczera, G. (2010). *Centralised urban stormwater harvesting for potable reuse*. https://doi.org/10.2166/wst.2011.003

Mcmahon, J., Heyenga, S., Marinoni, O., Jenkins, G., Maheepala, S., & Greenway, M. (2008). *Review of Stormwater Harvesting Practices*. http://www.griffith.edu.au/

Minghini, M., & Frassinelli, F. (2019). OpenStreetMap history for intrinsic quality assessment: Is OSM up-to-date? *Open Geospatial Data, Software and Standards*, *4*(1). https://doi.org/10.1186/s40965-019-0067-x

Mitchell, G., Hatt, B., Deletic, A., Fletcher, T., McCarthy, D., & Magyar, M. (2006). *Integrated Stormwater Treatment and Harvesting: Technical Guidance Report*. https://www.researchgate.net/publication/260391841

Mitchell, V. G., McCarthy, D. T., Deletic, A., & Fletcher, T. D. (2008). Urban stormwater harvesting - sensitivity of a storage behaviour model. *Environmental Modelling and Software*, *23*(6), 782–793. https://doi.org/10.1016/J.ENVSOFT.2007.09.006

Mkhize, T., Proude, M., & Thnadi, N. (n.d.). *2030 Water Resources Group – World Bank Group*. Retrieved March 23, 2022, from https://www.2030wrg.org/south-africa/background/

Mohanrao, I. P. (2014). *Selection and Evaluation of Potential Stormwater Harvesting Sites in Urban Areas*.

Ndeketeya, A., & Dundu, M. (2022). *Alternative water sources as a pragmatic approach to improving water security*. https://doi.org/10.1016/j.rcradv.2022.200071

O'Halloran, D. (n.d.). *Westfield Reserve Stormwater Harvesting Concept Design*. Retrieved December 19, 2022, from https://alluvium.com.au/project/westfield-reserve-stormwater-harvesting-concept-design/

Pordage, C. (2018, August 8). *Pioneering stormwater harvesting for potable use in Australia - Utility Magazine*. Utility Magazine. https://utilitymagazine.com.au/pioneering-stormwater-harvesting-for-potable-use-in-australia/

Roesner, L., & Matthews, R. (1990). *Stormwater Management for the 1990's*.

Rohrer, A. (2017). *The viability of using the stormwater ponds on the Diep River in the Constantia Valley for stormwater harvesting*. University of Cape Town.

Rossman, L., & Huber, W. (2016). *Storm Water Management Model Reference Manual Volume I-Hydrology (Revised)*. https://nepis.epa.gov/Exe/ZyPURL.cgi?Dockey=P100NYRA.txt

Roy, S. (2021). *ESRI 2020 Global Land Cover from Sentinel-2*. https://samapriya.github.io/awesome-gee-community-datasets/projects/esrilc2020/#credits-attributions-and-license

Siebritz, L.-A. (2014). *Assessing the Accuracy of OpenStreetMap Data in South Africa for the Purpose of Integrating it with Authoritative Data*.

Sirko, W., Kashubin, S., Ritter, M., Annkah, A., Bouchareb, Y. S. E., Dauphin, Y., Keysers, D., Neumann, M., Cisse, M., & Quinn, J. (2021). *Continental-Scale Building Detection from High Resolution Satellite Imagery*. https://developers.google.com/earth-engine/datasets/catalog/GOOGLE_Research_open-buildings_v1_polygons

Soulis, K. X., & Valiantzas, J. D. (2012). SCS-CN parameter determination using rainfall-runoff data in heterogeneous watersheds-the two-CN system approach. *Hydrol. Earth Syst. Sci*, *16*, 1001–1015. https://doi.org/10.5194/hess-16-1001-2012

South African National Roads Agency. (2013). *Drainage manual* (6th Edition).

SRTM Version 3.0. (2021, March 1). https://earthdata.nasa.gov/learn/articles/nasa-shuttle-radar-topography-mission-srtm-version-3-0-global-1-arc-second-data-released-over-asia-and-australia

SWMM | US EPA. (n.d.). Retrieved November 19, 2021, from https://www.epa.gov/water-research/storm-water-management-model-swmm

Tal, A. (2006). Seeking Sustainability: Israel's Evolving Water Management Strategy. *Science*, *313*(5790), 1081–1084. https://www.academia.edu/19715966/Seeking_Sustainability_Israels_Evolving_Water_Management_Strategy_2006_

Theeboom, E., Johnston, P., Braune, M., Hewitson, B., Coop, L., Phalatse, L., & Gwate, M. (2009). *City of Johannesburg Climate Change Adaptation Plan*.

Thukela_Vaal Transfer Scheme. (2013). *ORASECOM Report 001/2013*. https://wis.orasecom.org/content/study/UNDP-GEF/InfrastructureCatalogue/Documents/Transfers/Thukela_Vaal%20Transfer%20Scheme.pdf

Turok, I., & Borel-Saladin, J. (2014). Is urbanisation in South Africa on a sustainable trajectory? *Https://Doi-Org.Tudelft.Idm.Oclc.Org/10.1080/0376835X.2014.937524*, *31*(5), 675–691. https://doi.org/10.1080/0376835X.2014.937524

Turton, A., Schultz, C., Buckle, H., Kgomongoe, M., Malungani, T., & Drackner, M. (2007). Gold, Scorched Earth and Water: The Hydropolitics of Johannesburg. *Https://Doi-Org.Tudelft.Idm.Oclc.Org/10.1080/07900620600649827*, *22*(2), 313–335. https://doi.org/10.1080/07900620600649827

Urban Hydrology for Small Watersheds. (1986).

van Vuuren, L. (2008). *Vaal Dam - underlying Gauteng's Wealth*. https://journals.co.za/doi/abs/10.10520/EJC115724

van Zyl, J. J. (2001). Pergamon THE SHUTTLE RADAR TOPOGRAPHY MISSION (SRTM): A BREAKTHROUGH IN REMOTE SENSING OF TOPOGRAPHY. *Acta Astronautica*, *48*(12), 559–565.

Verma, P., Yadav, P., Deshpande, S., & Gubbi, J. (2016). *URBAN GROWTH STUDIES FOR JOHANNESBURG CITY USING REMOTELY SENSED DATA*.

Wang, H., Wang, T., Zhang, B., Li, F., Toure, B., Omosa, I. B., Chiramba, T., Abdel-Monem, M., & Pradhan, M. (2014). Water and Wastewater Treatment in Africa – Current Practices and Challenges. *CLEAN – Soil, Air, Water*, *42*(8), 1029–1035. https://doi.org/10.1002/CLEN.201300208

Wong, T. (2012). *Stormwater Management in a Water Sensitive City*.

Wong, T. H. F., & Brown, R. R. (2009). The water sensitive city: principles for practice. *Water Science and Technology : A Journal of the International Association on Water Pollution Research*, *60*(3), 673–682. https://doi.org/10.2166/WST.2009.436

ANNEXURE A – PCSWMM & SWMM

PCSWMM

The United States (US) Environmental Protection Agency (EPA) Surface Water Management Model (SWMM) was used to do the integrated hydrological & hydraulic modelling. SWMM is used primarily in urban areas and can model both single events and long-term continuous rainfall. SWMM is a dynamic rainfall-runoff modelling software that can model the hydrology, hydraulics and water quality (*SWMM | US EPA*, n.d.). The SWMM model schematic is shown below in **Figure A1**

PCSWMM uses the SWMM engine and includes GIS tools and scripting functionality as part of an improved graphical user interface & post processing of SWMM. PCSWMM was chosen as the software to do the modelling for this research due to its strong capability in integrating GIS & hydrological & hydraulic modelling. The PCSWMM model can also be viewed in the freeware SWMM as provided by the US EPA.

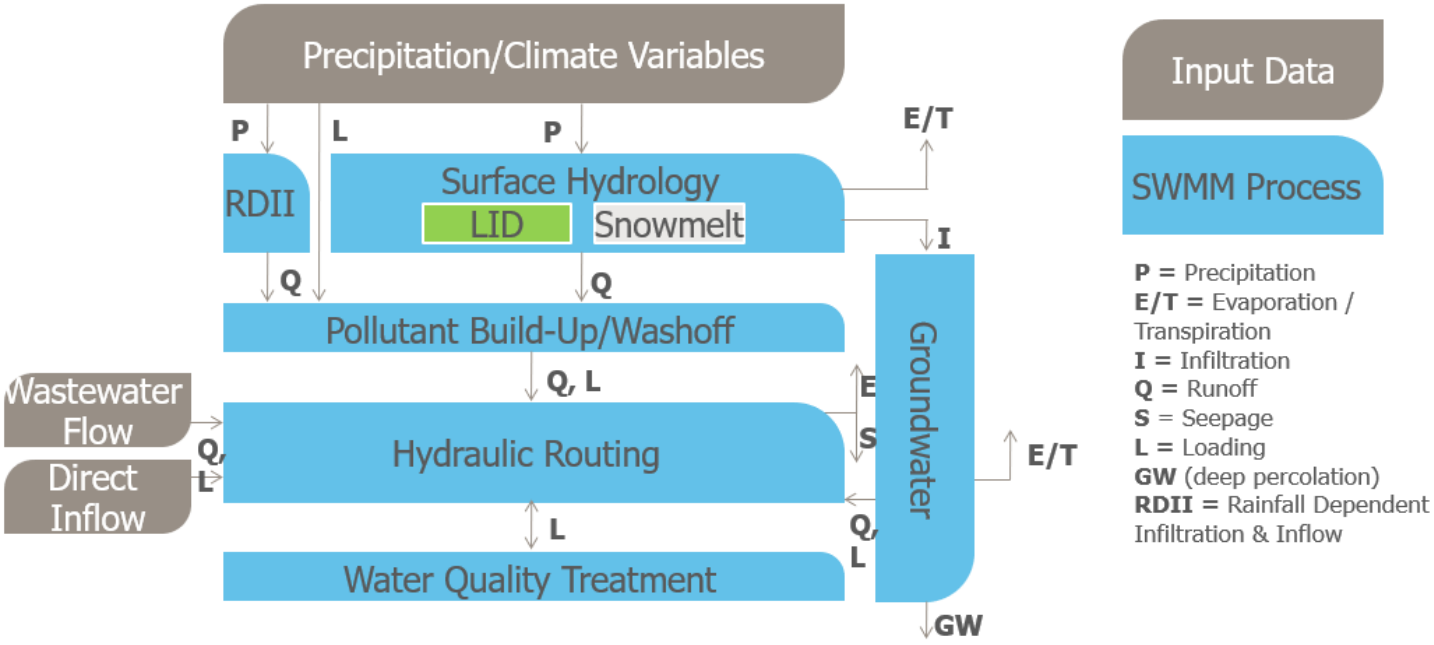

Figure A1: SWMM Processes

Hydrology

The hydrology of SWMM is modelled with subcatchments that are represented as non-linear reservoirs as is shown below in Error! Reference source not found. **A2**. The infiltration of the non-linear reservoir can be modelled with either the Horton's equation, the modified Horton's equation, the Green-Ampt equation, the modified Green-Ampt equation and SCS Curve Numbers (Computational Hydraulics International (CHI), n.d.-b). The groundwater module (which receives the infiltration as inflow) of SWMM was not utilised in this assessment.

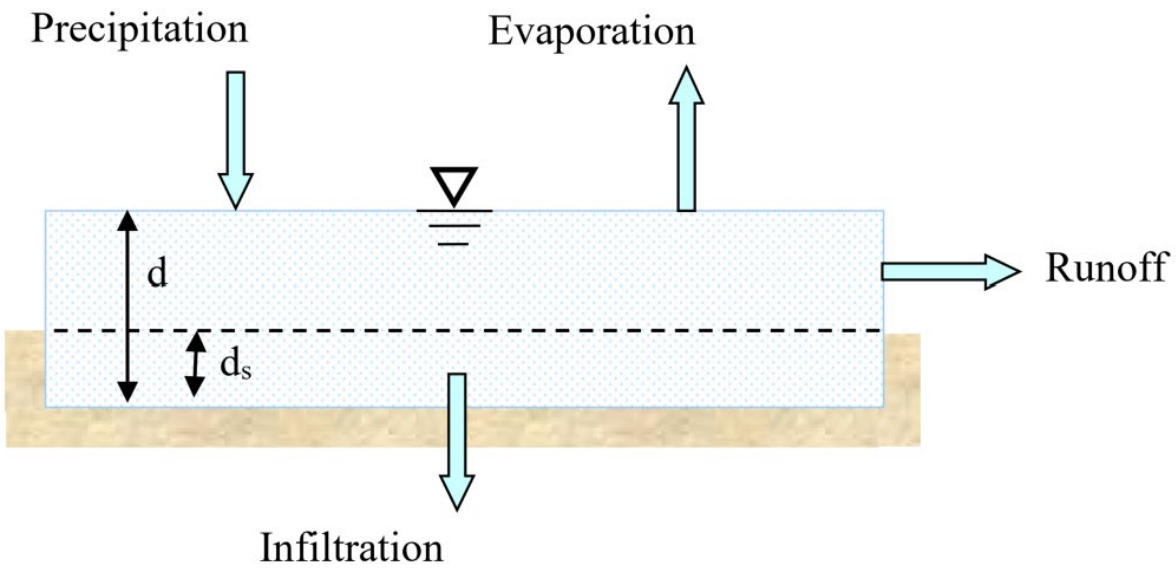

Figure A2: Non-Linear Reservoir *(SWMM | US EPA*, n.d.)

The subcatchments in SWMM are based on an idealized rectangular area where the land use is divided into two categories, namely pervious and impervious as is shown below in **Figure A3**. The pervious surfaces (fields, lawns etc.) allow rainfall to infiltrate into the soil, whereas the impervious surfaces (roads, roofs etc.) do not allow any infiltration. SWMM allows subcatchments to have both pervious and impervious subareas. The impervious subareas can further be discretized into impervious areas with depression storage (parking lots, roads, flat roofs etc.) and impervious areas without depression storage (pitched roofs).

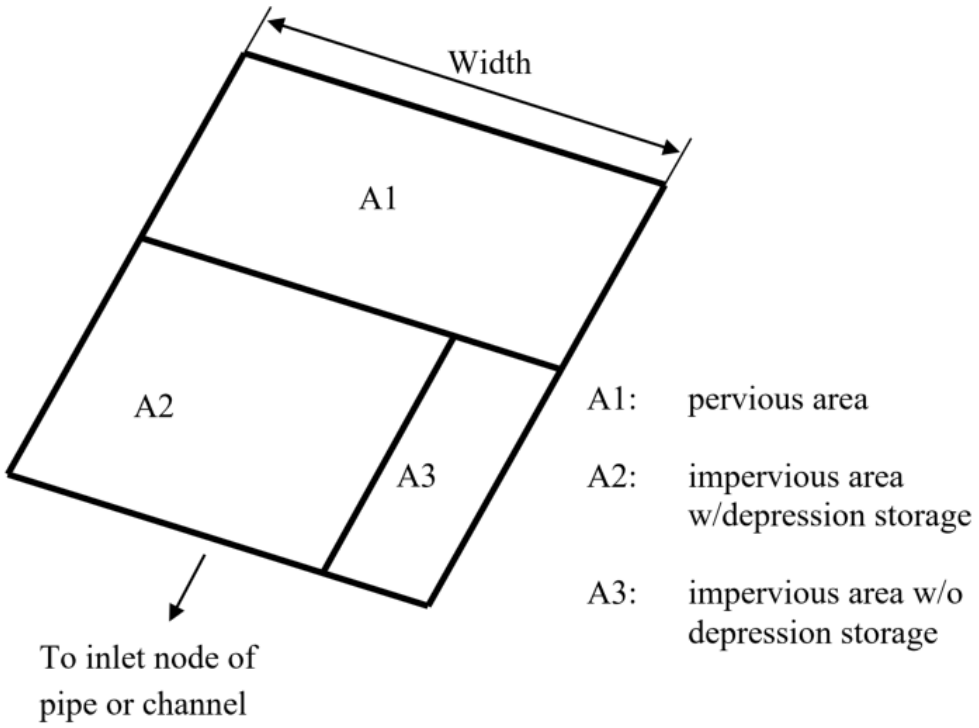

Figure A3: Idealized Rectangular SWMM Subcatchment *(SWMM | US EPA*, n.d.)

The hydrological input parameters needed for SWMM are:

- Area (Ha)
- Flow Length (m)
- Slope (%)
- Impervious Area (%)
- Impervious Area with No Depression Storage (%)
- Depression Storage for the Pervious Area (mm)
- Depression Storage for the Impervious Area (mm)
- Manning n for Pervious Area
- Manning n for Impervious Area
- Infiltration Parameters:
    - SCS Curve Number:
        - Curve Number (-)
        - Drying Time (Days)

The majority of the SWMM hydrology input parameters can be derived from land-use and soils maps through spatial weighting (Area Weighting).

Hydraulics

The hydraulics of SWMM is governed by the conservation of mass & the conservation of momentum where gradually varied unsteady flow is assumed, allowing the use of the Saint Venant Equations. The hydraulics can be modelled with either steady flow routing, kinematic wave routing or dynamic wave routing (Computational Hydraulics International (CHI), n.d.-a). The Dynamic Wave routing w used in this evaluation as it allows branched & looped networks, backwater, free surface flow, pressure flow and flow reversals. The use of dynamic wave routing makes it possible to model both the major and minor systems of urban stormwater system simultaneously. The hydraulics of SWMM are represented with nodes and conduits. The nodes have input parameters of Rim Elevation (m) & Invert Elevation (m). The conduits have input parameters on cross section type, length (m), and Manning n roughness.

ANNEXURE B - DETAILED METHODOLOGY

The workflow of this assessment is shown below in **Figure B1**. The methodology has 4 large blocks, namely, watershed delineation, hydrological model parameters, model forcing & water demand. The ranking of the SWH Hotspots was done by weighted calculation of various output parameters of the assessment. The methodology was executed in the software program PCSWMM.

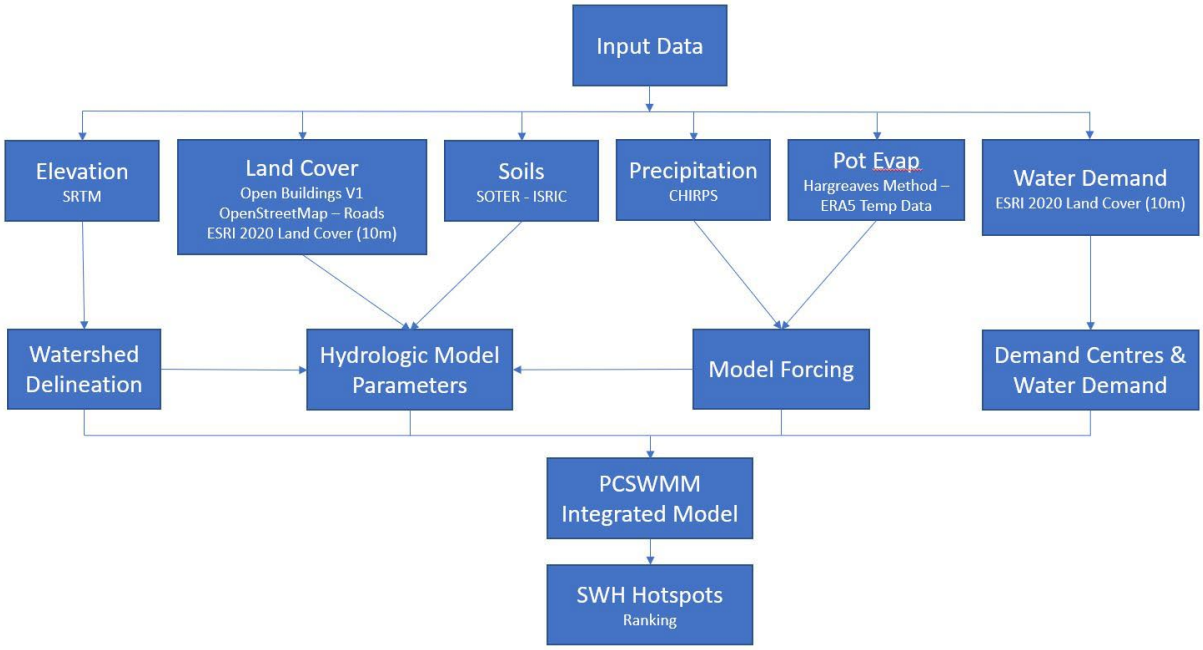

Figure B1: Workflow to Identify High-Yielding Stormwater Harvesting Sites

Watershed Delineation

The watershed delineation is done with the SRTM DEM data in PCSWMM with the Watershed Delineation Tool (WDT). The WDT creates several layers through sequential computations as per the visual representation in **Figure B2** below. The software first generates a pit filled DEM where localised ponding areas are filled in to create a smoother hydrological DEM. The program then uses the pit filled DEM to generate a flow direction grid, where each pixel analyses the eight pixels around it and determines in which direction a water droplet would flow (D8 method), based on the steepest slope to neighbouring pixels. The program then uses the flow direction grid to create a flow accumulation grid, where the upstream pixels that would contribute to flow through a pixel is determined. Lastly the program uses the flow accumulation grid to determine the watersheds and the stream network. The watersheds are defined as polygons (subcatchments) and the stream network is defined as nodes (junctions) and links (conduits) where each polygon (subcatchment) drains to a stream network node (junction). The SRTM DEM with the defined stream network links (conduits) of the Upper Jukskei catchment is shown below as **Figure B3**.

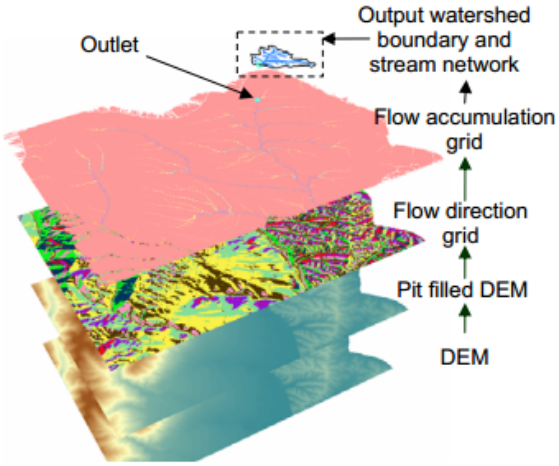

Figure B2: Watershed Delineation Process

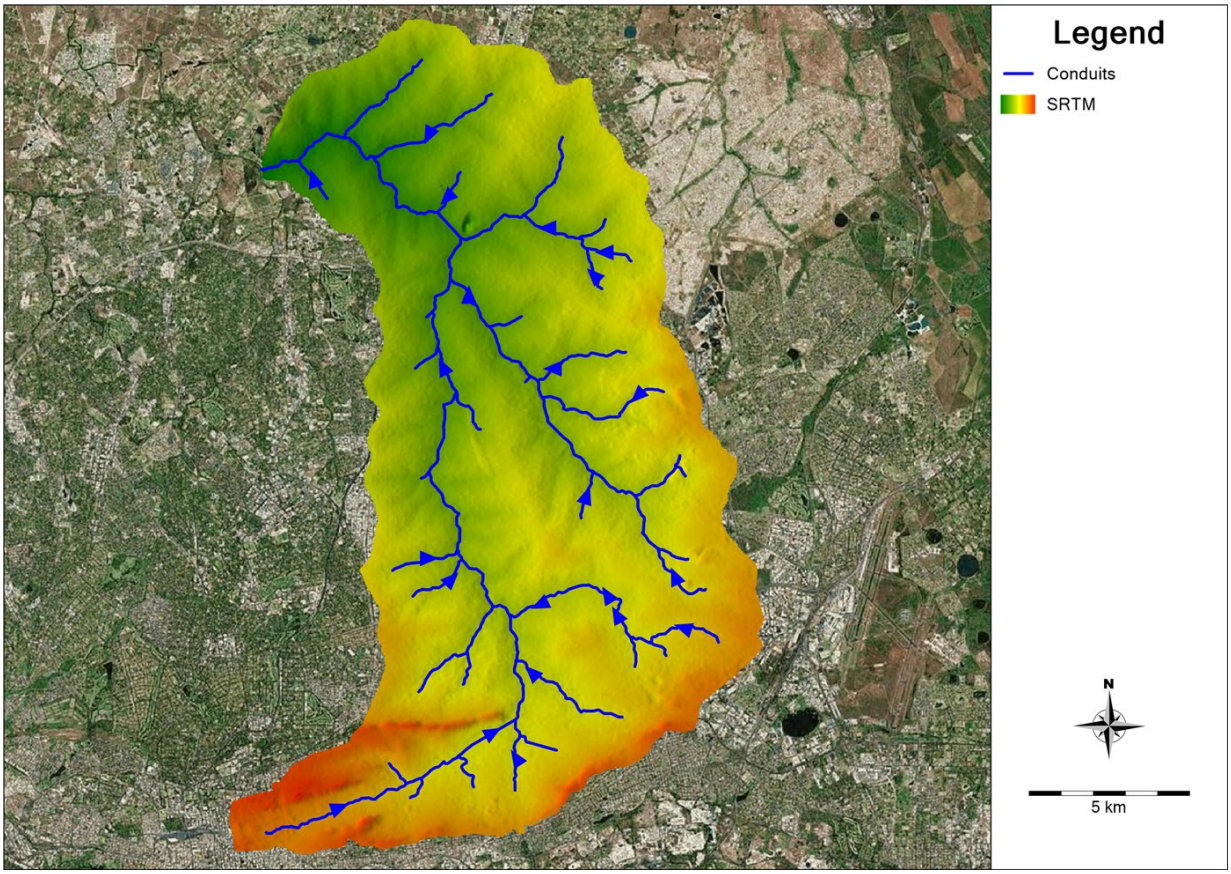

Figure B3: WDT - SRTM DEM & Stream Network Conduits of the Upper Jukskei

The polygons (subcatchments) and stream network links (conduits) that were created by the WDT of the Upper Jukskei are shown below in **Figure B4**.

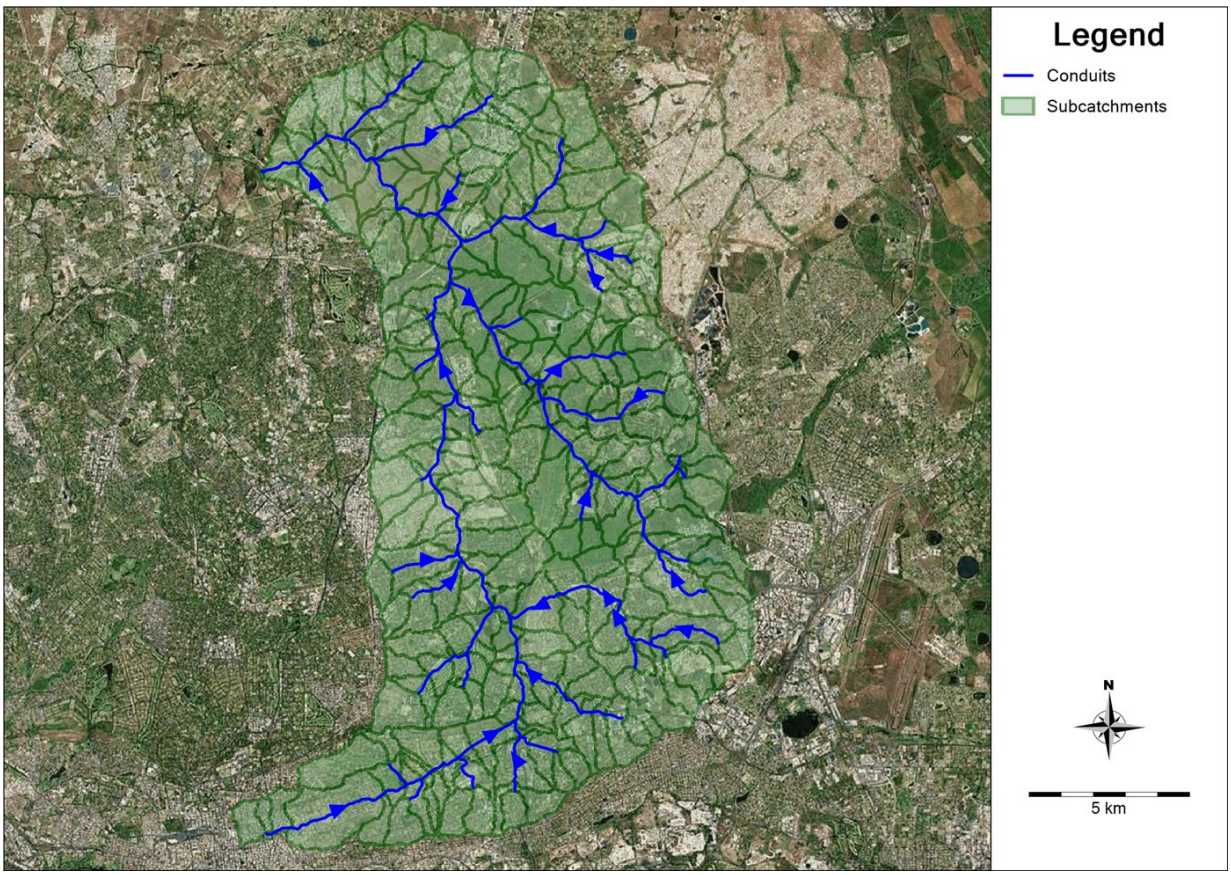

Figure B4: WDT - Subcatchments & Conduits of the Upper Jukskei

The WDT requires a target subcatchment discretization size, where the median subcatchment size of the subcatchments is specified. The software then attempts to define subcatchments roughly the size of the target discretization size, based on the topography from the DEM. The target subcatchment discretization size determines the number of subcatchments, and nodes created. The nodes are used for the determination of the SWH hotspots, and the location of these nodes can be critical in the final rankings of the SWH hotspots. The sensitivity of the target subcatchment discretization size and the number of nodes is discussed in Section 7 as part of the sensitivity analysis.

The subcatchment area is calculated from the defined watershed extent by the GIS. The subcatchment slope is determined based on the flow direction of each grid cell in the subcatchment. The flow length is determined using the method developed by Guo & Urbonas, that applies a kinematic wave approach to convert irregular shaped subcatchments to equivalent rectangular planes.

Hydrological Model Parameters

SWMM Hydrology

The subcatchments in SWMM are based on an idealized rectangular area where the land use is divided into pervious and impervious areas as is shown below in Error! Reference source not found.. The pervious surfaces (fields, lawns etc.) allow rainfall to infiltrate into the soil, whereas the impervious surfaces (roads, roofs etc.) do not allow any infiltration. The impervious subareas are further be discretized into impervious areas with depression storage (parking lots, roads, flat roofs etc.) and impervious areas without depression storage (pitched roofs). The infiltration from the pervious portion of the subcatchments were modelled with the SCS Curve Numbers. The groundwater module, which receives the infiltration as inflow, of SWMM was not utilised in this assessment, due to the time constraints of the research period and to keep the model as simple as possible. The SWMM hydrology input parameters were derived from land-use and soils maps through spatial weighting (Area Weighting).

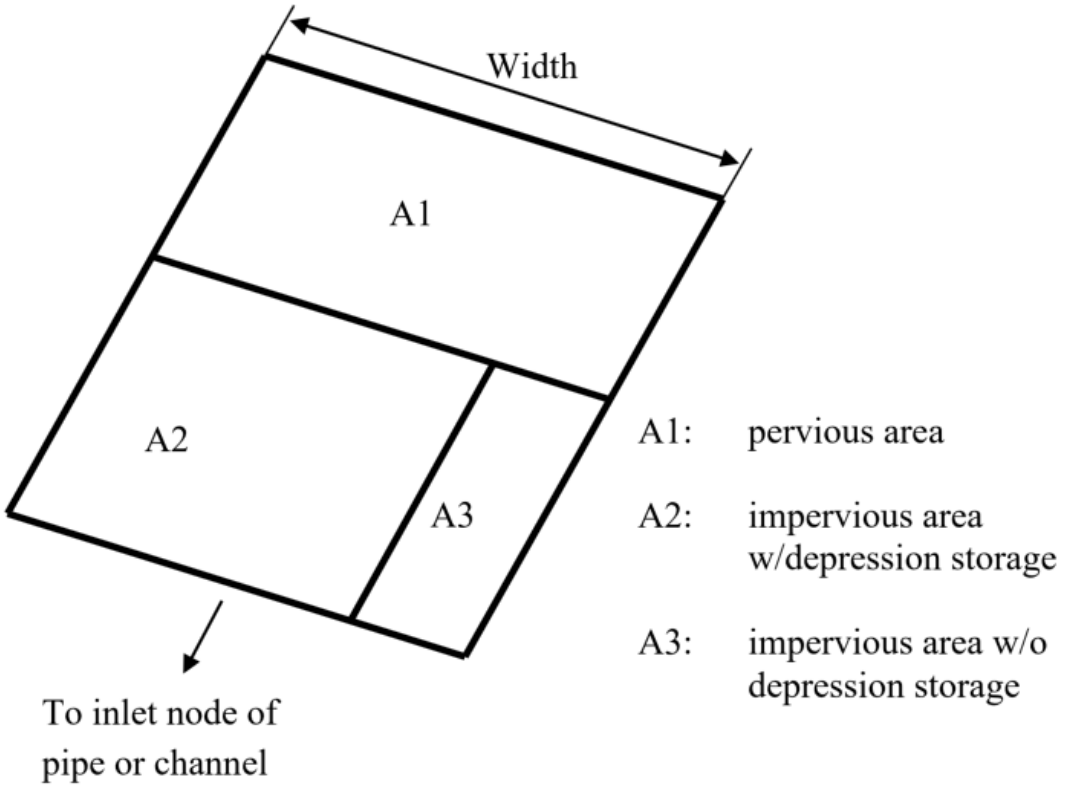

Figure B5: SWMM Idealized Rectangular Subcatchment *(SWMM | US EPA*, n.d.)

SCS Curve Number

The United States Department Soil Conservation Service (SCS) method was developed for catchments smaller than 30 km² and utilises a curve number to calculate the run-off generated by a subcatchment (South African National Roads Agency, 2013). The curve number integrates several factors including land cover, soil type, land use practices, surface condition and antecedent moisture condition (AMC) (Kumar & Jhariya, 2017). The SCS-CN is a very popular method due to its integration of the many factors that affect run-off and it's easy to obtain and well documented inputs. The SCS-CN does however not consider the intensity of rainfall, the effects of spatial scale and is highly sensitive to changes of the single curve number value (Soulis & Valiantzas, 2012).

The SCS Curve Number run-off equation is shown below in **Equation 1**

$$Q = \frac{(P - Ia)^2}{P - Ia + S} \tag{1}$$

where:

Q = run-off depth (mm)

P = rainfall depth (mm)

S = potential maximum soil water retention (mm)

Ia = initial losses prior to the commencement of run-off (mm)

The initial losses (Ia) are defined by the empirical relation in **Equation 2**. If **Equation 2** is substituted into **Equation 1** then **Equation 3** is found.

$$Ia = 0.2S \tag{2}$$

$$Q = \frac{(P - 0.2S)^2}{P + 0.8S} \tag{3}$$

The potential maximum soil water retention is related to the soil properties, land cover, land management and antecedent moisture condition of the catchment prior to the rainfall event and can be calculated with **Equation 4** below:

$$S = 25.4 * \left(\frac{1000}{CN} - 10\right) \tag{4}$$

Hydrological Soil Groups

The SCS-CN method has four hydrological soil groups (HSG) that relate to the soils run-off potential. High clay content soils produce higher run-off than low clay content soils. Similarly, well drained soils produce less run-off than poorly drained soils. The characteristics of the four hydrological soil groups are summarised below in Error! Reference source not found. from the South African Drainage Manual (6th Edition) and from the USDA.

Table B1: Characteristics of four basic SCS soil groups (South African National Roads Agency, 2013; *Urban Hydrology for Small Watersheds*, 1986)

HSG	Soil Texture	Soil Properties
Soil Group A	Sandy, loamy sand, sandy loam	Low run-off potential. Infiltration is high and permeability is rapid. Overall drainage is excessive to well-drained (Final infiltration rate ±25mm/hr, Permeability rate > 7.6 mm/hr)
Soil Group B	Silt loam or loam (Moderately fine to fine texture)	Moderately low run-off potential. Infiltration, effective depth, and drainage is moderate. Permeability is slightly restricted and soil depth tends to be shallow (Final infiltration rate ±13mm/hr, Permeability rate 3.8 mm/hr to 7.6 mm/hr)
Soil Group C	Sandy clay loam (Moderately fine to fine texture)	Moderately high run-off potential. Infiltration rate is slow and deteriorates rapidly. Soil depth tends to be shallow (Final infiltration rate ±6mm/hr, Permeability rate 1.3 mm/hr to 3.8 mm/hr)
Soil Group D	Clay loam, silty clay loam, sandy clay, silty clay, clay	High run-off potential. Infiltration is very low, with severely restricted permeability. Soils are very shallow and have a high shrink-swell potential. (Final infiltration rate ±3mm/hr, Permeability rate <1.3 mm/hr)

Notes:

1. Final infiltration and permeability rates are for a saturated soil
2. Final infiltration rates refer to soils with short grass cover
3. Infiltration rate is controlled by surface conditions, permeability is controlled by soil conditions.

Antecedent Moisture Conditions

The SCS curve numbers often found in curve number tables are for "normal" or "average" antecedent moisture conditions (AMC II). The below adjustments can be made for AMC I (low moisture) and AMC III (high moisture) conditions:

$$CN_I = \frac{4.2CN_{II}}{10 - 0.058CN_{II}} \tag{5}$$

$$CN_{III} = \frac{23CN_{II}}{10 - 0.13CN_{II}} \tag{6}$$

The SWMM hydrology manual recommends that the AMC I curve number should be used for long-term simulations to allow the soil to reach its maximum potential moisture retention capacity during extended dry spells (Rossman & Huber, 2016). Subsequently the AMC I curve numbers were used in the modelling for the upper Jukskei catchment assessment.

Drying Time

The drying time used in the SCS computations of SWMM are handled similar to the Horton and Green-Ampt recovery process. The drying time T*dry* in days can be related to the soil's saturated hydraulic conductivity K*s* in in/hr as shown below (Rossman & Huber, 2016):

$$T_{dry} = \frac{3.125}{\sqrt{K_s}} \tag{7}$$

The equation therefore predicts a drying time of 3 days for a Ks of 1 in/hr, and a drying time of 2 days for a Ks of 2 in/hr.

Subsequently to convert **Equation 7** from US units to SI units leads to **Equation 8** below for Ks in mm/hr:

$$T_{dry} = \frac{3.125}{\sqrt{K_s/25.4}} \tag{8}$$

SWMM Considerations for SCS-CN

The curve numbers typically given in the USDA manuals lump the pervious and impervious areas together for urban land cover situations. The curve number is therefore representative of both the impervious and pervious potions of the subcatchment.

SWMM does calculations for the pervious and impervious portions of the subcatchment separately before routing them both to the outlet of the subcatchment and determining the combined outflow hydrograph. To avoid double accounting of water (or the generation of too much run-off) the SWMM subcatchment should therefore not be partitioned into an impervious area and a pervious area when using the "combined" curve numbers, and the subcatchment should be modelled as 100% pervious.

Alternatively, if the partitioning of the subcatchment into impervious and pervious areas is of particular importance to the modeller the curve number assigned to the subcatchment must be representative of the pervious section of the subcatchment only (Rossman & Huber, 2016).

The SCS curve number method in SWMM is used for the infiltration calculations, which then affects the run-off calculations. Due to the infiltration calculations only being calculated for the pervious area of the subcatchment, it was decided to explicitly partition the impervious and pervious areas and to use SCS curve numbers that are only representative of the pervious section of the subcatchment.

Hydrological Model Parameter Determination

The following hydrological parameters were determined for the model:

- Impervious Area (%)
- Impervious Area with No Depression Storage (%)
- Depression Storage for the Pervious Area (mm)
- Depression Storage for the Impervious Area (mm)
- Manning n for Pervious Area
- Manning n for Impervious Area
- Infiltration Parameters:
    - SCS Curve Number:
        - Curve Number (-)
        - Drying Time (Days)
- Area (Ha)
- Flow Length (m)
- Slope (%)

The Area, Flow Length & Slope were calculated as part of the watershed delineation. The remaining SWMM hydrology input parameters were derived from the land-use and soils maps through spatial weighting (area weighting). The workflow for the hydrological parameter determination is shown below in **Figure B6**.

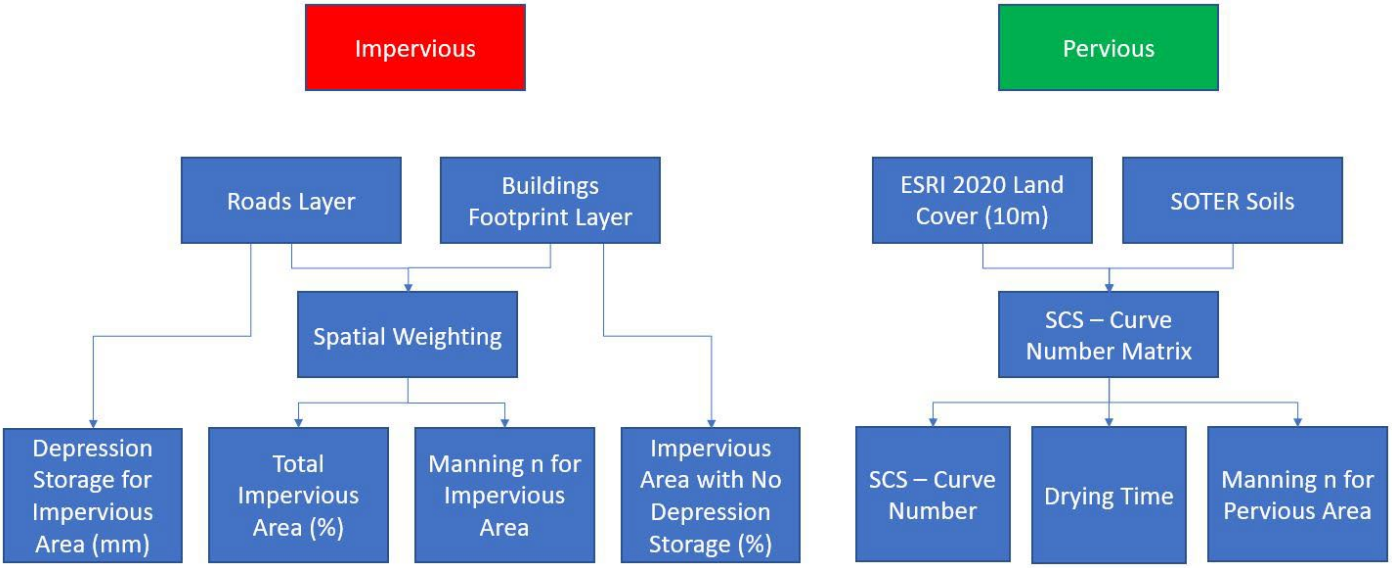

Figure B6: Hydrological Model Parameter Determination

Impervious and Pervious Areas

The impervious areas of the model were defined by the roads and the buildings footprint/roofs layers as is shown in Error! Reference source not found. for the Upper Jukskei Catchment. The total percentage impervious area of a subcatchment was calculated as the percentage of the subcatchment occupied by the roads and roofs through spatial weighting. The Impervious area of the subcatchment was further discretised into impervious area with depression storage and impervious area without depression storage. The subcatchments and their calculated impervious % is shown below in **Figure B8** for the Upper Jukskei Catchment. The pervious area of the subcatchments was determined as the total subcatchment area minus the impervious area of the subcatchment.

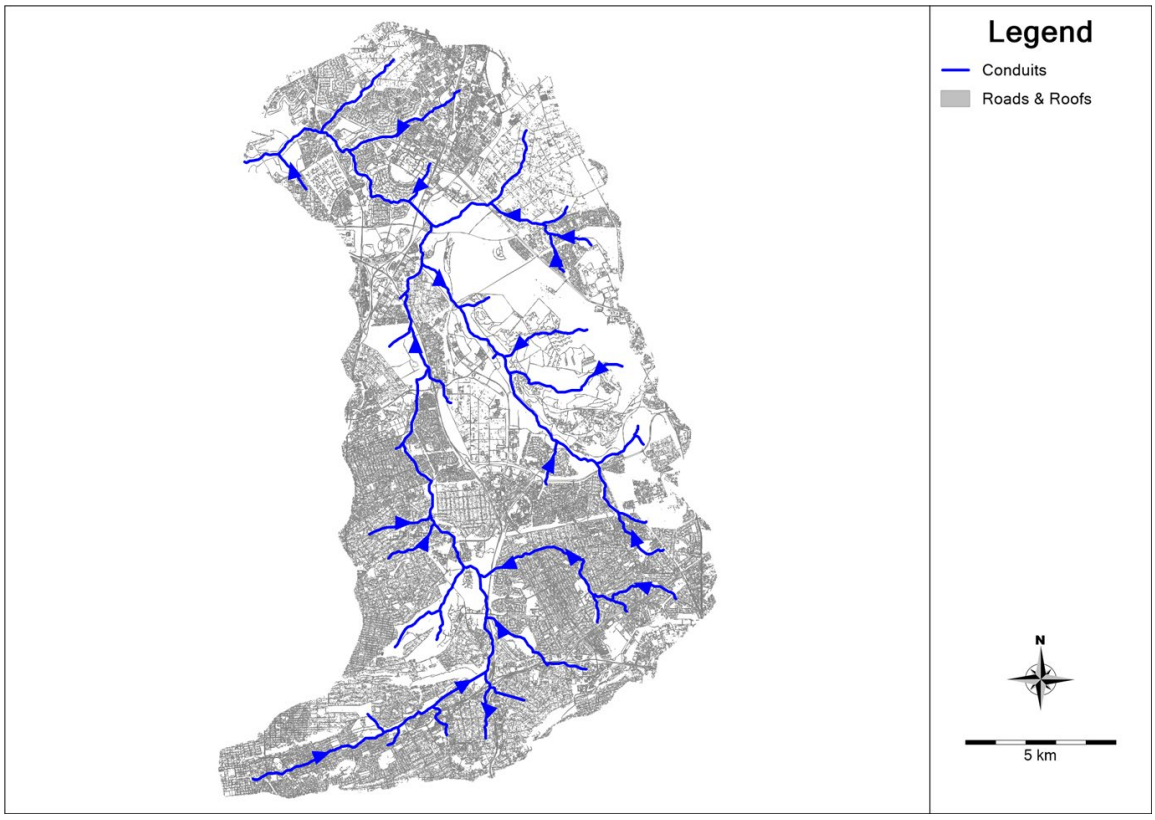

Figure B7: Roads & Roofs Layer

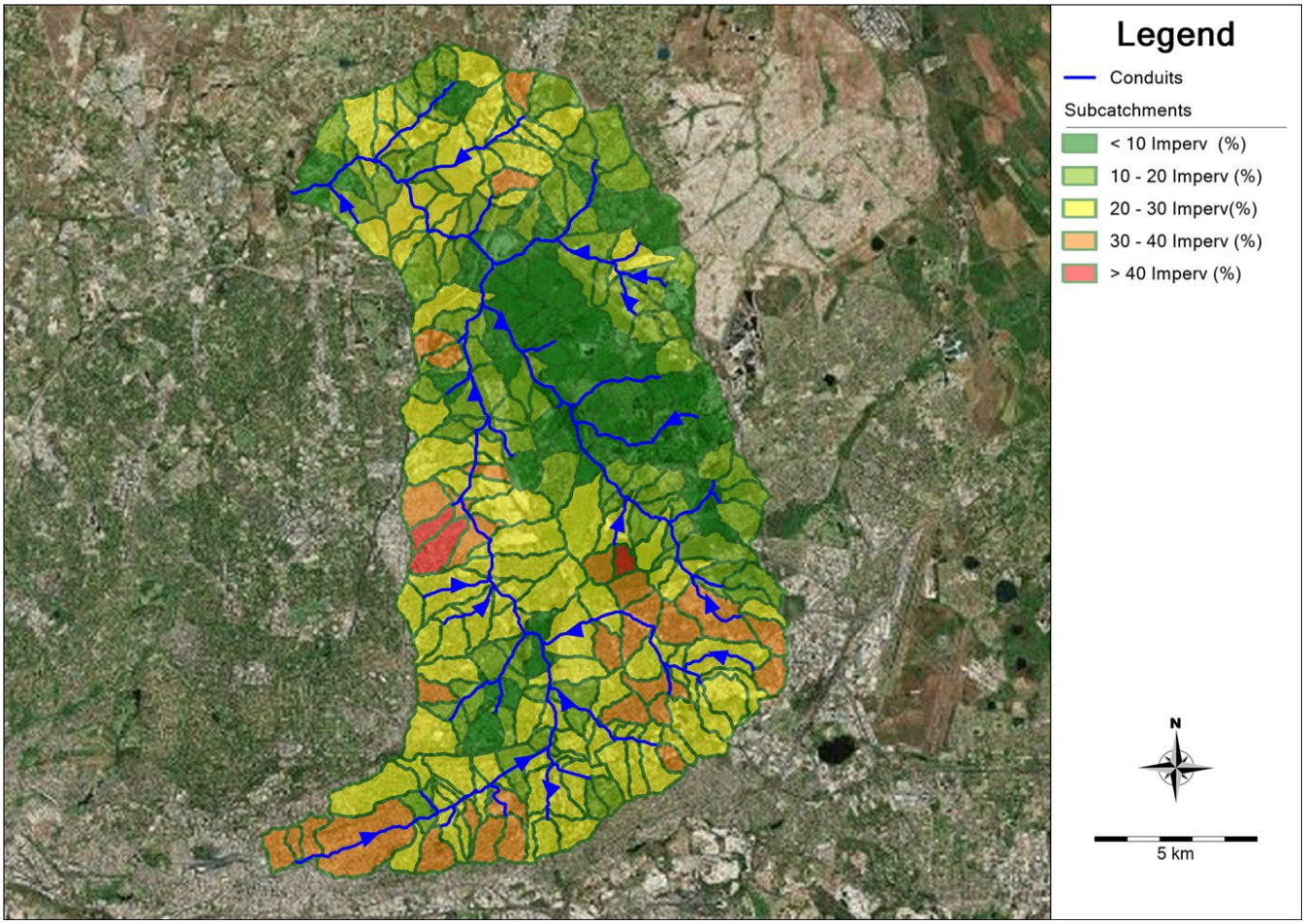

Figure B8: Subcatchment % Impervious

Depression Storage

Depression storage can visually be observed in parking lots and on roads where localised puddles occur that need fill up before run-off can occur. Steep pitched roofs are an example of impervious areas with no depression storage. The impervious area with no depression storage was taken as 40% of the roofs in the subcatchment. This is an assumption that was made based on visual observation from the satellite images and a parameter that was tested as part of the sensitivity analysis. The depression storage figures used in the model are based on the 1992 ASCE paper "Design and construction of urban stormwater management systems" (ASCE, 1992). The depression storage values used in the model for the various land uses are:

- Impervious Areas:
  - Roads: 2 mm
  - Pitched Roofs: 1.25 mm
- Pervious Areas:
  - Water: 0 mm
  - Trees: 4 mm
  - Grass: 2.5 mm
  - Flooded Areas: 6 mm
  - Crops: 5 mm
  - Shrub: 5 mm
  - Built Up: 2.5mm
  - Bare Ground: 2 mm

Manning n – Overland Flow

The Manning n overland flow values for the pervious and impervious areas are based on the Table in **Annexure C** from SWMM hydrology manual (Rossman & Huber, 2016), which is based on studies done by Crawford & Lindsey (1966), Engman (1986) and Yen (2001). The Manning n overland flow values used in the model for the various land uses are:

- Impervious Areas:
  - Roads: 0.015
  - Roofs: 0.013
- Pervious Areas:
  - Water: 0.010
  - Trees: 0.090
  - Grass: 0.075
  - Flooded Areas: 0.150
  - Crops: 0.100
  - Shrub: 0.120
  - Built Up: 0.075
  - Bare Ground: 0.030

SCS Curve Numbers

The SCS curve numbers were determined from a ERSI 2020 land-cover and SOTER soils matrix. The SOTER soils FAO soil drainage classes, shown below in **Figure B9,** were translated to SCS soil groups as shown below in **Table B2 below**.

Table B2: FAO Drainage Class to SCS Soil Group

FAO Soil Drainage Class	SCS Soil Group
Excessively Drained	A
Somewhat excessively drained	
Well drained	B
Moderately well drained	C
Imperfectly drained	
Poorly drained	D
Very Poorly Drained	

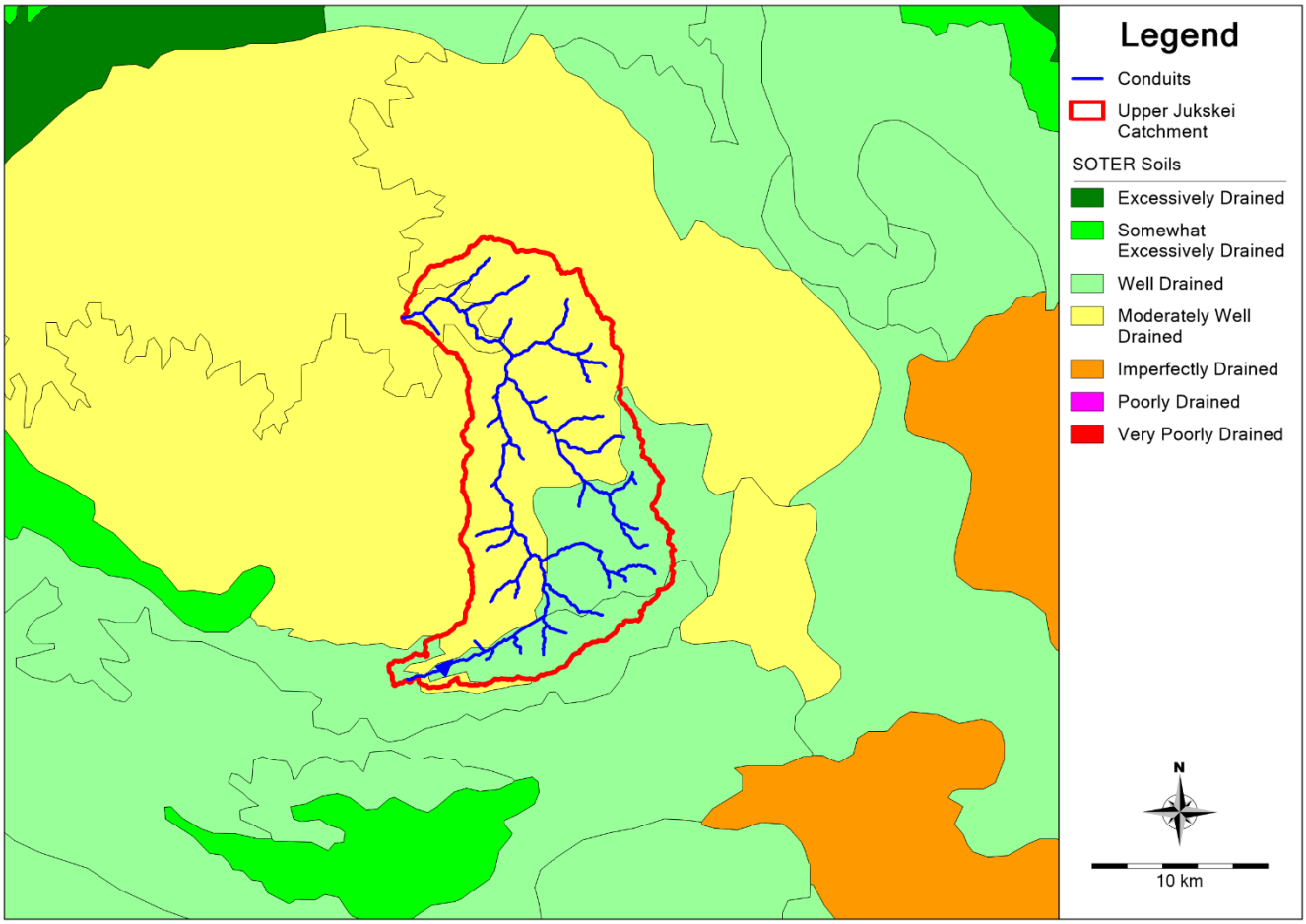

Figure B9: SOTER Soils - FAO Drainage Classes

The ESRI Land Cover classes were assigned SCS curve numbers for each hydrological soil group based on the pervious contribution of each land cover class. It was decided to partition the impervious and pervious areas of each subcatchment and subsequently the curve numbers are only representative of the pervious area of each land cover class. The SCS curve numbers for each land cover class were determined by consulting several tables in the SANRAL Drainage Manual (South African National Roads Agency, 2013) and the USDA publication (*Urban Hydrology for Small Watersheds*, 1986). The SCS curve numbers in the SANRAL and USDA publications are for "normal or average" antecedent conditions (CN_{II}). The SCS-CN_{II} for the ERSI Land Cover classes are shown below in **Table B3**.

Table B3: SCS-CN_{II} for 2020 ESRI Land Cover Classes

ESRI Land Cover	Hydrological Soil Group			
	A	B	C	D
Water	98	98	98	98
Trees	34	59	69	75
Grass	49	69	79	84
Flooded Vegetation	30	56	66	72
Crops	63	74	82	85
Shrub	45	66	77	83
Built Up	56	72	80	87
Bare Ground	72	82	87	89

The SWMM hydrology manual recommends that SCS-CN_I or low moisture SCS curve numbers are assigned when conducting continuous simulations to allow the soil to reach its maximum potential moisture retention

capacity during extended dry spells. Subsequently **Equation 5** was applied to the SCS-CN_{II} values in **Table B3**, to determine the SCS-CN_I as is shown below in **Table B4**. The SCS-CN_I values that were used in the model are shown below in **Figure B10**.

Table B4: SCS-CN_I for 2020 ESRI Land Cover Classes

ESRI Land Cover	Hydrological Soil Group			
	A	B	C	D
Water	95	95	95	95
Trees	18	38	48	56
Grass	29	48	61	69
Flooded Vegetation	15	35	45	52
Crops	42	54	66	70
Shrub	26	45	58	67
Built Up	35	52	63	74
Bare Ground	52	66	74	77

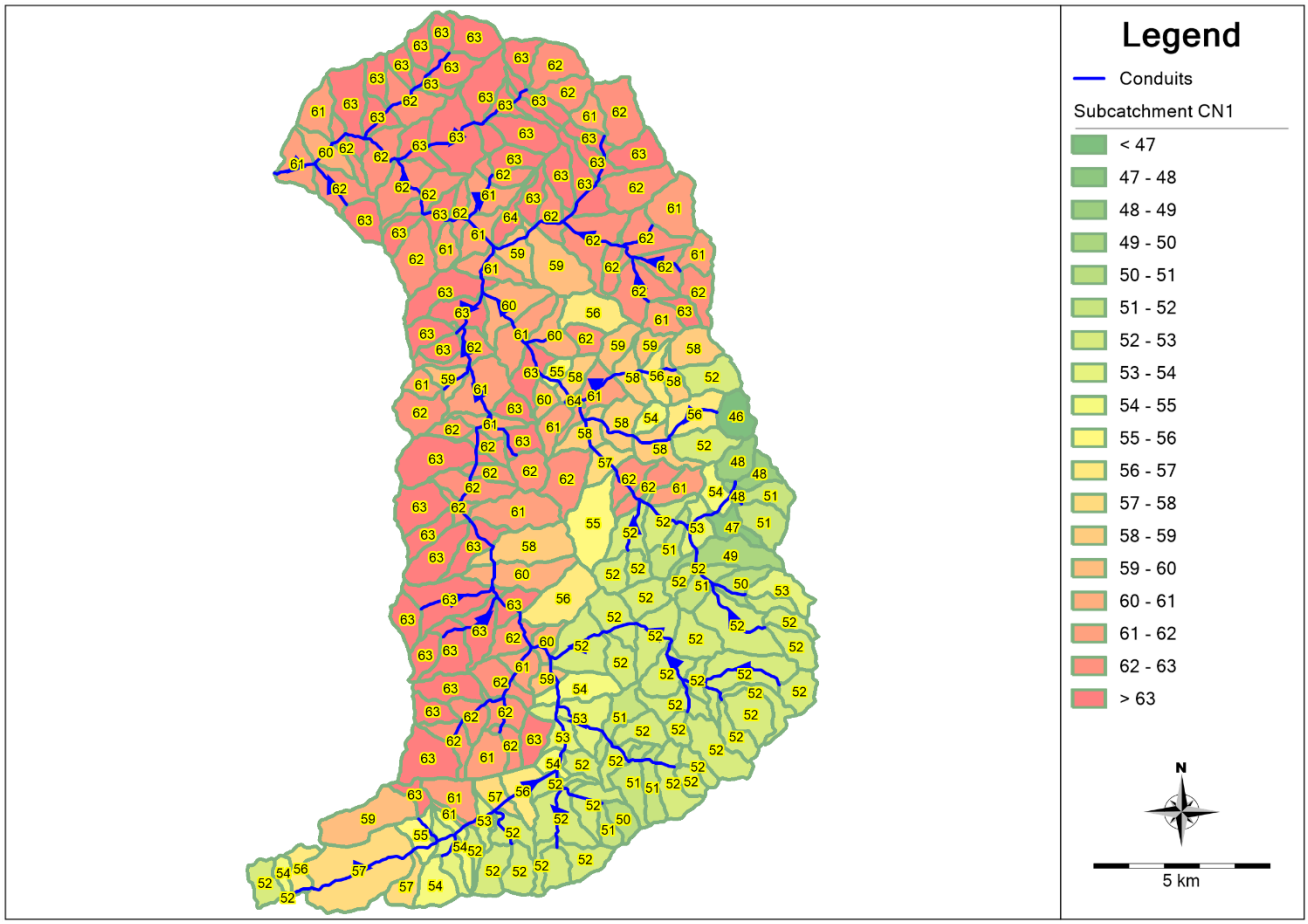

Figure B10: Upper Jukskei Catchment – SCS-CN_I Curve Numbers

Drying Time

The drying time T*dry* in days can be related to the soil's saturated hydraulic conductivity K*s* (mm/hr) by applying **Equation 8**. The SANRAL drainage manual (South African National Roads Agency, 2013) gives ranges for the permeability rates of the four hydrological soil groups. The permeability rates were used as the saturated hydraulic conductivity rates as the "…permeability rates are controlled by the properties of the soil profile…". The chosen permeability rates are shown below with the SANRAL ranges shown in brackets:

- Soil Group A: 7.6 mm/hr (> 7.6 mm/hr)
- Soil Group B: 5.7 mm/hr (3.8 mm/hr to 7.6 mm/hr)

- Soil Group C: 2.55 mm/hr (1.3 mm/hr to 3.8 mm/hr)
- Soil Group D: 1.3 mm/hr (< 1.3 mm/hr)

The drying times were calculated with **Equation 8** and are shown below for the hydrological soil groups:

- Soil Group A: 5.71 days
- Soil Group B: 6.60 days
- Soil Group C: 9.86 days
- Soil Group D: 13.81 days

Model Forcing

CHIRPS Rainfall

The CHIRPS rainfall has a gridded spatial resolution of 0.05° where the data is available from 1981 to present and produces daily precipitation estimates. The rainfall record used in this study is from 1981 to 2021 (41 years) where the rainfall from each of the 0.05° grids is assigned to the subcatchment below it. The 0.05° grids over the Upper Jukskei Catchment are shown below in **Figure B11**. The daily rainfall from Grid 43 is shown below in **Figure B12** where it can be seen that the maximum daily rainfall is 101mm on 11 March 2014.

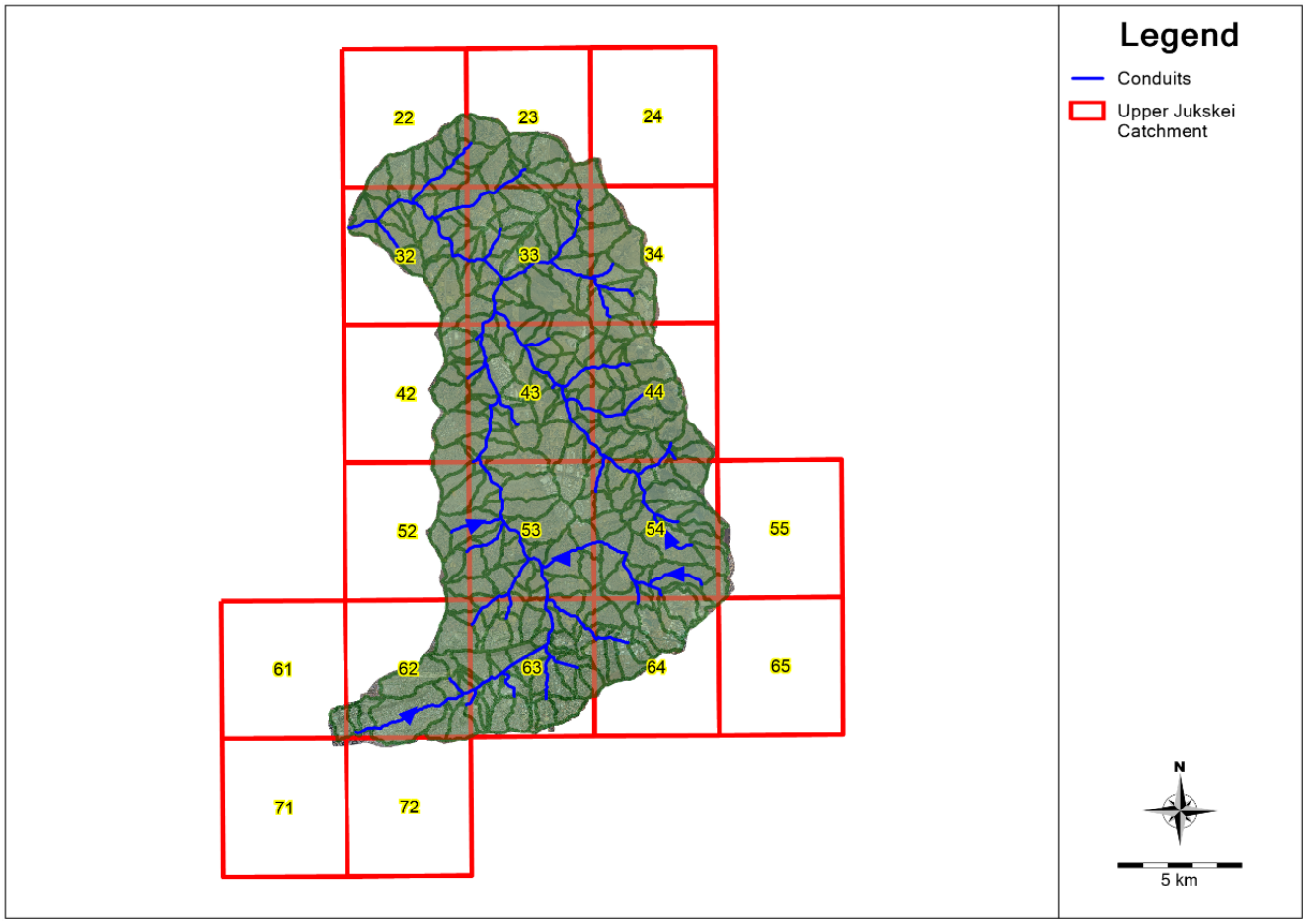

Figure B11: CHIRPS Rainfall 0.05° Grids

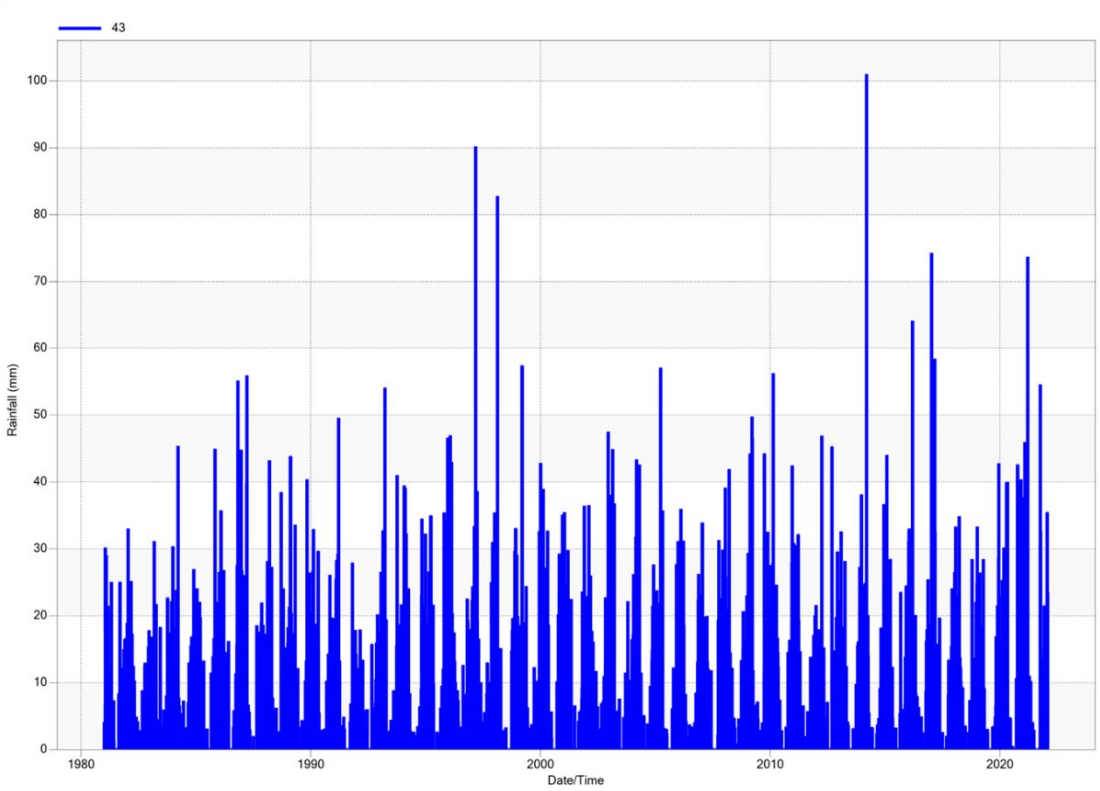

Figure B12: Grid 43 - CHIRPS Daily Rainfall

The CHIRPS precipitation varies between the various grids that cover the study area. The Mean Annual Precipitation (MAP) for the CHIRPS grids that cover the study area is shown below in **Figure B13**. The general trend observed is that the Southern part of the catchment receives more precipitation than the Northern part of the catchment. This could be due to the Witwatersrand Ridge situated in CHIRPS Grids 61 to 63. This is an interesting pattern and could be investigated in more detail in future.

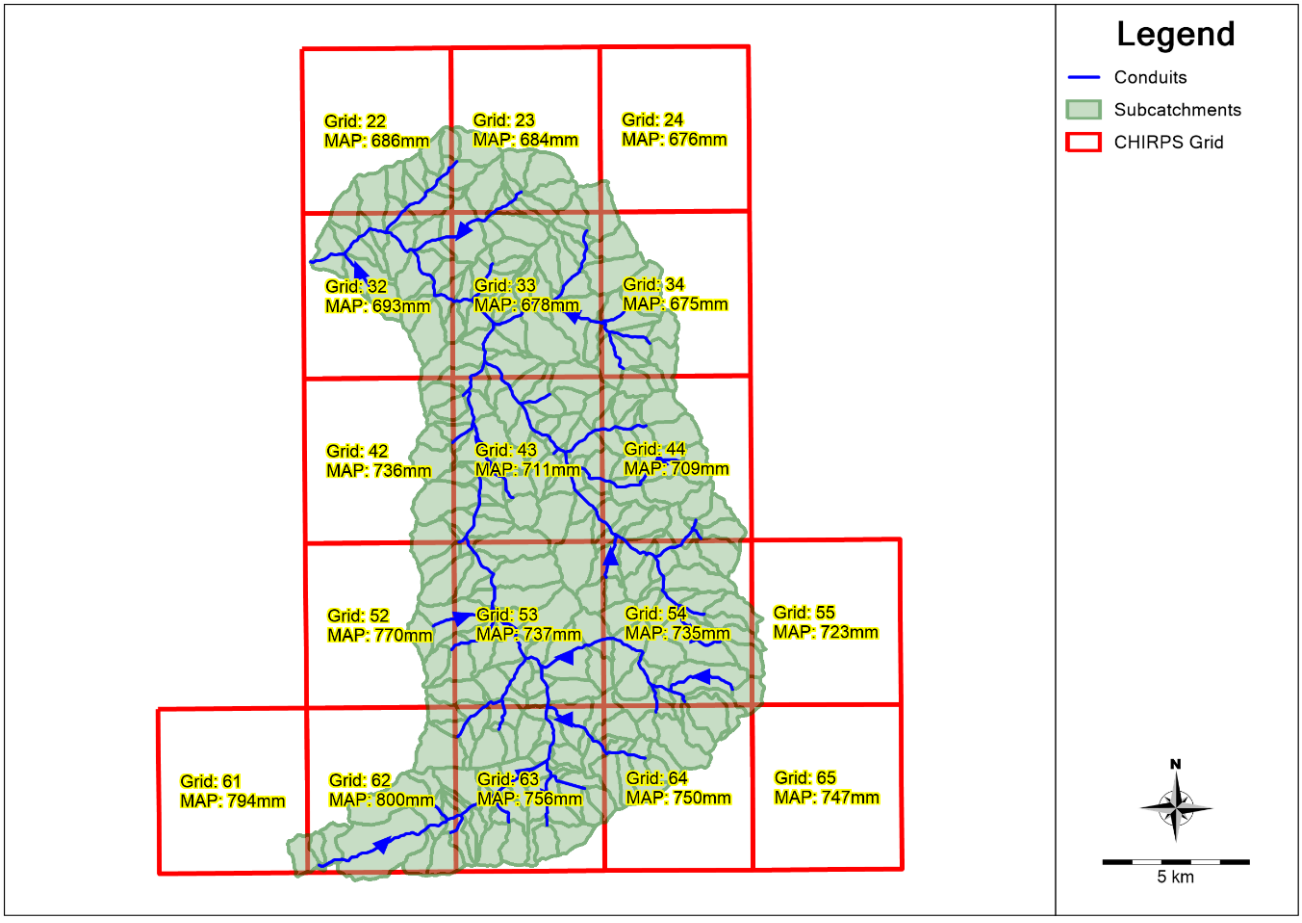

Figure B13: Mean Annual Precipitation (MAP) of the CHIRPS Grids

The average annual precipitation of all the CHIRPS Grids over the study area is shown below in **Figure B14**. The average annual precipitation for all the CHIRPS grids is 726mm. The year 1986 has an average precipitation closest to the average annual precipitation of all the CHIRPS grids with 729mm. The highest precipitation year (wettest year) is the year 2000 with an average of 920mm. The precipitation for the various CHIRPS grids for the year 2000 is shown below in **Figure B15**. The lowest precipitation year (driest year) is the year 1999 with an average of 498mm. The precipitation for the various CHIRPS grids for the year 1999 is shown below in **Figure B16**. The trend of higher precipitation in the Southern part of the catchment than the Northern part of the catchment is also visible in both Error! Reference source not found. and Error! Reference source not found..

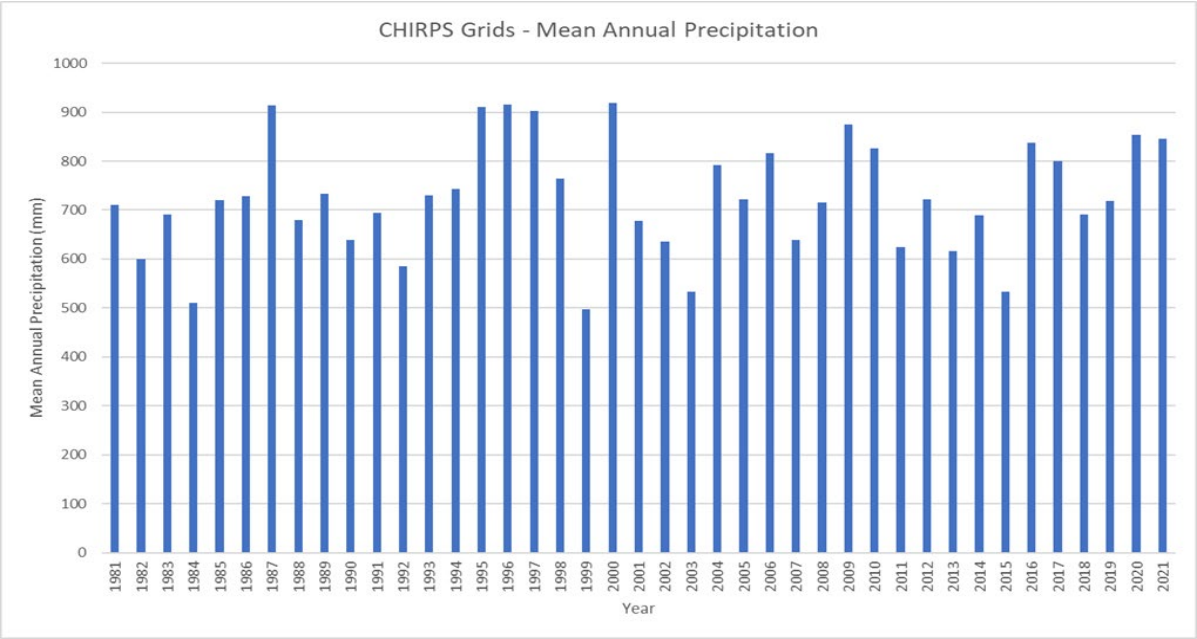

Figure B14: Average Annual Precipitation of all CHIRPS Grids

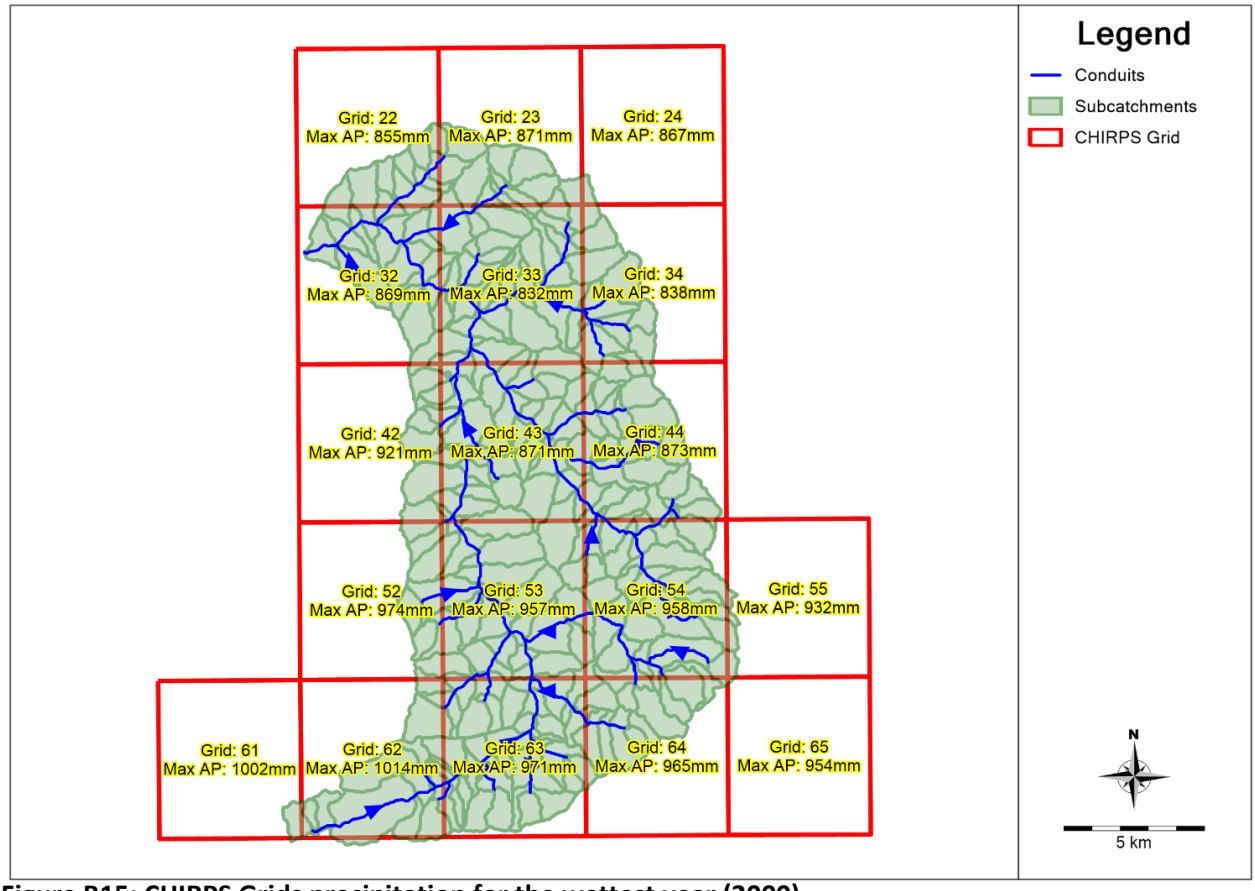

Figure B15: CHIRPS Grids precipitation for the wettest year (2000)

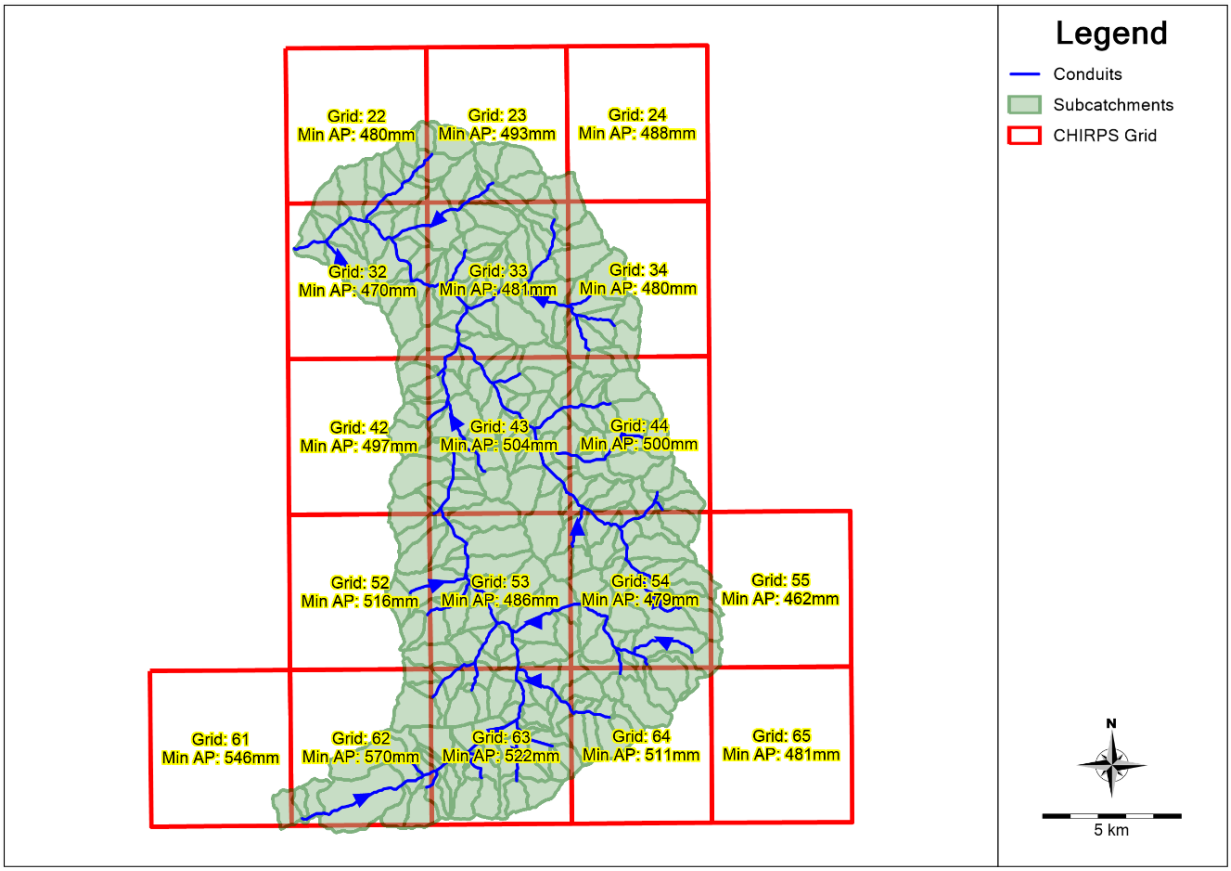

Figure B16: CHIRPS Grids precipitation for the driest year (1999)

Hargreaves Potential Evaporation

The Hargreaves Potential Evaporation is calculated by PCSWMM based on the method set out in Hargreaves et al., 1998. The method utilises the daily maximum and minimum temperatures as well as the study site latitude ,to determine the extra-terrestrial radiation, in the calculation of the potential evaporation. ERA5 reanalysis data with a spatial resolution of 0.25° was used to determine the daily maximum and minimum temperatures. The monthly distribution of the ERA5 daily maximum and minimum temperatures is shown below in **Figure B17**, where it is clear that the warmer summer months are from October to March and the colder winter months are from April to September. The summer months often have maximum temperatures in excess of 30 C°, where the winter months have minimum temperatures approaching 0 C°. The Hargreaves potential evaporation from 1981 to 2021 for the Upper Jukskei Catchment is shown below in **Figure B18**.

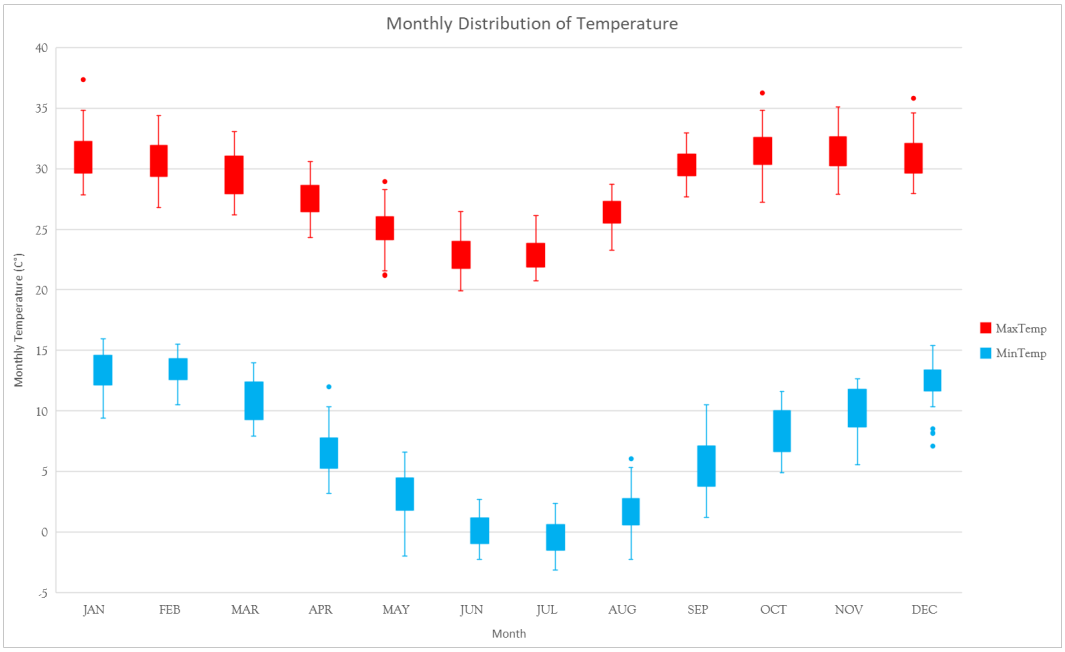

Figure B17: Monthly Distribution of ERA5 Daily Maximum and Minimum Temperatures

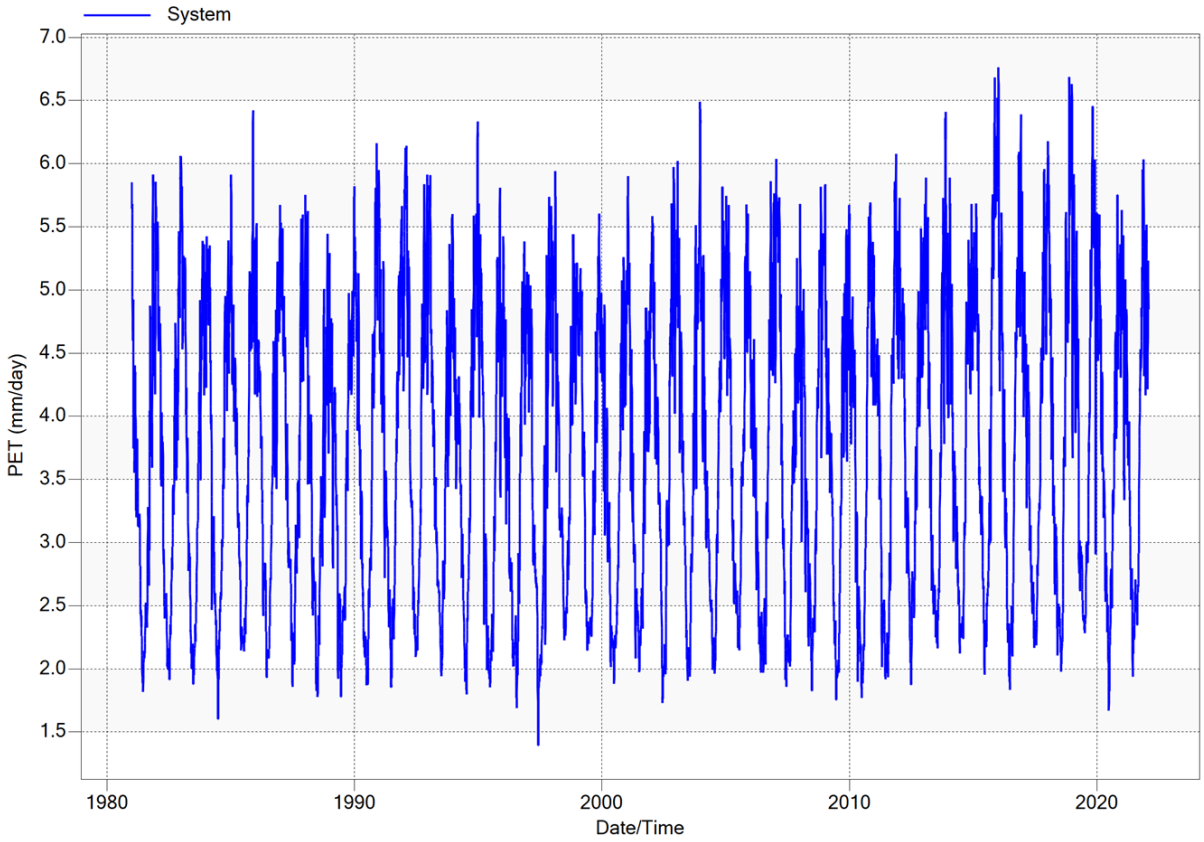

Figure B18: Hargreaves Potential Evaporation for the Upper Jukskei Catchment

Water Demand

The non-potable water demand for this assessment was determined in CROPWAT by considering a grass that is planted in loamy soil in Johannesburg and its water demand during the warmer months of October to March as it assumed that irrigation is not applied during the colder winter months. The evaporation and rainfall data were used from the pre-defined station available for Johannesburg in CROPWAT. It is recommended that for each assessment the water demand be calculated for local conditions with CROPWAT as the rainfall period and irrigation period could have a mismatch. The total gross irrigation demand that was calculated is 290.1mm as is shown in **Figure B19.** This equates to 2.917 Mℓ/Ha/annum and was rounded up to 3 Mℓ/Ha/annum. Inamdar (2013) used a non-potable water demand of 2 Mℓ/Ha/annum for the demand of the city parks in Melbourne, Australia.

The total water demand was therefore calculated by calculating the total area of all the applicable demand areas and then multiplying the area with 3 Mℓ/Ha/annum to determine the annual water demand.

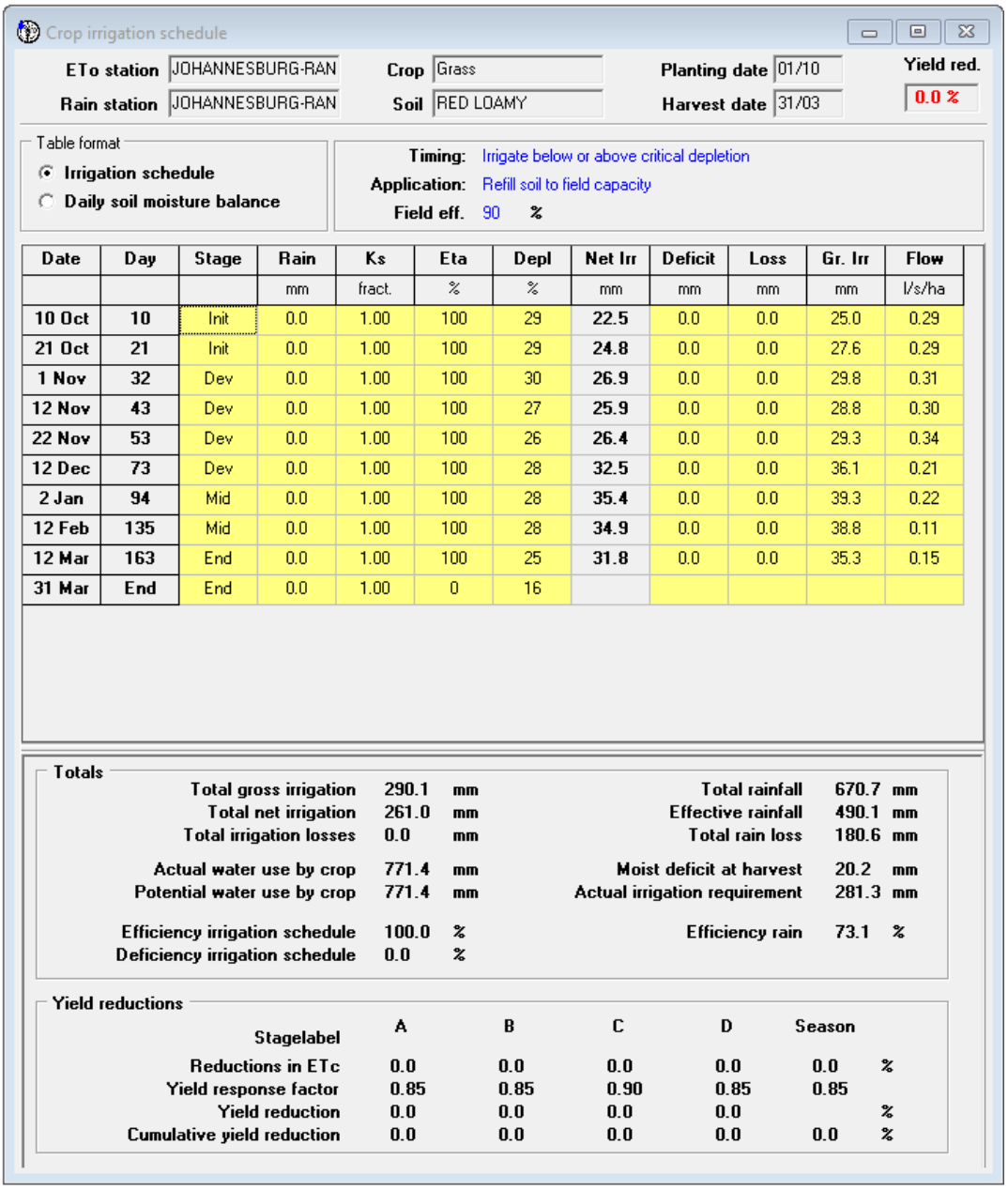

Date	Day	Stage	Rain	Ks	Eta	Depl	Net Irr	Deficit	Loss	Gr. Irr	Flow
			mm	fract.	%	%	mm	mm	mm	mm	l/s/ha
10 Oct	10	Init	0.0	1.00	100	29	22.5	0.0	0.0	25.0	0.29
21 Oct	21	Init	0.0	1.00	100	29	24.8	0.0	0.0	27.6	0.29
1 Nov	32	Dev	0.0	1.00	100	30	26.9	0.0	0.0	29.8	0.31
12 Nov	43	Dev	0.0	1.00	100	27	25.9	0.0	0.0	28.8	0.30
22 Nov	53	Dev	0.0	1.00	100	26	26.4	0.0	0.0	29.3	0.34
12 Dec	73	Dev	0.0	1.00	100	28	32.5	0.0	0.0	36.1	0.21
2 Jan	94	Mid	0.0	1.00	100	28	35.4	0.0	0.0	39.3	0.22
12 Feb	135	Mid	0.0	1.00	100	28	34.9	0.0	0.0	38.8	0.11
12 Mar	163	End	0.0	1.00	100	25	31.8	0.0	0.0	35.3	0.15
31 Mar	End	End	0.0	1.00	0	16					

Figure B19: CROPWAT Gross Water Requirement for Grass in Johannesburg

ANNEXURE C - OVERLAND FLOW MANNING N VALUES

Source	Ground Cover	n	Range
Crawford and Linsley (1966)a	Smooth asphalt	0.01	
	Asphalt of concrete paving	0.014	
	Packed clay	0.03	
	Light turf	0.2	
	Dense turf	0.35	
	Dense shrubbery and forest litter	0.4	
Engman (1986)b	Concrete or asphalt	0.011	0.010-0.013
	Bare sand	0.01	0.01-0.016
	Graveled surface	0.02	0.012-0.03
	Bare clay-loam (eroded)	0.02	0.012-0.033
	Range (natural)	0.13	0.01-0.32
	Bluegrass sod	0.45	0.39-0.63
	Short grass prairie	0.15	0.10-0.20
	Bermuda grass	0.41	0.30-0.48
Yen (2001)c	Smooth asphalt pavement	0.012	0.010-0.015
	Smooth impervious surface	0.013	0.011-0.015
	Tar and sand pavement	0.014	0.012-0.016
	Concrete pavement	0.017	0.014-0.020
	Rough impervious surface	0.019	0.015-0.023
	Smooth bare packed soil	0.021	0.017-0.025
	Moderate bare packed soil	0.03	0.025-0.035
	Rough bare packed soil	0.038	0.032-0.045
	Gravel soil	0.032	0.025-0.045
	Mowed poor grass	0.038	0.030-0.045
	Average grass, closely clipped sod	0.05	0.040-0.060
	Pasture	0.055	0.040-0.070
	Timberland	0.09	0.060-0.120
	Dense grass	0.09	0.060-0.120
	Shrubs and bushes	0.12	0.080-0.180
	Business land use	0.022	0.014-0.035
	Semi-business land use	0.035	0.022-0.050
	Industrial land use	0.035	0.020-0.050
	Dense residential land use	0.04	0.025-0.060
	Suburban residential land use	0.055	0.030-0.080
	Parks and lawns	0.075	0.040-0.120

a Obtained by calibration of Stanford Watershed Model.
b Computed by Engman (1986) by kinematic wave and storage analysis of measured rainfall-runoff data.
c Computed on basis of kinematic wave analysis.

ANNEXURE D – SCENARIO 1 COLLECTION MODELS - SCATTER PLOTS

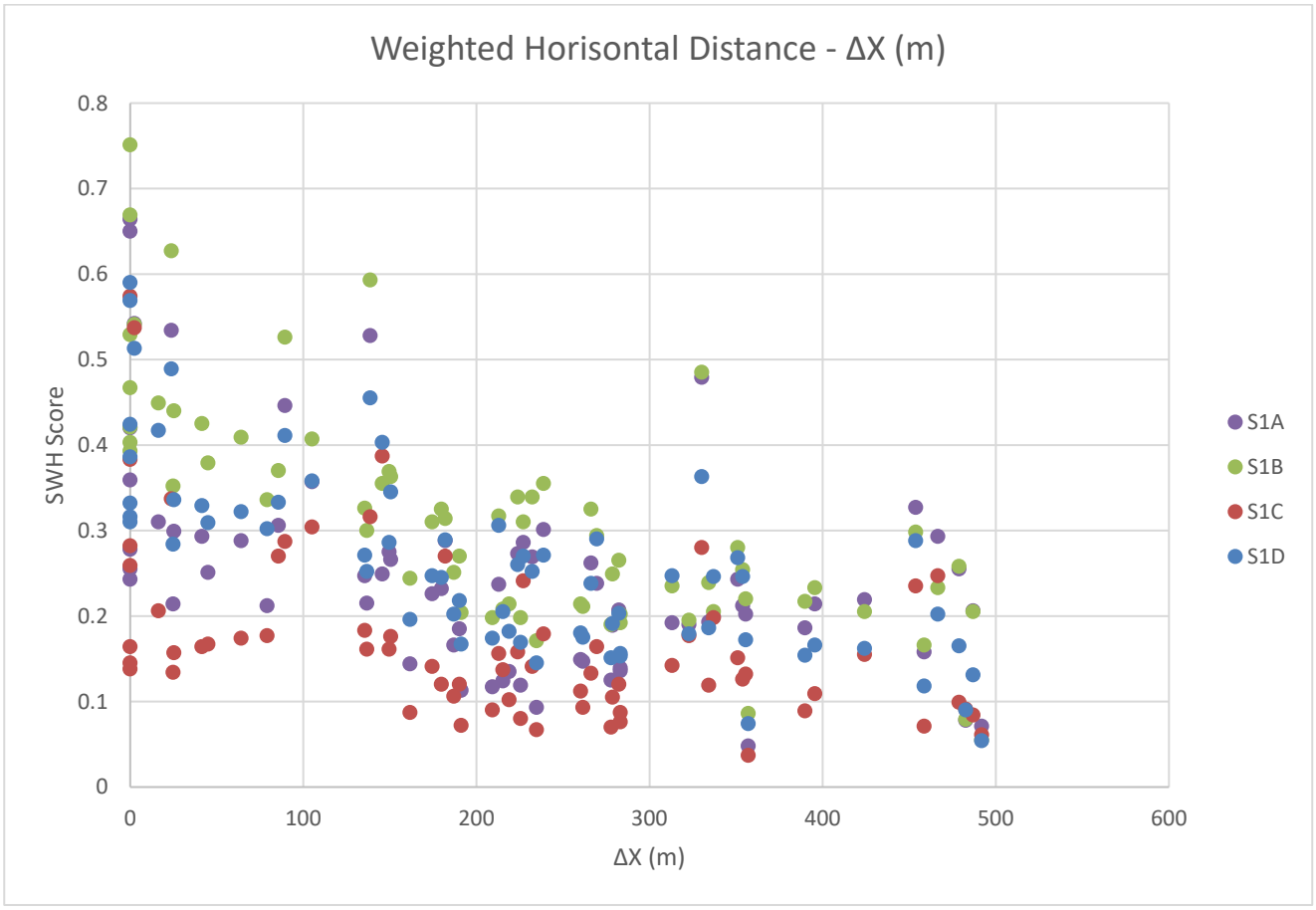

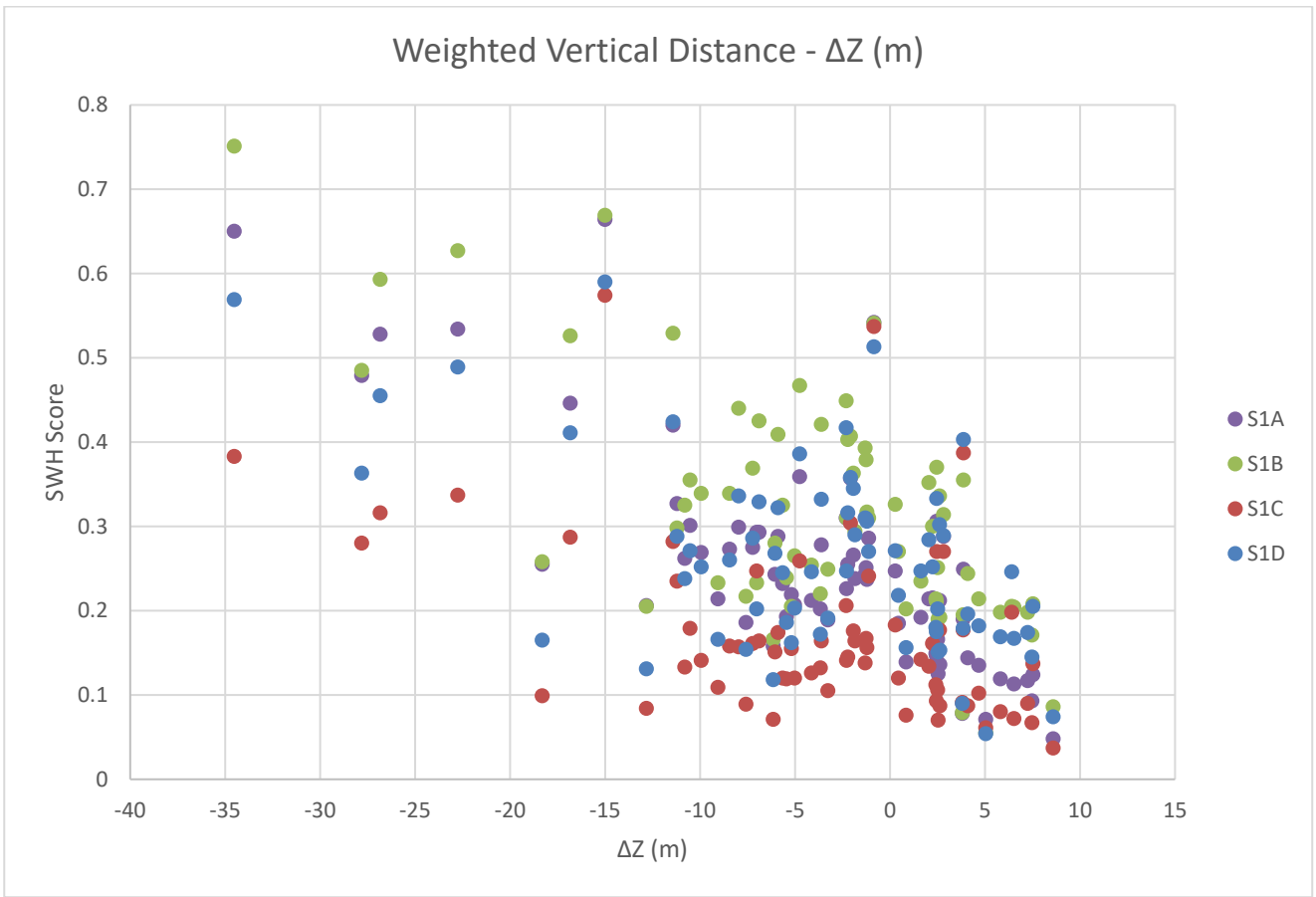

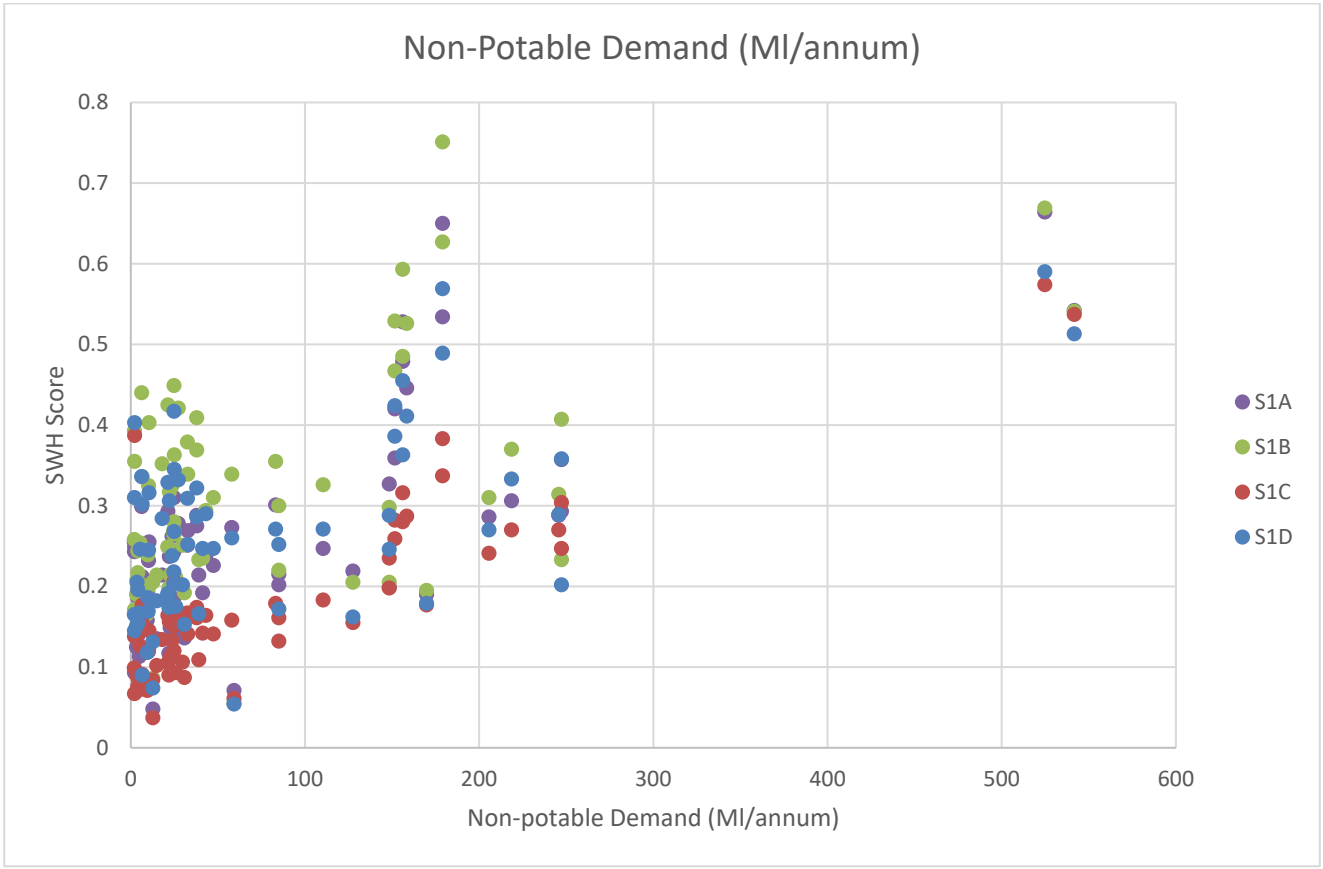
Non-Potable Demand (Ml/annum)
SWH Score
0.8
0.7
0.6
0.5
0.4
0.3
0.2
0.1
0
0
100
200
300
400
500
600
Non-potable Demand (Ml/annum)
S1A
S1B
S1C
S1D

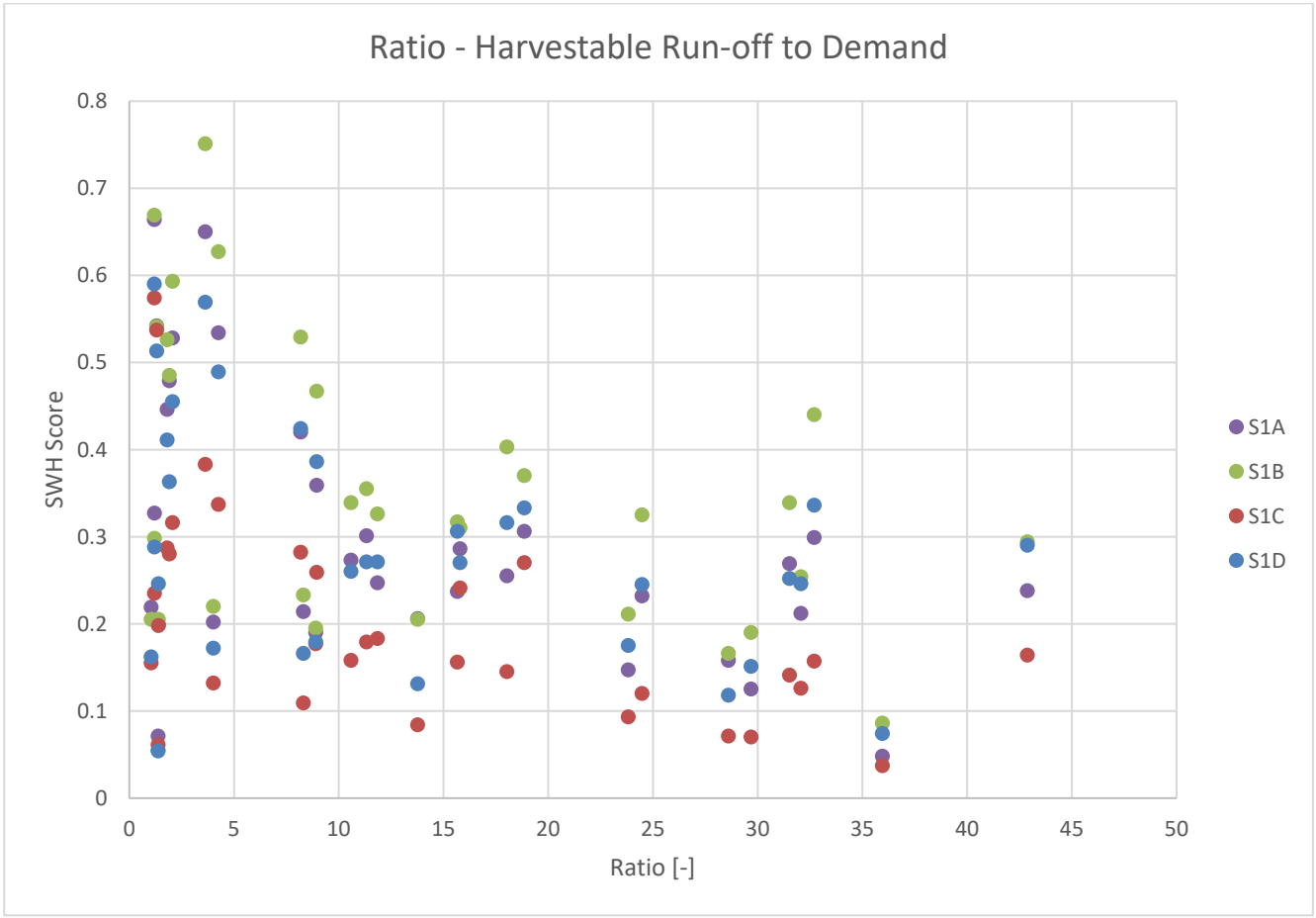
Ratio - Harvestable Run-off to Demand
SWH Score
0.8
0.7
0.6
0.5
0.4
0.3
0.2
0.1
0
0
5
10
15
20
25
30
35
40
45
50
Ratio [-]
S1A
S1B
S1C
S1D

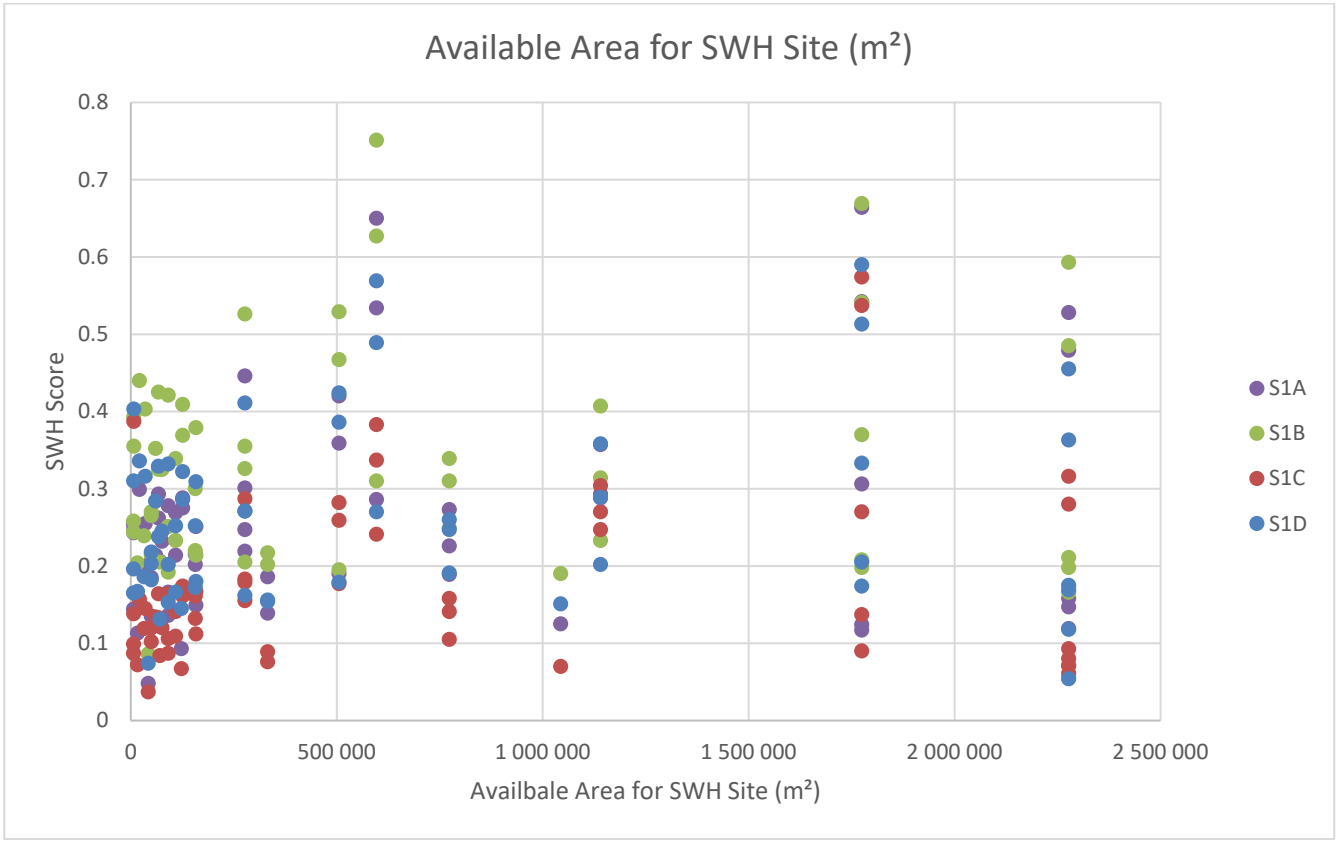
Available Area for SWH Site (m²)
SWH Score
0.8
0.7
0.6
0.5
0.4
0.3
0.2
0.1
0
0
500 000
1 000 000
1 500 000
2 000 000
2 500 000
Availbale Area for SWH Site (m²)
S1A
S1B
S1C
S1D

ANNEXURE E – SCENARIO 2 COLLECTION MODELS - SCATTER PLOTS

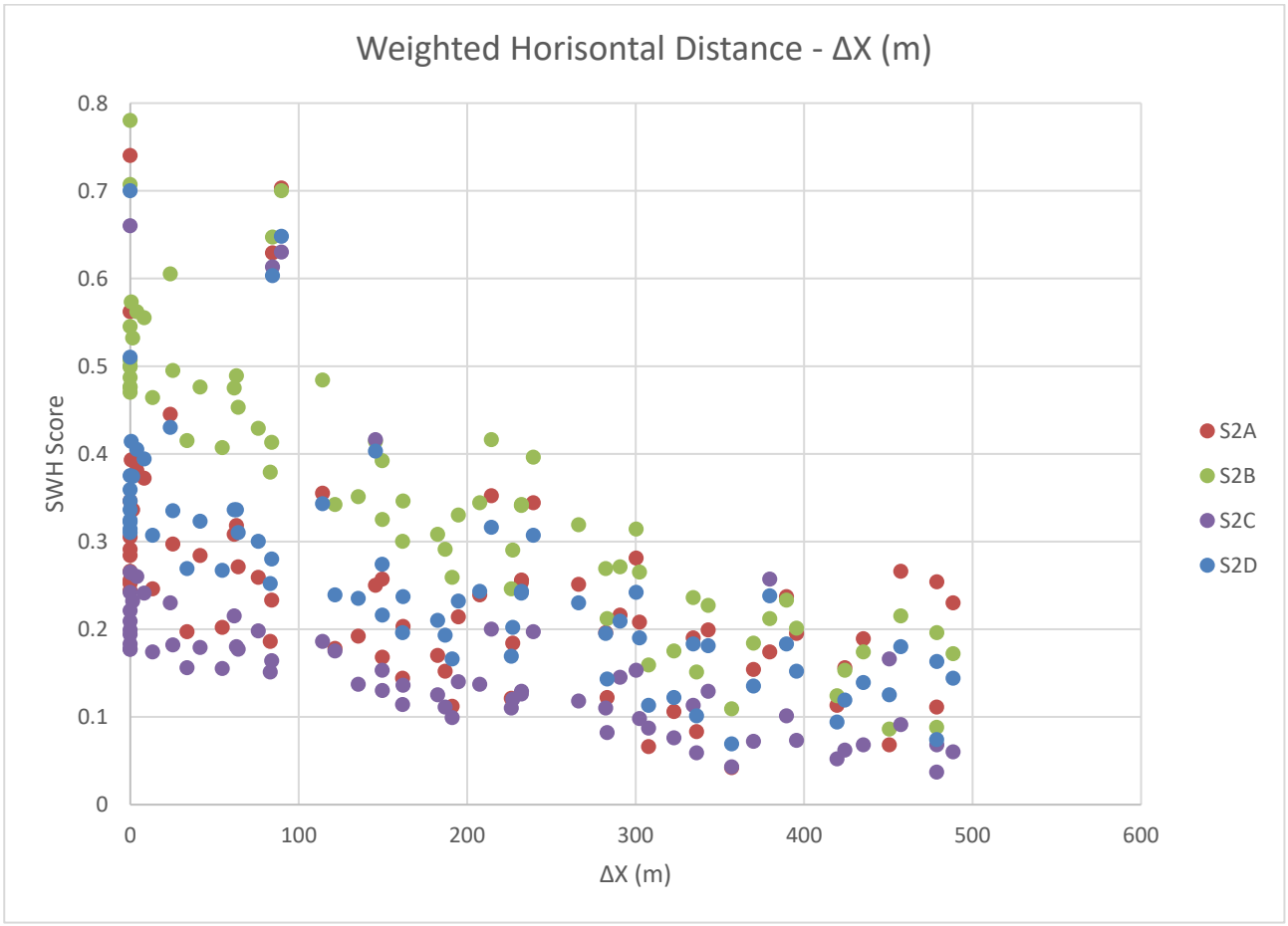

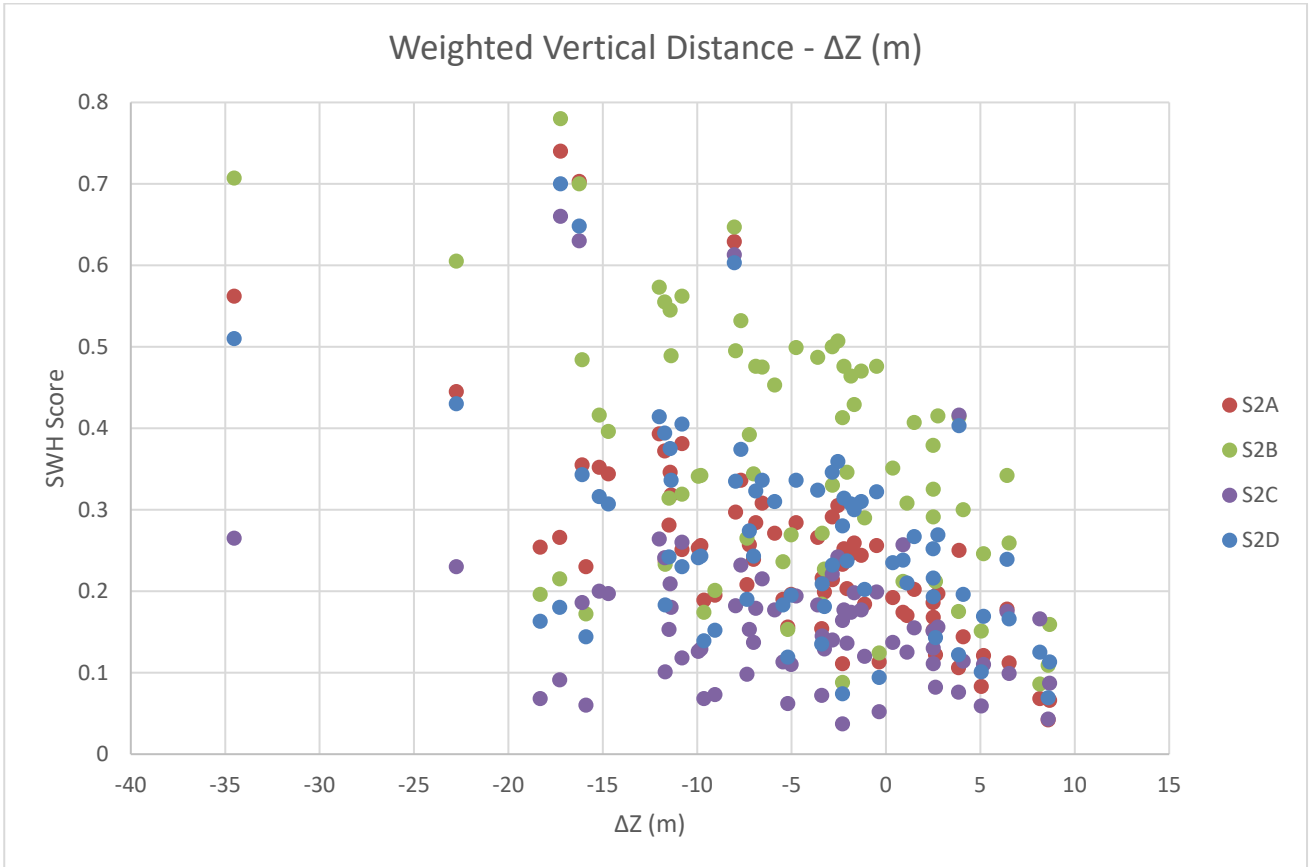

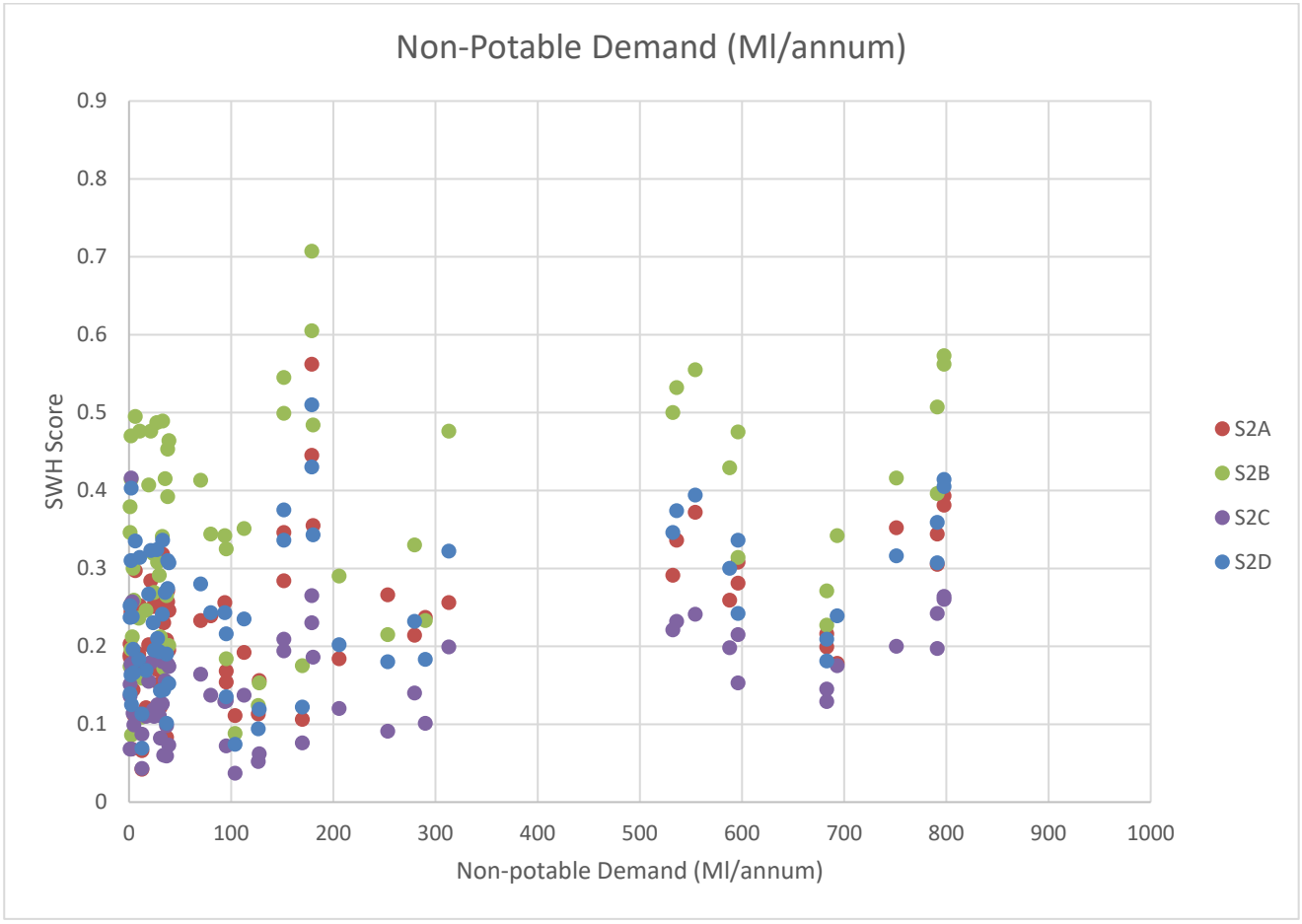
Non-Potable Demand (Ml/annum)
SWH Score
0.9
0.8
0.7
0.6
0.5
0.4
0.3
0.2
0.1
0
0
100
200
300
400
500
600
700
800
900
1000
Non-potable Demand (Ml/annum)
S2A
S2B
S2C
S2D

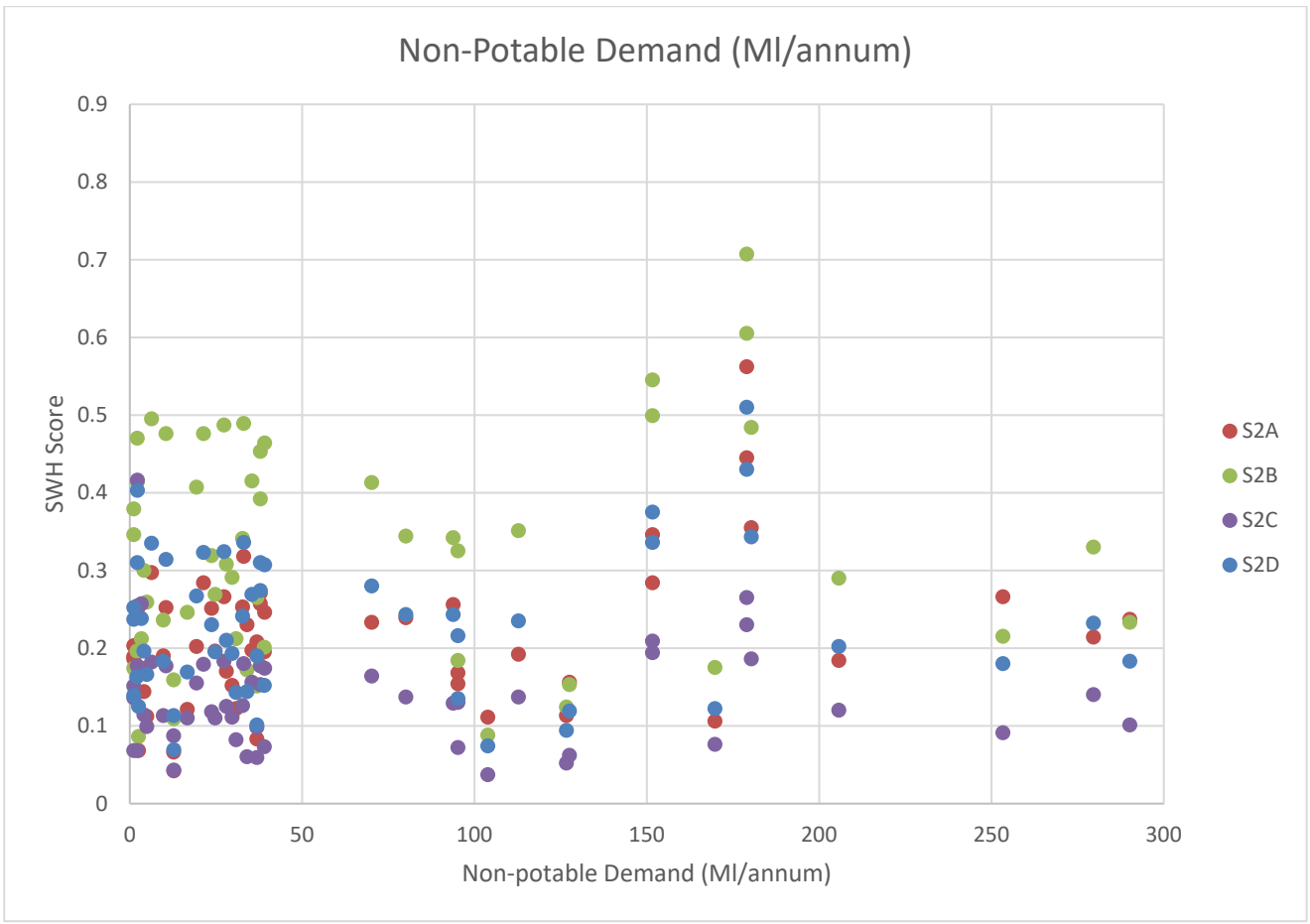
Non-Potable Demand (Ml/annum)
SWH Score
0.9
0.8
0.7
0.6
0.5
0.4
0.3
0.2
0.1
0
0
50
100
150
200
250
300
Non-potable Demand (Ml/annum)
S2A
S2B
S2C
S2D

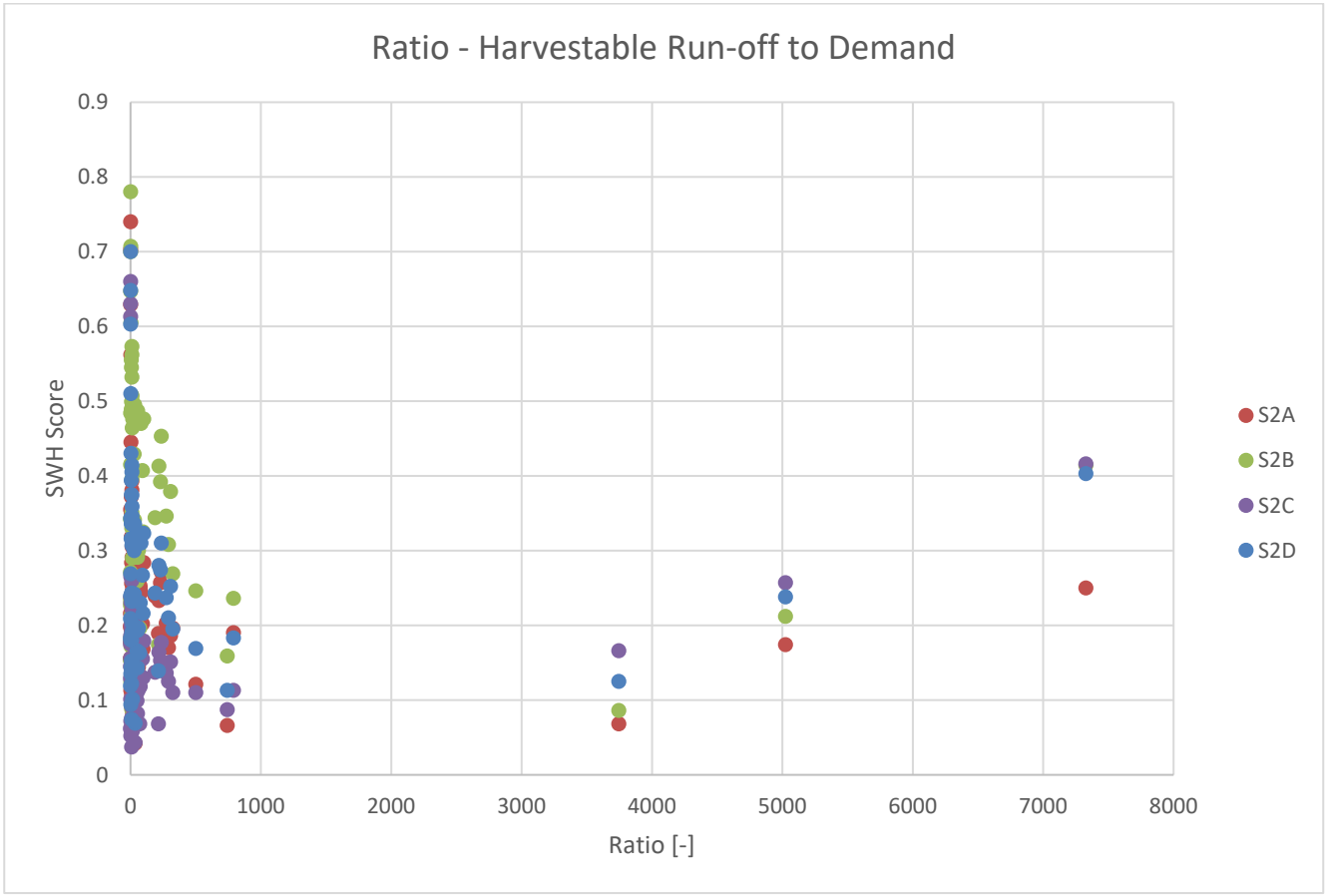
Ratio - Harvestable Run-off to Demand
SWH Score
0.9
0.8
0.7
0.6
0.5
0.4
0.3
0.2
0.1
0
0
1000
2000
3000
4000
5000
6000
7000
8000
Ratio [-]
S2A
S2B
S2C
S2D

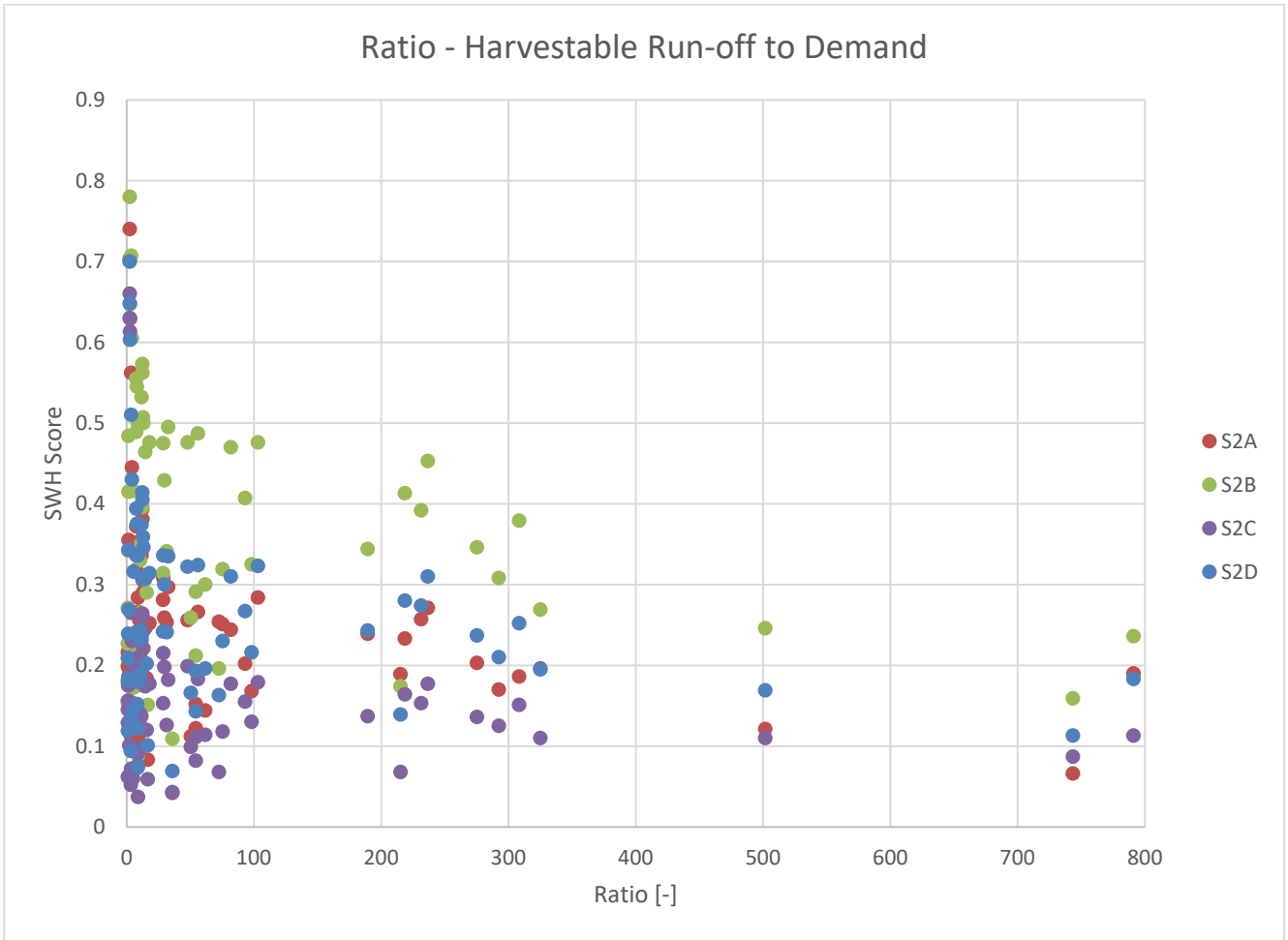
Ratio - Harvestable Run-off to Demand
SWH Score
0.9
0.8
0.7
0.6
0.5
0.4
0.3
0.2
0.1
0
0
100
200
300
400
500
600
700
800
Ratio [-]
S2A
S2B
S2C
S2D


Available Area for SWH Site (m²)
SWH Score
0.9
0.8
0.7
0.6
0.5
0.4
0.3
0.2
0.1
0
0
500 000
1 000 000
1 500 000
2 000 000
2 500 000
Availbale Area for SWH Site (m²)
S2A
S2B
S2C
S2D

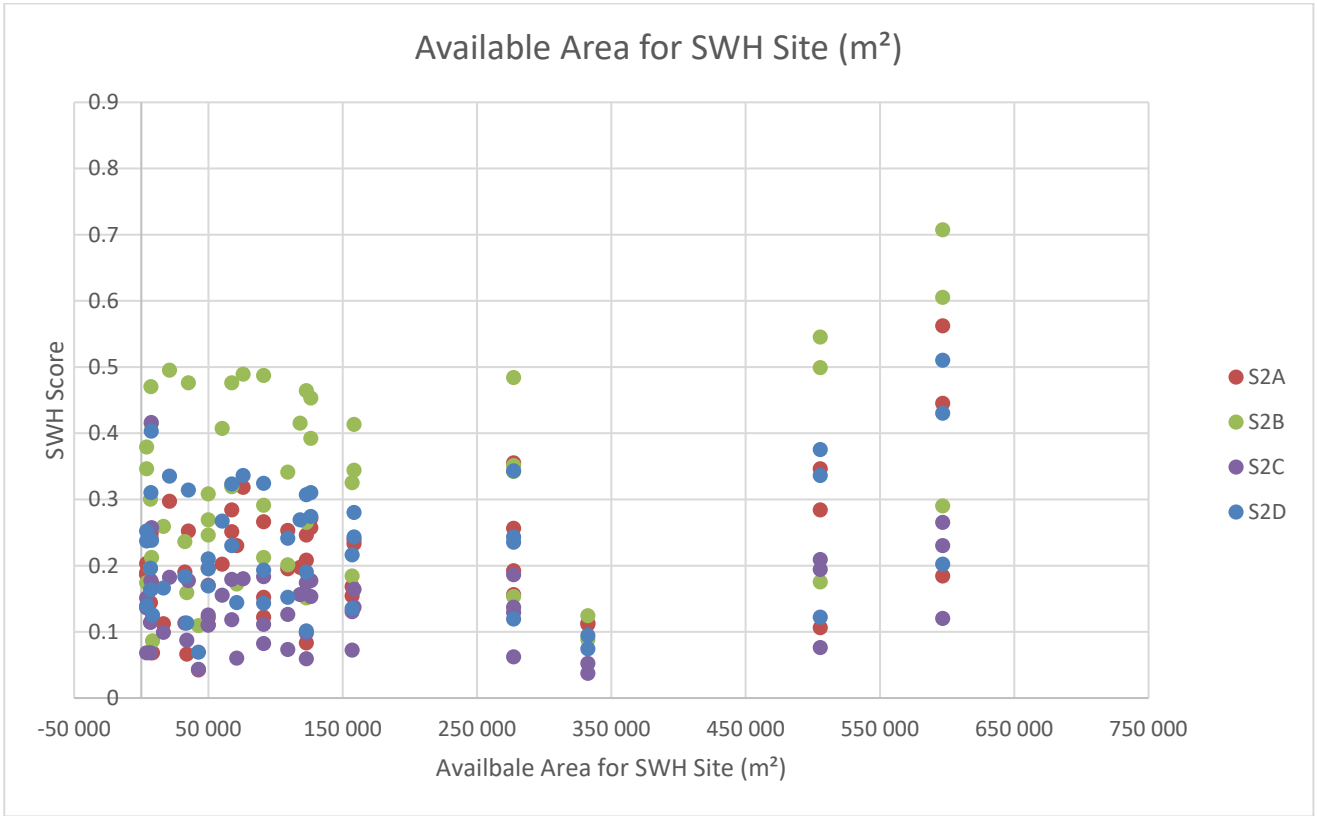
Available Area for SWH Site (m²)
SWH Score
0.9
0.8
0.7
0.6
0.5
0.4
0.3
0.2
0.1
0
-50 000
50 000
150 000
250 000
350 000
450 000
550 000
650 000
750 000
Availbale Area for SWH Site (m²)
S2A
S2B
S2C
S2D

ANNEXURE F – PCSWMM PYTHON SCRIPTS

Script 1 – Annual Harvestable inflows

```
#Interpreter64:IronPython (Python 2.7)
# tags: Support,SWH JHB
# file: Calculate Harvestable Volume


def diff_attr(lyr1_name, lyr2_name, comp_attr_name, new_attr_name):
  #lyr1_name = first layer name
  #lyr2_name = second layer name
  #comp_attr_name = the attribute common to both layers to be compared
  #new_attr_name = create this attribute in the first layer to store the difference
  lyr = pcpy.Map.Layer[lyr1_name]
  if not new_attr_name in lyr.Attributes:
    new_attr = pcpy.Attribute(new_attr_name, 'Number')
    lyr.add_attribute(new_attr_name)
  #open the second layer to compare
  lyr2 = pcpy.Map.Layer[lyr2_name]
  #loop through entities to calculate the attribute value difference
  entities = lyr.get_entities()
  for en in entities:
    en2 = lyr2.get_entities("Name='{0}'".format(en['Name']))[0]  # get entitiy in the other layer
    v, v2 = en[comp_attr_name], en2[comp_attr_name]
    en[new_attr_name] = v - v2


diff_attr('Junctions', 'ENV Flow Junctions', 'TotInflow', 'HarTotInf')
```

Script 2 – Harvestable Inflow Hydrograph

```
#Interpreter64:IronPython (Python 2.7)

#out files already loaded in the graph panel:

pre_out_fname = r'C:\Users\rober\OFC Dropbox\OFC\Delft\Thesis\Stormwater Harvesting\PCSWMM\Land Use Model\2023-01-14 Jukskei CMP - SWH Assessment (PreDevelopment).out'

post_out_fname = r'C:\Users\rober\OFC Dropbox\OFC\Delft\Thesis\Stormwater Harvesting\PCSWMM\Land Use Model\2023-01-14 Jukskei CMP - SWH Assessment (Current).out'

#tsb file to be created:

diff_tsb_fname = r'C:\Users\rober\OFC Dropbox\OFC\Delft\Thesis\Stormwater Harvesting\PCSWMM\Land Use Model\diff.tsb'


def create_tsb_file():
    tsb_fname = diff_tsb_fname


    #Check if tsb file already exists
    for file in pcpy.Graph.Files:
        if file.FilePath == tsb_fname:
            break
    else:
        file = pcpy.Graph.add_file(tsb_fname)


    # clear data in the file
    for func in file.Functions:
        file.delete_function(func.Name, 'm3/s')


    # add one function Flow difference
    flow_func = file.add_function('Flow_difference', 'm3/s')
    return file, flow_func


try:
    #open both out files
    files = pcpy.Graph.Files
    for f in files:
        if f.FilePath == pre_out_fname: pre_out=f
        if f.FilePath == post_out_fname: post_out=f
```

```
    #create empty tsb file
    tsb_file, flow_func = create_tsb_file()

    #loop all junctions computing the difference between post and pre development total flows
    junctions = pcpy.SWMM.Junctions
    for name, junction in junctions.items():
        pre_values = pre_out.get_data('Nodes', 'Total inflow', 'm3/s', name)
        post_values = post_out.get_data('Nodes', 'Total inflow', 'm3/s', name)
        diff_values = []

        #loop each time step
        for pre_value, post_value in zip(pre_values,post_values):
            diff_value = post_value.Value - pre_value.Value
            diff_values.append(pcpy.DateTimeValue(pre_value.DateTime, diff_value))

        #save new time series as a new location in the tsb file
        tsb_location = flow_func.add_location(name)
        tsb_location.Data = diff_values

    tsb_file.save()

except Exception as e:
    print str(e)
```

Script 3 – SWH Site Metrics

```
# tags: Support,SWH JHB
# file: agg_polygons_to_node

BUFFER_DIST = 500



def get_within_polygons_area(junc_entity, polygons):
    # return the weighted distance & height difference of the polygons within 500 m of the junction
    # if height difference is more than 10m (1 Bar pressure) then polygon area is disregarded
    junc_geo = junc_entity.Geometry
    tot_distance = 0.0
    count = 0.0
    tot_elev = 0.0
    elev_count = 0.0
    tot_area = 0.0
    elev_product = 0.0
    dist_product = 0.0
    np_demand = 0.0
    #np_R_D = 0.0
    for pn in polygons:
        pn_geo = pn.Geometry
        if not pn.Geometry.within(junc_geo, BUFFER_DIST): continue
        if not pn['MIN_ELEV_M'] - junc_entity['InvertElev'] < 10 : continue
        if not pn_geo.AreaInM2 > 2500 : continue
        tot_distance += junc_geo.distance(pn.Geometry)
        count += 1.0
        tot_elev += pn['MIN_ELEV_M'] - junc_entity['InvertElev']
        elev_count += 1.0
        pn_geo = pn.Geometry
        tot_area += pn_geo.AreaInM2
        elev_product += (pn['MIN_ELEV_M'] - junc_entity['InvertElev'])*pn_geo.AreaInM2
        dist_product += (junc_geo.distance(pn.Geometry))*pn_geo.AreaInM2
    print(dist_product)
```

```
    print (count)
    print(elev_product)
    print(elev_count)
    print (tot_area)
    if count < 1:
        dist_weigh = 9999
    else:
         dist_weigh = dist_product/tot_area
    if elev_count < 1:
        height_weigh = 9999
    else:
        height_weigh = elev_product/tot_area
    print(dist_weigh)
    print(height_weigh)
    np_demand = tot_area*0.0003 #Demand in ML/annum
    #np_R_D = ((junc_entity['TotHarInf'])/41)/np_demand
    print(np_demand)
    #print(np_ro_to_dem)
    return dist_weigh, height_weigh, tot_area, np_demand, #np_R_D


def Ratio_run_off_to_demand(junc_entity):
    # loop over junctions and use junction entity to set the new attributes
    Np_Demand = 0.0
    Np_R_D = 0.0

    Np_Demand = junc_entity['Np_Demand']
    if Np_Demand < 1:
        Np_R_D = 0
    else:
         Np_R_D = (junc_entity['HarTotInf']/40)/Np_Demand #Check Number of Years of Simulation
    return Np_R_D

#Define New Attributes to be Calculated & Populated
```

```
lyr = pcpy.Map.Layer['Junctions']
if not 'Np_Delta_h' in lyr.Attributes:
 new_attr = pcpy.Attribute('Np_Delta_h', 'Number')
 lyr.add_attribute(new_attr)

lyr = pcpy.Map.Layer['Junctions']
if not 'Np_Delta_w' in lyr.Attributes:
 new_attr1 = pcpy.Attribute('Np_Delta_w', 'Number')
 lyr.add_attribute(new_attr1)

 lyr = pcpy.Map.Layer['Junctions']
 if not 'Np_Area' in lyr.Attributes:
  new_attr = pcpy.Attribute('Np_Area', 'Number')
  lyr.add_attribute(new_attr)

 lyr = pcpy.Map.Layer['Junctions']
 if not 'Np_Demand' in lyr.Attributes:
  new_attr = pcpy.Attribute('Np_Demand', 'Number')
  lyr.add_attribute(new_attr)

 lyr = pcpy.Map.Layer['Junctions']
 if not 'Np_R_D' in lyr.Attributes:
  new_attr = pcpy.Attribute('Np_R_D', 'Number')
  lyr.add_attribute(new_attr)

# get the two layers
junc_layer = pcpy.Map.Layer['Junctions']
poly_layer = pcpy.Map.Layer['ESRI Grass Areas with Elev']          #Check the Name

# get all junctions and polygons
junctions = junc_layer.get_entities()
polygons = poly_layer.get_entities()

# loop each junction to set its attribute
```

```
for junc_entity in junctions:
    junc_entity['Np_Delta_w'],junc_entity['Np_Delta_h'], junc_entity['Np_Area'], junc_entity['Np_Demand'] = get_within_polygons_area(junc_entity, polygons)


# loop each junction to set its attribute
for junc_entity in junctions:
    junc_entity['Np_R_D'] = Ratio_run_off_to_demand(junc_entity)
print('Done')
```

Script 4 – SWH Location

```
#Interpreter64:IronPython (Python 2.7)
# tags: Support,SWH JHB

BUFFER_DIST = 500

def get_within_polygons_area(junc_entity, polygons):
    # return the if SWH facility is possible within 500m of the junction
    # if height difference is more than 10m (1 Bar pressure) then polygon area is disregarded
    junc_geo = junc_entity.Geometry
    SWH_Sites = 0.0
    SWH_Area = 0.0
    for pn in polygons:
        pn_geo = pn.Geometry
        if not pn.Geometry.within(junc_geo, BUFFER_DIST): continue
        if not pn['MIN_ELEV_M'] - junc_entity['InvertElev'] < 10 : continue
        if not pn_geo.AreaInM2 > 2500 : continue
        SWH_Sites += 1.0
        if pn_geo.AreaInM2 > SWH_Area:
            SWH_Area = pn_geo.AreaInM2
        else:
            SWH_Area = SWH_Area
    return SWH_Sites, SWH_Area


lyr = pcpy.Map.Layer['Junctions']
if not 'SHW_Sites' in lyr.Attributes:
 new_attr = pcpy.Attribute('SWH_Sites', 'Number')
 lyr.add_attribute(new_attr)

if not 'SWH_Area' in lyr.Attributes:
 new_attr1 = pcpy.Attribute('SWH_Area', 'Number')
 lyr.add_attribute(new_attr1)
```

```
# get the two layers
junc_layer = pcpy.Map.Layer['Junctions']
poly_layer = pcpy.Map.Layer['ESRI GrassShrub Areas with Elev']        #Check Name

# get all junctions and polygons
junctions = junc_layer.get_entities()
polygons = poly_layer.get_entities()

# loop each junction to set its attribute
for junc_entity in junctions:
   junc_entity['SWH_Sites'], junc_entity['SWH_Area'] = get_within_polygons_area(junc_entity, polygons)
```

Script 5 – SWH Ranking

```
# -*- coding: utf-8 -*-
# tags: SWH Ranking, PCSWMM Automation
# file: calc_swh_rank_short

################################################################################
# USER SETTINGS – weights & metric behaviour
################################################################################
WEIGHTS = {
   'Np_Delta_h': 0.25,   # lower is better
   'Np_Delta_w': 0.25,   # lower is better
   'Np_Demand' : 0.2,   # higher is better
   'Np_R_D'    : 0.2,   # higher is better
   'SWH_Area'  : 0.1    # higher is better
}

LOWER_IS_BETTER   = {'Np_Delta_h', 'Np_Delta_w'}
DISCARD_THRESHOLD = 1
DISCARD_SCORE     = 9999
# ---- new field names (≤ 10 chars) ---------------------------------
SCORE_FIELD = 'SWHScore'   # 8 chars
RANK_FIELD  = 'SWHRank'    # 7 chars
################################################################################

import math
junc_layer = pcpy.Map.Layer['Junctions']

# ------------------------------------------------------------------
# 1. Ensure new attributes exist
# ------------------------------------------------------------------
def ensure_attribute(layer, name, attr_type='Number'):
   if name not in layer.Attributes:
      layer.add_attribute(pcpy.Attribute(name, attr_type))
```

```
ensure_attribute(junc_layer, SCORE_FIELD, 'Number')   # float
ensure_attribute(junc_layer, RANK_FIELD,  'Number')   # integer

# ---------------------------------------------------------------------
# 2. Collect junction entities and split into eligible / discarded
# ---------------------------------------------------------------------
junctions = junc_layer.get_entities()
eligible   = [j for j in junctions
              if j['Np_R_D'] is not None and j['Np_R_D'] >= DISCARD_THRESHOLD]
discarded  = [j for j in junctions if j not in eligible]

# ---------------------------------------------------------------------
# 3. Calculate min-max ranges for normalisation (eligible only)
# ---------------------------------------------------------------------
ranges = {}
for m in WEIGHTS:
    vals = [j[m] for j in eligible]
    ranges[m] = (min(vals), max(vals))

def normalise(val, mn, mx, higher_is_better):
    span = mx - mn
    if abs(span) < 1e-12:
        return 1.0
    return (val - mn) / span if higher_is_better else (mx - val) / span

# ---------------------------------------------------------------------
# 4. Compute rank score for every junction
# ---------------------------------------------------------------------
scored = []   # (score, entity)

for j in eligible:
    score = 0.0
    for metric, w in WEIGHTS.items():
        mn, mx  = ranges[metric]
```

```
        hi_best = metric not in LOWER_IS_BETTER
        score  += normalise(j[metric], mn, mx, hi_best) * w
    j[SCORE_FIELD] = score
    scored.append((score, j))

for j in discarded:
    j[SCORE_FIELD] = DISCARD_SCORE
    j[RANK_FIELD]  = None

# ---------------------------------------------------------------------
# 5. Rank eligible junctions by descending score
# ---------------------------------------------------------------------
scored.sort(key=lambda tup: tup[0], reverse=True)
for rk, (_, j) in enumerate(scored, start=1):
    j[RANK_FIELD] = rk

print("SWH ranking complete - {0} eligible, {1} discarded."
      .format(len(scored), len(discarded)))
```